U.PORTO
FACULDADE DE CIÊNCIAS
UNIVERSIDADE DO PORTO

FEUP FACULDADE DE ENGENHARIA
UNIVERSIDADE DO PORTO

Optimal Control of Shell Models of Turbulence

Nagwa Mohamed Arafa Mohamed

Tese de Doutoramento apresentada à
Faculdade de Ciências da Universidade do Porto
Applied Mathematics

2017

Optimal Control of Shell Models of Turbulence

Nagwa Mohamed Arafa Mohamed
Applied Mathematics
Mathematics Department
2017

Supervisor
Sílvio Marques de Almeida Gama, Professor Associado, FCUP

Co-supervisor
Fernando Manuel Ferreira Lobo Pereira, Professor Catedrático, FEUP

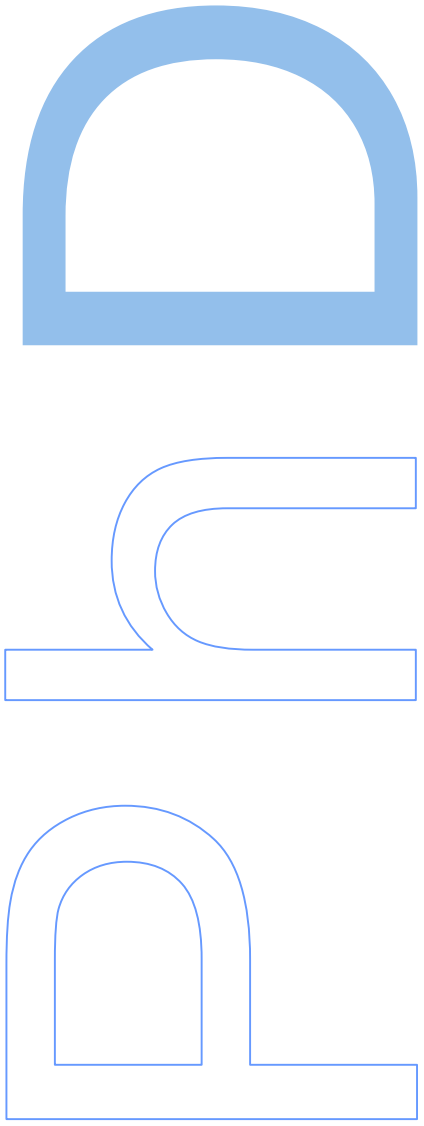

Abstract

The aim of this thesis is threefold: (i) to derive first order optimality conditions, where the state variable dynamics is given by a shell model of turbulence, (ii) to apply the Pontryagin maximum principle for the optimal control of the Obukhov model, and (iii) to present a conceptual recursive algorithm based on the maximum principle of Pontryagin.

First, we present work on the development of a theoretical methodology based on optimization schemes and on optimal and control approaches in order to optimize and control the forcing of turbulence, and we applied this methodology to the Obukhov and Gledzer-Okhitani-Yamada shell models.

Secondly, we apply the Pontryagin maximum principle to the Obukhov continuous hydrodynamic shell model in one space dimension restricted only to three shells. We show that many information can be extracted by simply reasoning with the conditions of the maximum principle, and, on the other hand, that this effort can become cumbersome, and, thus, there are limits to what can be achieved in an efficient way in terms of computing the solution to the optimal control problem. Numerical computation of solutions to this optimal control problem based on a "brute-force" type of shooting method evidences the existence of switching points in the control.

Lastly, we reports findings in designing a conceptual optimal control algorithm based on the maximum principle of Pontryagin and of the steepest descent type for a relaxed version of the original problem. Allowing the relaxation of initial condition in order to rewrite the two boundary value problem as one with boundary conditions in the same endpoint, key properties of this algorithm are proved. Then, some results are obtained by using an optimization algorithm of the same type for which off-the-shelf routines taking into account the numerical issues, which are always tricky for infinite dimensional problems.

Keywords: Optimal control; Maximum principle; Optimal control algorithms; Obukhov, GOY and Gledzer models.

Resumo

O objetivo desta tese é triplo: (i) derivar condições de optimalidade de primeira ordem, onde a dinâmica das variáveis de estado é dada por um dos modelos de camada de turbulência, (ii) aplicar o princípio máximo de Pontryagin para o controle ótimo do modelo de Obukhov e (iii) apresentar um algoritmo recursivo conceptual baseado no princípio máximo de Pontryagin.

Em primeiro lugar, apresentamos o desenvolvimento de uma metodologia teórica baseada em esquemas de optimização e em abordagens óptimas e de controle, a fim de optimizar e controlar a forçagem da turbulência, e aplicamos essa metodologia ao modelos de turbulência de Obukhov e de Gledzer-Okhitani-Yamada.

Em segundo lugar, aplicamos o princípio máximo de Pontryagin ao modelo de camada hidrodinâmico contínuo de Obukhov a uma dimensão espacial restrita apenas a três camadas. Mostramos que muita informação pode ser extraída por simples raciocínio das condições do princípio máximo e, por outro lado, que esse esforço pode tornar-se incômodo e, portanto, há limites para o que pode ser alcançado de forma eficiente em termos de computação da solução para o problema de controle ótimo. A computação numérica de soluções para este problema de controle ótimo com base em um método de disparo de "força bruta" evidencia a existência de pontos de comutação no controle.

Por fim, apresentamos resultados e um algoritmo de controle conceptual tendo, por bases, o princípio do máximo de Pontryagin e um esquema do tipo de descida mais rápida para uma versão relaxada do problema original. Permitindo o relaxamento da condição inicial de forma a reescrever o problema com valores de fronteira como um com condições de limite no mesmo ponto inicial (ou final), provamos as propriedades chave deste algoritmo. Terminamos, mostrando alguns resultados numéricos, mas agora, usando algoritmos de otimização, de tipo semelhante, mas para o quais existe software disponível.

Palavras-chave: Palavras-chave: controle óptimo; Princípio do máximo; Algoritmos de controle óptimos; Modelos de Obukhov, GOY e Gledzer.

Acknowledgments

All appreciation and thanks to Allah who guided and helped me to achieve this thesis, and to all those who somehow contributed to the accomplishment of this PhD work.

First of all, I would like to express my most sincere gratitude to my supervisor, Prof. Sílvio Marques de Almeida Gama, Associate Professor in the Department of Mathematics (and CMUP) at the Faculty of Science (FCUP) and Director of the Doctoral Course in Applied Mathematics, University of Porto, Portugal and my co-supervisor Prof. Fernando Manuel Ferreira Lobo Pereira, Full Professor in the Department of Electrical and Computer Engineering (DEEC) of the Faculty of Engineering University of Porto (FEUP), and Coordinator of SYSTEC Portugal. I want to thank them primarily for accepting to jointly supervise this thesis, for their guidance, support, encouragement, accessibility, their remarks and comments during the meetings we held together, that helped me to understand the relevant concepts of the problem, and their friendship during my studies at the University of Porto. This thesis would not have been possible without their expertise.

I am grateful for the financial support given by Erasmus Mundus-Deusto University through the grant Erasmus Mundus Fatima Al Fihri Scholarship Program. Also, I am thankful to the Portuguese coordinator, Ana Paiva, and to all the Erasmus Mundus team in Porto.

The participation of the personnel of FEUP was partially supported by FCT R&D Unit SYSTEC - POCI-01-0145-FEDER-006933/SYSTEC funded by ERDF | COMPETE2020 | FCT/MEC | PT2020, and Project STRIDE - NORTE-01-0145-FEDER-000033, funded by ERDF | NORTE 2020.

The participation of the personnel of FCUP was partially supported by CMUP (UID/MAT/00144/2013), which is funded by FCT (Portugal) with national (MEC) and European structural funds (FEDER), under the partnership agreement PT2020, and Project STRIDE - NORTE-01-0145-FEDER-000033, funded by ERDF | NORTE 2020.

I thank some colleagues from the Mathematics Department of the University of Porto, especially Muhammad Ali Khan, Azizeh Nozad, Marcelo Trindade and Teresa Daniela Grilo, for their support and assistance on mathematical questions and valuable insights.

Special thanks go to those friends that gave me the right motivation at the right time and make me feel that I am not alone. In particular, Hossameldeen Ahmed, Hend Mysara and Ranya Al-Emam.

I am grateful as well to all my friends here in Porto and also in Egypt, for their support,

assistance, friendship over the past years, and for the entertainment that they provided to me. I would like to thank Lar Luísa Canavarro for their assistance in the last year who stood beside me as a family to finish this thesis. Specially, the sisters Maria Eduarda Viterbo, Leontina de Conceição Sousa, and all my friends there.

This humble effort is dedicated to my parents for their encouragement, support, and prayers for me, that always gave me strength in difficult times. I really thank you for the most important values you have given me, and I would like to thank my brothers, sister and all my family.

Last but no means the least, I cannot thank enough my beloved husband, Mohamed Soliman, for his love and encouragement that have stood beside me at all times, and who pushed me ahead with his unwavering faith. I would also like to acknowledge the most important persons in my life: my beloved daughter Hoor and my son Malek.

Finally, I express my humble apologies to those whom I might have forgotten to thank.

Contents

Chapter 1

Introduction

1.1 Objectives

This thesis concerns the important problem of fluid dynamics first considered by Kolmogorov to characterize the energy spectrum. The general objective is to investigate how the forcing, for appropriately chosen shell models, can be designed in order to obtain the scaling laws of the structure functions in an as efficient as possible manner. Thus, the general goal is of methodological nature, in the sense that it investigates approaches and tools that are better suited to, for given contexts, characterize the energy spectrum in fluid dynamics.

The goals of this thesis are the following:

a) Investigate alternatives to the traditional computationally intensive and time consuming numerical approaches by investigating two new methods for the computation of the optimal forcing associated with the energy cascade spectrum at the stationary regimen. These novel approaches to compute the optimal forcing to this problem were investigated along two directions:

   - Iterative optimization procedure in appropriate infinite dimensional spaces, and
   - Optimal control algorithms using the maximum principle of Pontryagin

   both seeking to minimize the distance to the target energy spectrum following the Kolmogorov's 1941 (K41) scaling laws for three-dimension, and the Kraichnan-Leith-Batchelor (KLB) scaling laws for two-dimension turbulence so that they are attained in a significantly more efficient way.

   For this purpose, the Obukhov shell model was considered. The optimization algorithm was of the steepest descent type in an infinite dimension space. The optimal control procedure based on the necessary conditions of optimality in the form of the Maximum Principle of Pontryagin and tailored to take advantage of the specific features of the dynamics of the controlled system.

b) Based on both frameworks constructed in a), the effect of the space-time structure of the forcing on the energy spectrum is investigated. Moreover, the effect of the forcing on the scaling properties of the energy spectrum in forced shell models of turbulence is studied.

1.2 General overview

In this section, we will introduce a brief review of fluid dynamics, turbulence, shell models of turbulence, and optimal control problems.

1.2.1 Fluid dynamics and turbulence

Fluid dynamics is considered one of the most relevant branches of applied sciences. It concerns the movement of liquids and gases, and how they are affected by forces. Water and air are the most important fluids which are present in many application areas that affect the human life. Most of mathematical, physical, biological, chemical, and astronomical investigations involving these fluids can be found in a wide range of key challenges such as designing models for weather forecast, climate change analysis, modeling ocean dynamics (currents, waves, etc.) that affect the spatial and evolution marine life, and both the oceanic and atmospheric weather, understanding volcanoes and earthquakes in geophysics, and for some important technological design applications such as air conditioning systems, wind turbines for electrical power production, and rocket engines, to name just a few.

In general, the flow represents the movement of liquids and gases, and reflect how fluids behave and how they interact with their surrounding environment, such as the moving of water over a surface or through a channel. It can be either steady or unsteady, laminar or turbulent, being the laminar flows smoother and the turbulent flows more chaotic.

Turbulent behavior in flowing fluids is one of the most interesting and important problems in all of classical physics. The problem of turbulence has been studied intensively by many mathematicians and engineers throughout the 19th and 20th centuries. However, we do not fully understand why or how turbulence occurs. There are a lot of definitions for turbulence but, in general, it refers to a complicated fluid motion which occurs in high speed flow over large length scales. There are countless examples of fluid flows in nature which are designated by turbulent. These include the water in the ocean, the air in the atmosphere, or even the rapid mixing of coffee and cream being stirred in a coffee cup. In spite of the huge difference of contexts, these flows share important features.

- They encompass a number of different scales of motion with entangled dynamics. The energy is always transferred among these scales in a complicated way. Even if the initial state of the flow includes only a few scales of motion, progressively,

an increasing number of scales will emerge, and the initially simple flow becomes a complicated turbulent flow.

- A change in a particular point of the flow can affect the flow far away from that point and this mean that there is a strong correlation between the flow points.

Moreover, turbulence has a lot of applications, including the turbulent motion occurring in the ocean on scales ranging from millimeters to hundreds of kilometers, and we can see how the turbulence varies, and transfers from one part of the ocean to another. For more details about its properties and how it is measured see, e.g., [142], and for interesting techniques and tools of measuring turbulence in the ocean which have been developed by various scientific - from geophysical to biological - oceanographic communities, see, e.g., [69]. It is important to note that simulation studies have been an important means of understanding these phenomena, notably, the dispersion of turbulence in the ocean. See, e.g., [70].

It is well known that the equations, the so called Navier-Stokes equations with suitable initial and boundary conditions, that describe turbulent flows have analytical solutions only in particular cases. In spite of the intense research effort during around two centuries, there are no general analytic solutions to these equations. For this reason, sophisticated numeric simulation tools emerged with the development of powerful computers. A lot of progress has been achieved in various engineering fields, like aerodynamics, hydrology, and weather forecasting, with the ability to perform extensive numerical calculations on computers, enabling the direct numerical solution of these equations even if only for relatively small problems with simple geometries. However, under some simplifying assumptions, one can make some predictions about the statistical properties of turbulent flows.

Richardson [129] described the turbulence phenomena, and Kolmogorov [91–93] developed the scaling theory. Their theoretical results were strongly corroborated by many experiments and observations. However, there are some observations which are not explainable by the Kolmogorov theory. These are due to deviations in the scaling exponents of the scaling of correlation functions. Moreover, except for the so-called four-fifth law, describing the scaling of a third order correlation function [61], the Kolmogorov theory is not based on the Navier-Stokes equation. This issue of the Kolmogorov theory will be raised later in this thesis.

1.2.2 Shell models

Shell models of turbulence were introduced by Obukhov [116], and Gledzer [75]. These models consist of a set of ordinary differential equations structurally similar to the spectral Navier-Stokes equations, but they are much simpler and numerically much easier to investigate than the Navier-Stokes equations. For these models, a scaling theory identical to the Kolmogorov theory has been developed, and they show the same kind of deviation

from the Kolmogorov scaling as real turbulent systems do. Thus, understanding the behavior of shell models will provide an important insight for the understanding of systems governed by the Navier-Stokes equations. The shell models are constructed to obey the same conservation laws and symmetries as the Navier-Stokes equations. Besides energy conservation, these models exhibit the conservation of a second quantity which can be identified with helicity or enstrophy that depends on a free parameter. This second quantity reveals whether the models are either 3D or 2D turbulence-like depending on whether either helicity or enstrophy is conserved. Thus, it is not surprising the abundance of works investigating shell models. For references, check, e.g., [26], [105], [103], [87]).

1.2.3 Optimal control

Optimal Control emerged essentially by the end of the first half of the 20^{th} century and can be regarded as a certain extension of the much older field of Calculus of Variations. The general optimal control problem formulation consists in the minimization of a cost functional on a given space subject to, at least, a differential or integral constraint, and possibly other type of "static" constraints on the so called state, and control variables, or jointly on both. Although the differential or integral constraint might be of any type, the most common ones - for which the theory is also more developed - are ordinary and partial differential equations. A feature that sets apart optimal control from calculus of variations in the differential context is that the function specifying the derivative of the state variable that depends on the control variable to steer its evolution takes values on a closed set.

Due to the large versatility of its formulation, it is not surprising that Optimal Control Problem (OCP) paradigm has been used in a wide range of applications arising in many different fields in real life problems. This spans:

- Engineering - see, e.g., [33], [160],
- Resource allocation and management - see, e.g., [47], [134],
- Biology - see, e.g., [23], [79], [86], [99],
- Medicine - see, e.g., [2], [139],
- Ecology - see, e.g., [53], [78],
- Economics - see e.g., [134], [160],
- Finance - see e.g., [46], [57], and
- Fluid dynamic - turbulence, climate, atmosphere) studies - see e.g., [137],[143], [3], [64], [114], [138], [25],

to name just a few.

These days, we have at our disposal a rich body of theory that spans a wide range of issues pertinent to address many practical challenges arising when solving real-life problems. The credits for the initiation of these developments are due essentially to the pioneering work of Pontryagin and his team [126], in which a wide range of OCPs have been considered, notably, state constraints, discrete-time and the sophisticated concept of relaxed solution had already been exploited, conventional optimal control theory went over the years through extremely-complicated developments, in which the assumptions of the problem were strongly weakened. Many diverse formulations and issues, such as posedness, nonsmoothness, sensitivity, and non-degeneracy, to name just a few, have, since then, been considered by a large number of authors. For references on these works, you may consider the relatively recent publications [148], [48], [50], [121], [6], and [17].

1.3 Contributions

The contributions of this thesis can be directly mapped in the proposed objectives. More precisely, results and algorithms for two different optimization approaches that exhibit a performance superior to the numerical experimentation carried out to corroborate Kolmogorov's 1941 (K41), and Kraichnan-Leith-Batchelor (KLB) scaling laws, respectively, for three-dimension and for two-dimension turbulence. These constributions involve the following:

i) Iterative optimization procedure of the steepest descent direction in appropriate infinite dimensional spaces in the context of the Obukhov model. This involves the explicit specification of the appropriate operators which are here derived for the first time.

ii) An original optimal control algorithm using necessary conditions of optimality in the form of the maximum principle of Pontryagin again using the Obukhov model as the controlled dynamic system. In this effort, there is the development of a conceptual algorithm involving an extended version of the optimization that allows the relaxation of the initial condition in order to improve the rate of convergence. Various results concerning the properties of the relaxed problem and required for the proof of convergence are also produced.

1.4 Organization

This thesis is organized as follows:

- In chapter 2, we list a number of important challenges for which the results of this thesis are relevant. Given the extremely wide range of possibilities, we decide to select one that is specially remarkable not only for its complexity but also for its huge role

in the future of our planet and, as consequence, for human kind: climate and weather. We present the context of relevance and provide some insight on how our results can impact in studies advancing knowledge, and, as a consequence, improved models, as well as, in supporting tools for short and long term forecasting methods.

- Chapter 3, we present some preliminary concepts and definitions, as well as a brief review of Navier-Stokes equations, Kolmogorov's 1941 theory (K41), The Kraichnan-Leith-Batchelor theory (KLB), shell models, and an overview of conventional optimal-control theory.

- In Chapter 4, we introduce our formulation of the control problem for shell models of turbulence, where we study four examples of shell models, continues with the some remarks about the computational method we use to solve the equations.

- In Chapter 5, we present our formulation of a simple optimal control model in which the dynamics are given by Obukhov shell model with dimension $N = 3$. This is a simple toy model that serves as basis to easily test the effectiveness of the approach. We characterize the set of candidates to the solution - optimal forcing which will be associated with the distributed energy over the spectrum as predicted by K41 model whose dynamics is given by Obukhov shell model - via the necessary conditions of optimality in the form of Pontryagin maximum principle.

  This chapter is organized in three distinct phases. In the first one, we attempt to derive the solution to the optimal control problem by using methods of mathematical analysis and we rapidly conclude that only very simple general cases - in fact two - can be solved. Then, in the second phase, we use "brute force" shooting methods to numerically compute the solution to the two point boundary value problem associated to the application of the maximum principle. This approach proved to be computationally heavy and not scalable.

  This led to the third phase that consisted in designing a conceptual optimal control algorithm based on the maximum principle and of the steepest descent type for a relaxed version of the original problem. Key properties of this algorithm were proved. Then, some results were obtained by using an optimization algorithm of the same type for which off-the-shelf routines taking into account the numerical issues, which are always tricky for infinite dimensional problems. In this process, we conclude that this last approach is much more efficient and scalable. Moreover, we also concluded for the problem at hand that the impact of the relaxation procedure initially considered was not relevant.

- In Chapter 6, we present the key conclusions of this effort and outline perspectives for future directions.

Chapter 2

Motivation

2.1 Introduction

Fluid dynamics plays an important role in our daily lives and is one of the keys to address critical challenges that human kind is facing today. It is surprising the extent to which the motion of gases and liquids and their interactions with surrounding environment, specially the air in the atmosphere and water in rivers, lakes and oceans, affect life on planet earth.

Moreover, fluid dynamics is nuclear to the understanding of phenomena arising in key areas: climate change in climatology, weather forecasting in meteorology, studies in energy, astrophysics, medicine, biology, chemistry, electronics, communications, and mobility, to name just some of the more general areas. It is worth remarking that the challenges underlying climate changes constitute one of the most relevant scientific problems and, possibly, the greatest challenge that human kind is facing. Significant disruption of current weather patterns will translate into intense natural disasters with very significant damages in the current human made infra-structures. This naturally will affect virtually all economic sectors leading to social and financial instabilities, and, eventually to the demise of human societies as we know them today. Thus, a better understanding of the wealth of phenomena of the climate system is key in order to define policies enabling the mitigation of the negative impacts that future changes in the climate will have in human societies.

In one way or another, the challenges in all these areas involve the need to solve fluid dynamics equations in order to support the design of the associated systems. However, the governing Navier-Stokes equations have no general analytic solutions. This explains the huge effort in the investigation of the required mathematical models by using sophisticated numerical solutions.

2.2 Weather and climate

The weather is the atmospheric condition at a particular time and place and, usually, its state depends on the type and motion of air masses. The characteristics of the air masses and the interactions between them can either keep the weather constant on a given area or make it change rapidly. The state of the weather depends on air temperature, atmospheric pressure, fog, cloud cover, humidity (the amount of water contained in the atmosphere), wind velocity, and precipitation (rain, snow, sleet, and hail). All these features are related to the amount of energy (heat) in the system (atmosphere) and how it is distributed. In addition, because this energy varies with location above the Earth's surface, and differing in different parts of the atmosphere. Thus, weather is always changing in a dynamic and complex manner.

On the other hand, climate change is assessed by the change of the average weather state in a given region over time. Thus, statistical information about the mean and variability of relevant quantities is needed in order to determine the nature and extent of climate change. A number of factors, such as the angle of the Sun, air pressure and cloud cover, heat stored in the water bodies, among others, enable the determination of the amount of energy in a given region. This data fed into appropriate models allow the prediction of how the climate in the given region will change.

Thus, the use of numerical models is considered of vital importance and plays a major role in predicting both the weather and climate change trends. Indeed, the basic ideas of weather forecasting and climate modeling were developed about one century ago (see, e.g., [125], [106]). However, the observations were irregular, and, as a result, it makes the weather forecasting imprecise, particularly over the ocean and air upper layers. By the same token, the fluid mechanics represent the set of basic physical principles that govern flows in the atmosphere and in the ocean. For example, the first mathematical approach to forecasting has been proposed by Abbe [1], and Bjerknes [27] employed a graphical approach for solving the fluid dynamics equations describing the state of the atmosphere some hours later.

Richardson [129] was the pioneer of numerical weather prediction. He was the first one to use finite difference methods to get a direct solution to the equations of motion. The quasi-geostrophic vorticity system has been developed by Charney, and it consists in a set of equations to compute large-scale motions of planetary-scale waves. Moreover, he developed a theory to produce accurate prediction of the atmospheric flow (see, e.g., [42], [43], [45], [44]). The rapid progress in computing technologies enabled more sophisticated numerical weather predictions leading to significant improvements in many aspects of forecast operations, and of the used models which became increasingly deendent on the numerical solution of the Navier-Stokes equations and of the thermal energy equation (see, e.g., [41], [124], [136]). Moreover, these computational capabilities also enable the consideration of probabilistic models and the production of forecasts for a wide range of

weather events. Sophisticated modeling and forecast approaches have been in use in major operational centers such as, the European Center for Medium-Range Weather Forecasts, National Center for Environmental Prediction, National Center for atmospheric Research, and Max Plank Institute for Meteorology.

In simple words, the simulation of the fluid dynamics equations in the atmosphere constitute the key issue. However, vital problem in the use of these equations is the need of accurate values for the associated parameters in order to corroborate phenomenologies of interest such as heat exchange, surface-water exchange, soil and vegetation, moisture, precipitation, evaporation, and small-scales processes (see, e.g., [135], [158]).

2.3 Weather and climate modeling

As we mentioned above, the simulation and prediction of the atmospheric phenomena with computer models by using numerical methods means that we can model the weather and forecast how it may evolve over a period of time. There are many weather and climate models.

- Troposphere models. The troposphere is the lowest layer of the atmosphere in which most of the phenomena weather occur. It contains most of the atmospheric moisture, and, when the temperature decreases, the warm air near the surface of the earth will rise and, as a result, we have a convection of air causing clouds, typically leading to rain (see, e.g., [122], [34], [123]).

- Barotropic models. These models are based on a quasi-geostrophic system, which is derived from Euler equations of motion and consider short-range prediction models (see, e.g., [24], [131], [38]).

- Baroclinic models. These models concern large vertical temperature gradients in the troposphere that lead to the convection in air currents transporting energy to the high layers with cooler air. This induces instability in the atmosphere, which is said to be baroclinic (see, e.g., [58], [111]).

- Primitive equation models. These models depend on Navier-Stokes equations and thermal energy equation. They simulate the energy and the dynamics of the atmosphere (see, e.g., [81], [124], [106]).

Now, to model the climate, one should has to take into account the interactions of air masses, energy, water, and momentum [133], since large-scale phenomena are generated from the interaction of small-scale physical systems. These models are used to study the dynamics of the climate system, and to generate predictions of its evolution. There are many phenomena that contribute to change the climate such as, the ocean circulation, the

atmospheric chemistry, the global carbon cycle, El Niño, La Niña, volcanic eruptions and greenhouse effects, among others.

In spite of all the intensive studies and models in weather and climate change that have been made until now, we still can not have a great forecasts accuracy, because they depend on initial state errors and on the model accuracy. Moreover, due to the non-linearity of the equations, information on the initial conditions is not of interest after a few days, and, as a result, the exact state of the weather system is not predictable. Accordingly, it is impossible to observe all the atmosphere's initial state details and create an accurate forecast system (see, e.g., [108]).

2.4 Turbulence and climate

The movement of air (atmosphere) and water (ocean) can be laminar or turbulent, where the turbulent behavior characterized by chaotic changes in flow velocity and pressure and represent an important unsolved problem of classical physics. Sergei S. Zilitinkevich said "Turbulence is the key to the atmospheric machine", and we can never understand the weather systems without knowing the interaction between their multiple components in the atmosphere. In engineering applications, we can understand turbulence by using statistical methods, but for turbulence in weather and climate, these methods are difficult, because in the atmosphere and in the ocean, the density of the medium changes with the altitude and this leads to convection, instability, and stratification.

Turbulence in the atmosphere represents irregular air motions characterized by winds that alter its direction and speed. In simple words, this phenomenon is important, because it mixes the atmosphere and causes smoke, water vapor, and energy. Moreover, turbulence plays an important role in the air-sea heat fluxes, and momentum which has an essential role in weather, global climate, ocean and atmosphere studies (see, e.g., [132], [147]).

There are some simulations emphasizing the applications of the turbulence-resolving modeling with large-eddy simulation numerical technique to planetary boundary layer research, and climate studies. The large-eddy simulation is considered very useful in the understanding of the ocean and atmospheric turbulence (see, e.g., [63]). In addition, there are many contributions to the study of atmospheric turbulence and diffusion (see, e.g., [112], [72], [83]).

It is worth to mention that most of the turbulent properties can be associated with the turbulent energy dissipation rate, and this considers a very important parameter in the design of chemical processing equipment. In order to develop a better chemical processing equipment design, we should have the knowledge of the effect flow structure on local turbulence parameters like turbulent kinetic energy, energy dissipation rate, and the eddy diffusivity (see, e.g., [84], [141], [146]).

2.5 Energy transfer in turbulence

Energy cascade mean that the energy is transferred from the large scales to the smaller scales until it reaches scales sufficiently small where the viscosity dissipates the energy into internal energy of the fluid. There is a range of scales between the large scales and small scales, the so-called inertial subrange [91–93]. The distribution of the energy of turbulence over the scales has been described in terms of Fourier analysis, where the velocity field u is expressed as a Fourier series

$$u(x) = \sum_{k} \hat{u}(k) e^{ikx} \,. \tag{2.1}$$

The energy spectrum

$$E(k) = \frac{1}{2} \sum_{k \leq \ell < k+1} \hat{u}(\ell) \hat{u}(\ell)^* \,, \tag{2.2}$$

where (*) denotes to the complex conjugate, gives the distribution of energy among turbulence vortices in terms of wavenumber, k. Kolmogorov derived a formula for the energy spectrum and founded the field of mathematical analysis of turbulence. He found that, in the inertial subrange, the effects of molecular and external forcing are negligible, and the energy cascades to the smaller scales due to the quadratic nonlinearities. At these small scales, the energy transfer rate must balance the energy dissipative rate. Therefore, the energy spectrum $E(k)$, for three dimensions, depends only on the energy dissipation rate, ϵ, and wavenumber, k, and it must have the form

$$E(k) = C\, \epsilon^{2/3}\, k^{-5/3} \,, \tag{2.3}$$

where C is the Kolmogorov constant.

Moreover, the success of Kolmogorov theory for three dimension turbulence encouraged the scientists to adapt it for two dimensional. Kraichnan [95], Leith [98], and Batchelor [21] (KLB) were the first pioneers to study two dimension turbulence, where they assumed an analogous theory for (statistically) isotropic, homogeneous and stationary two-dimensional forced turbulence. The KLB theory proposes the existence of inertial ranges: (i) one for the energy $E(k)$, which depends on the energy dissipation ϵ and the wavenumber k, and (ii) the other range for the enstrophy, which depends on the enstrophy dissipation η and k, where the effects of external forcing and viscosity are negligible. Then, they derived the scaling laws $E(k) \propto k^{-5/3}$ in the energy inertial range, and $E(k) \propto k^{-3}$ in the enstrophy inertial range.

2.6 Motivation of this work

In this thesis, we propose to introduce the necessary mathematical methodology in order to control the energy cascades in the shell models of turbulence. Shell models are a kind

of Navier-Stokes equations of the poor, in the sense that they only share the same form of non-linearity and dissipation terms. In fact, the phenomenology developed by Kolmogorov and his followers, proven experimentally and numerically within certain limits, is strongly based on the form of the Navier-Stokes equations.

Years later, researchers raised the question of whether Kolmogorov's phenomenology would be successful for other equations that had the same structural form as the Navier-Stokes equations. This is how the shell models of turbulence, inspired by Obukhov's works, came about. The reached conclusions show that Kolmogorov's phenomenology (and its adaptations to other spatial dimensions) depends, in essence, on the structural form of the equations.

The cascades of energy that are observed in the shell models of turbulence, or more generally, the scaling laws of the structure functions, require intensive numerical integrations that take extremely long computing time. The purpose of this thesis is to seek alternative approaches that are computationally effective in tuning shell models forcing terms in order to obtain the sought after scaling laws of the structure functions.

Chapter 3

State-of-the-art

In this chapter, we will present a brief review of Navier-Stokes equations, shell models of turbulence and optimal-control theory, which are relevant for the research developed in the thesis. Moreover, this overview will be also helpful to appreciate the added value of this thesis with respect to the state-of-art.

3.1 Preliminary concepts and definitions

There is no good definition of turbulence. Among the various attempts to achieve this goal (see, e.g., T. von Kármán [150], Hinze [82], Chapman and Tobak [40]), probably the most cited and consensual definition is due to Richardson [129]: "Big whorls have little whorls, which feed on their velocity, and little whorls have lesser whorls, and so on to viscosity".

This definition describes the physical concept that energy injected into a flow, at some large scale, is transferred from the larger to smaller scales (energy cascade) until it is finally dissipated by molecular viscosity. This describes that the turbulence deals with two physical phenomena simultaneously: diffusion and dissipation of kinetic energy.

The study of turbulent fluids is a tangle that involves several physical features including (i) chaotic and disorganized structures, (ii) very large range of space and time scales, (iii) diffusion (mixing) and dissipation, (iv) sensitivity to the initial conditions and nonrepeatability, and (v) intermittency in both space and time.

One of the major steps in the analysis of turbulence was taken by G. I. Taylor during the 1930s. He was the first one to use statistical methods involving correlations, Fourier transforms and power spectra to analyse fluids. In his 1935 paper [140], he presents the assumption that turbulence is a random phenomenon, and, then, proceeds to introduce statistical tools for the analysis of stationary, homogeneous and isotropic turbulence. A further contribution, especially valuable for analysis of experimental data, was the introduction of the Taylor hypothesis, which provides a means of converting temporal

data to spatial data (in von Kármán [153], von Kármán and Howarth [152], and Weiner [155], the reader can find other scientific advances dring this period of time in this domain).

In the 40s of last century, the ideas of Landau and Hopf on the transition to turbulence became popular, and there were numerous additional contributions to the study of turbulence (see, e.g., Batchelor [22], Burgers [37], Corrsin [56], Heisenberg [80], von Kármán [151], Obukhov [115] and Townsend [144], and the first full-length books on turbulence theory began to appear in the 1950s. In addition, in 1941, A. N. Kolmogorov published three papers [91–93] that provide some of the most important results of turbulence theory, in particular, the so-called K41 theory.

Two decades later, new directions were taken in the attack of the turbulence closure problem (existence of more unknowns than equations). There was also significant progress in experimental studies of turbulence during the 1960s. Efforts were made to address aspects of turbulence such as decay rates of isotropic turbulence, return to isotropy of homogeneous anisotropic turbulence, boundary layer transitions, transition to turbulence in pipes and ducts, effects of turbulence on scalar transport, etc. These include the works of Comte-Bellot and Corrsin [54] on return to isotropy, Tucker and Reynolds [145] on effects of plain strain, Wygnanski and Fiedler [157] on boundary layer transition, Gibson [71] on turbulent transport of passive scalars, and Lumley and Newman [102], also on return to isotropy. Also, particular attention was devoted to wall-bounded shear flows, flow over and behind cylinders and spheres, jets, plumes, etc. (Blackwelder and Kovasznay [28], Antonia et al. [4], Reynolds and Hussain [128], Wood and Bradshaw [156]).

In 1971, Ruelle and Takens [130] present the sequence of transitions (bifurcations) that a flow undergoes through (steady $\rightarrow$ periodic $\rightarrow$ quasiperiodic $\rightarrow$ turbulent), as the Reynolds number, Re, increases. One decade later, the Ruelle transitions were observed in many experimental results.

From the viewpoint of present-day turbulence investigations, probably the most important advances of the 1970s and 80s were due to the computational techniques. One of the first of theses techniques was the large-eddy simulation (LES), proposed by Deardorff [59] in 1970. This was rapidly followed by the first direct numerical simulation (DNS) by Orszag and Patterson [118] in 1972, and the introduction of a wide range of Reynolds-averaged Navier-Stokes (RANS) approaches (see, e.g., Launder and Spalding [96] and Launder et al. [97]).

Turbulent motions occur over a wide range of length and time scales, creating difficulties in the analysis of turbulent flow.

Turbulent length scales. Let us consider the range of length scales (eddy sizes) that one may expect to observe in turbulent flows. Let L be the size of the largest eddies in the flow, and η the size of the smallest eddies. The sizes of these eddies are constrained by the physical boundaries of the flow, e.g., boundary layer, depth, etc. Now, we will refer to L as the integral length scale for the energy-containing eddies. The size of the smallest

scales of the flow is determined by the viscosity, where the smallest length scales act in the turbulent flow and are those where the kinetic energy is dissipated into heat. For the very high Reynolds number flows, the viscous forces become small with respect to the inertial forces. Smaller scales of motion are, then, necessarily generated until the effects of viscosity become important and energy is dissipated.

For a statistically steady turbulent flow, the energy dissipated at the small scales must be equal to the energy supplied by the large scales. Now, let us form a length scale based only on the energy flux, ϵ, and viscosity, ν. Then, from dimensional analysis, the dissipative length scale is:

$$\eta \sim \left(\frac{\nu^3}{\epsilon}\right)^{1/4} . \tag{3.1}$$

This is the so-called Kolmogorov length scale and is the smallest hydrodynamic scale in turbulent flow. Now, to relate this length scale to the largest length scales in the flow, we need an estimation for the dissipation rate in terms of the large scale flow features. Since the energy flux is equal to the kinetic energy production rate, the kinetic energy of the flow is proportional to U^2 over the inverse of the time scale of the large eddies L/U. In other words,

$$\epsilon \sim \frac{U^2}{L/U} \sim \frac{U^3}{L} . \tag{3.2}$$

Substituting in (3.1), we obtain

$$\eta \sim \left(\frac{\nu^3 L}{U^3}\right)^{1/4} . \tag{3.3}$$

We can see from these estimations that the energy flux does not depend on the viscosity. Viscosity serves only to determine the dissipation length scale. The ratio of the largest to smallest length scales in the flow is:

$$\frac{L}{\eta} \sim \left(\frac{UL}{\nu}\right)^{3/4} = Re^{3/4}, \tag{3.4}$$

where Re is the Reynolds number. Thus, the separation of the largest and smallest length scales increases as the Reynolds number increases.

Another typical length scale in turbulence is the Taylor microscale for the inertial subrange eddies, λ, defined by:

$$\left(\frac{\partial u'}{\partial x}\right)^2 = \frac{u'^2}{\lambda^2} , \tag{3.5}$$

where

$$u' = \left\langle (u - \bar{u})^2 \right\rangle^{1/2}$$

is the root mean square of the fluctuating velocity field. Sometimes the Taylor microscale,

called turbulence length scale, because it is related to the turbulent fluctuation. The turbulent Reynolds number is defined by

$$Re_\lambda = u'\lambda/\nu \ .$$

Summarizing, the main scales in a turbulent flow are:

i) the largest length scales, usually imposed by the flow geometry. Because turbulence kinetic energy is extracted from the mean flow at the largest scales, they are often referred to as the "energy-containing" range;

ii) the integral scale;

iii) the Taylor microscale which is an intermediate scale for which turbulence kinetic energy is neither generated nor destroyed, but is transferred from larger to smaller scales, basically corresponding to Kolmogorov's inertial subrange; and

iv) the Kolmogorov (or dissipative) scales which are the smallest scales present in the fluid.

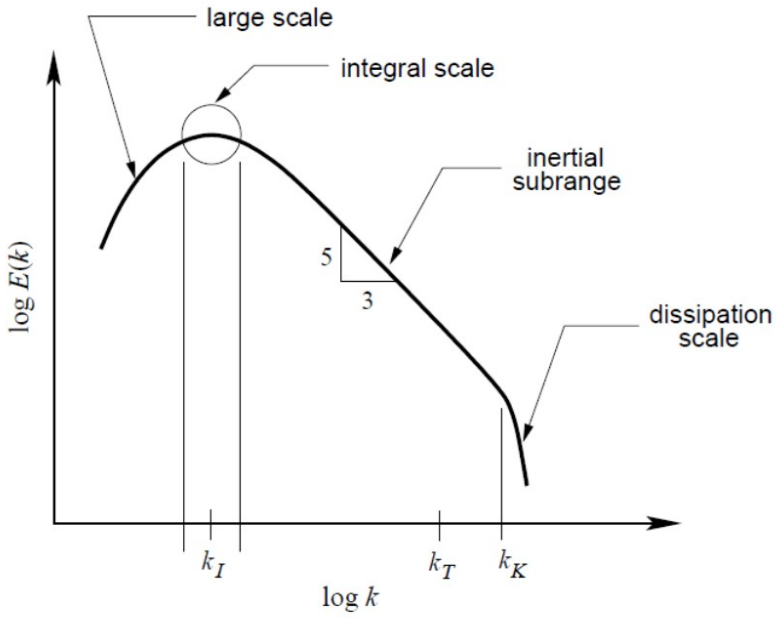

Figure 3.1: Energy spectrum of turbulence.

The Figure 3.1 displays the main details of energy cascade corresponding to $Re \gg 1$. The wavenumbers corresponding to the dissipative scales are strongly influenced by Re. Thus, the wavenumber range covered by the inertial scales must increase with increasing Re.

Time scales. The large eddy turnover time is defined by

$$t_L = \frac{L}{U}\,. \tag{3.6}$$

We can also generate a time scale for the small eddies using the viscosity and the dissipation:

$$t_\eta = \left(\frac{\nu}{\epsilon}\right)^{1/2}\,. \tag{3.7}$$

By using the scaling for the energy flux, we have

$$t_\eta = \left(\frac{\nu L}{U^3}\right)^{1/2}\,. \tag{3.8}$$

Thus, the ratio of these time scales is

$$\frac{t_L}{t_\eta} = \left(\frac{UL}{\nu}\right)^{1/2} = Re_L^{1/2}\,. \tag{3.9}$$

The large scale structures in the flow are seen to have a much larger time scale than the smallest energy dissipating eddies. Thus, as the Reynolds number of the flow increases, the magnitude of the separation between both time and length scales increases.

3.2 The Navier-Stokes equations

The Navier-Stokes equations, which are now almost widely believed to embody the physics of all fluid flows, including turbulent ones, were introduced in the early to mid 19th Century by Claude-Louis Navier and George Gabriel Stokes. These equations are used to model the ocean currents, the weather, the air flow around a wing, the water in a pipe, etc..

The Eulerian velocity of the fluid parcel with position $\boldsymbol{x} = (x, y, z)$, or (x_1, x_2, x_3), is denoted $\boldsymbol{u}(\boldsymbol{x}, t) = (u(\boldsymbol{x}, t), v(\boldsymbol{x}, t), w(\boldsymbol{x}, t))$, or $\boldsymbol{u}(\boldsymbol{x}, t) = (u_1(\boldsymbol{x}, t), u_2(\boldsymbol{x}, t), u_3(\boldsymbol{x}, t))$. The motion of this fluid parcel is due to the advection, pressure, viscosity, and external forces. The change in the momentum per unit volume is

$$\frac{\partial(\rho \boldsymbol{u})}{\partial t} = \sum (\text{Forces per unit volume})\,, \tag{3.10}$$

where ρ is the density of the fluid and the right-hand side is a sum over the advection, pressure, viscous effects, and external forces. For incompressible flows the density is constant. The advective force can be represented via the Lagrangian derivative

$$\frac{\partial \boldsymbol{u}}{\partial t} + \boldsymbol{u} \cdot \nabla \boldsymbol{u}\,, \tag{3.11}$$

and represents how the fluid parcel reacts to the motion of fluid parcels in its neighborhood in absence of other forces. Here, $\nabla = \left(\frac{\partial}{\partial x}, \frac{\partial}{\partial y}, \frac{\partial}{\partial z}\right)$ is the gradient differential operator.

By combining all the forces and assuming that the fluid is incompressible, the incompressible Navier-Stokes equations read:

$$\frac{\partial \boldsymbol{u}}{\partial t} + \boldsymbol{u} \cdot \nabla \boldsymbol{u} = -\frac{1}{\rho}\nabla P + \nu \nabla^2 \boldsymbol{u} + \boldsymbol{F}\,, \tag{3.12a}$$

$$\nabla \cdot \boldsymbol{u} = 0\,. \tag{3.12b}$$

The incompressible Navier-Stokes equations conserve the energy, when both the forcing and viscosity are zero. The energy is defined by

$$E = \frac{1}{2}\int_\Omega |\boldsymbol{u}(\boldsymbol{x},t)|^2 d\boldsymbol{x}\,, \tag{3.13}$$

where Ω is the physical domain of the fluid. Let us prove that energy is indeed conserved for the case where the boundary conditions are periodic and the velocity is continuous. By taking the time derivative of the energy with respect to time, we obtain

$$\begin{aligned}
\frac{dE}{dt} &= \frac{1}{2}\frac{d}{dt}\int_\Omega |\boldsymbol{u}(\boldsymbol{x},t)|^2 d\boldsymbol{x} \\
&= \int_\Omega \boldsymbol{u} \cdot \frac{\partial \boldsymbol{u}}{\partial t} d\boldsymbol{x} \\
&= \int_\Omega \boldsymbol{u} \cdot (-\boldsymbol{u} \cdot \nabla \boldsymbol{u} - \nabla P) d\boldsymbol{x} \\
&= -\int_\Omega \boldsymbol{u} \cdot \nabla \left(\frac{|u|^2}{2} + P \right) d\boldsymbol{x} \\
&= -\int_\Omega \nabla \cdot \boldsymbol{u} \left(\frac{|u|^2}{2} + P \right) d\boldsymbol{x} \\
&= 0\,,
\end{aligned}$$

where we have used $\nabla \cdot \boldsymbol{u} = 0$. In three dimensions, the Navier-Stokes equations have another non-trivial invariant, called helicity, defined by

$$H = \frac{1}{2}\int_\Omega \boldsymbol{u} \cdot (\nabla \times \boldsymbol{u}) d\boldsymbol{x}\,. \tag{3.14}$$

If $\boldsymbol{F} = 0$, then

$$\frac{dH}{dt} = \nu \int_\Omega \boldsymbol{\omega} \cdot (\nabla \times \boldsymbol{\omega}) d\boldsymbol{x}\,. \tag{3.15}$$

In two dimensions, the helicity is trivially conserved, since $\boldsymbol{\omega}$ and $\boldsymbol{u}$ are perpendicular, and thus H is constant. Also in two dimensions, if $\nu = 0$, the flow conserves the enstrophy, which is defined by

$$Z = \frac{1}{2}\int_\Omega |\boldsymbol{\omega}|^2 d\boldsymbol{x}\,. \tag{3.16}$$

Indeed,

$$\frac{dZ}{dt} = \frac{1}{2}\frac{d}{dt}\int_\Omega |\boldsymbol{\omega}|^2 d\boldsymbol{x}$$

$$
\begin{aligned}
&= \int_\Omega \boldsymbol{\omega} \cdot \frac{\partial \boldsymbol{\omega}}{\partial t} d\boldsymbol{x} \\
&= \int_\Omega \boldsymbol{\omega} \cdot (-\boldsymbol{u} \cdot \nabla) \boldsymbol{\omega} d\boldsymbol{x} \\
&= \int_\Omega (\nabla \cdot \boldsymbol{u}) \frac{|\boldsymbol{\omega}|^2}{2} d\boldsymbol{x} \\
&= 0\,,
\end{aligned}
$$

since $\nabla \cdot \boldsymbol{u} = 0$. Note that the enstrophy is positive-definite quantity.

3.3 Kolmogorov's 1941 theory (K41)

In 1941, Kolmogorov proposed a statistical theory for statistically isotropic, homogeneous and stationary three-dimensional incompressible turbulence [91–93] (see Frisch [68] for a more recent reading on this subject). Kolmogorov considered the transfer of energy between scales to be a cascade, where the energy moves from larger scales to smaller scales through intermediate scales. The viscous term in the Navier-Stokes equations is usually active at the small scales, where it acts to remove energy, while energy injection (via forcing) is restricted to large scales.

In statistically steady three-dimensional turbulence, the energy is transferred by the nonlinear (advective) term from the large scales to the small scales. The region of Fourier space in which this energy transfer takes place, in the absence of forcing and dissipation, is called the inertial range. Kolmogorov showed that the energy spectrum in the inertial range is

$$
E(k) \sim \varepsilon^{2/3} k^{-5/3}\,, \tag{3.17}
$$

where ε is the energy dissipation rate.

3.4 The Kraichnan-Leith-Batchelor theory (KLB)

The Kolmogorov's concept of a downscale energy cascade in three dimensions (3D) turbulence inspired the researchers to adapt the theory to two dimensions (2D) turbulence. Indeed, Kolmogorov's theory does not apply directly to 2D flow, since the 2D flow dynamics are different from 3D flow ones, due to(i) the enstrophy conservation in 2D, and (ii) the vortex stretching which plays a key role in the energy transfer between scales in 3D, and it is absent in 2D.

Kraichnan [95], Leith [98], and Batchelor [21] (KLB) were the first to study the 2D turbulence. Their work has contributed to the development of an analogous theory for homogeneous, isotropic and statistically stationary 2D forced turbulence. They have discovered the phenomenon known as an inverse cascade of energy. In other words, they proposed that in 2D turbulence there is an upscale energy cascade and a downscale

enstrophy cascade, where the effects of the viscosity and the external forces are negligible, respectively, when the force injects energy and enstrophy in a narrow band of intermediate length scales.

By assuming that the energy flows upscale and the enstrophy flows downscale, the KLB dimensional analysis argument gives

$$E(k) \sim \epsilon^{2/3} k^{-5/3}\,, \tag{3.18}$$

and,in the downscale enstrophy range, namely direct or forward cascade, is

$$E(k) \sim \beta^{2/3} k^{-3}\,, \tag{3.19}$$

where ϵ and β are the energy dissipation rate, and the enstrophy dissipation rate, respectively. In the KLB idealization, there is only a single flux in each inertial range: a pure energy upscale cascade on the upscale side of injection, and a pure downscale enstrophy cascade on the downscale side of injection (see Fig. 3.2). This situation is called the dual-pure cascade.

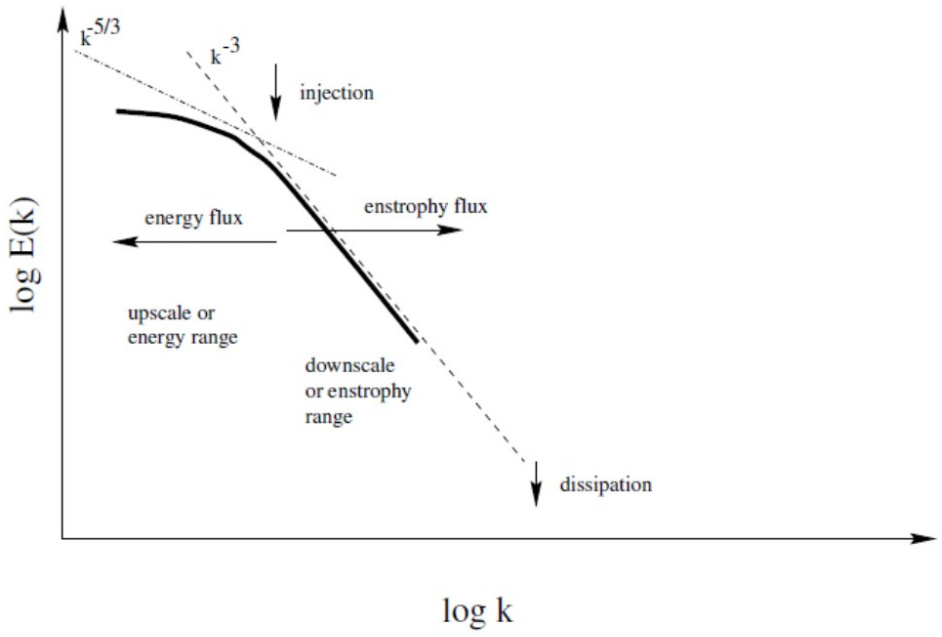

Figure 3.2: The Kraichnan-Leith-Batchelor (KLB) scenario of a dual-pure cascade. There is a pure energy upscale cascade upscale and a pure downscale enstrophy cascade.

In addition, the idea of a dual cascade was first suggested by Fjørtoft [66], who naively showed that in a 2D incompressible Navier-Stokes flow the energy is transferred to larger scales, while the enstrophy is transferred to smaller scales. This so-called dual cascade is quite different from the 3D case where the energy cascades down to smaller scales in the

inertial range. A later study by Merilees and Warn [107] has provided more quantitative detail.

Many numerical and laboratory experiments have been performed in attempting to test the KLB theory (see, e.g., [100], [119], [30], [90], [29] and [35]). These studies confirm the general setting of the theory. Each of the cascades have been observed independently with the predicted slopes. However, there is a controversy. The KLB theory predicts that if enough energy and enstrophy are injected into the system these dual cascades (i.e. inverse cascade of energy and direct or forward cascade of enstrophy) must be realizable simultaneously in a statistically stationary state. (Indeed, the inverse cascade of energy can be only quasi-stationary in an infinite domain since the energy is transferred to ever larger scales.)

Some attempts have been made to explain this departure from the KLB theory. First, it should be noted that while the KLB theory assumes unbounded domains the numerical and laboratory experiments are necessarily performed on bounded domains. Kraichnan [95] pointed out from the very beginning that this may affect the results of the experiments since the energy transferred by the inverse cascade accumulates in the largest available scales. This problem is avoided by adding a friction-type dissipation to remove energy at the largest scales. This type of dissipation, usually called Rayleigh friction, is natural in atmospheric flow because of the friction between flow and the earth's surface [20].

3.5 The spectral Navier-Stokes equations

The spectral Navier-Stokes equations are obtained by performing the Fourier transform on the incompressible Navier-Stokes equations (3.12). Consider the Fourier transform $\boldsymbol{u_k}$ of $\boldsymbol{u}(\boldsymbol{x})$ (the velocity field is 2π-periodic in each space direction),

$$\boldsymbol{u_k} = \frac{1}{(2\pi)^3} \int_B \boldsymbol{u}(\boldsymbol{x})\, e^{-i\boldsymbol{k}\cdot\boldsymbol{x}} d\boldsymbol{x}\,, \tag{3.20}$$

where $\boldsymbol{k}$ is the wavevector for the mode with complex amplitude $\boldsymbol{u_k}$, and $B = [0, 2\pi]^3$. Since $\boldsymbol{u}(\cdot)$ is real-valued, the Fourier-transformed data is Hermitian symmetric, i.e.

$$\boldsymbol{u}_{-\boldsymbol{k}} = \boldsymbol{u}_{\boldsymbol{k}}^*\,, \tag{3.21}$$

where $(*)$ denotes complex-conjugation. By taking into account the divergence on both sides of the Navier-Stokes equations and by applying the incompressible condition, we get the Poisson equation

$$-\nabla^2 P = \nabla \cdot [(\boldsymbol{u}\cdot\nabla)\boldsymbol{u}]\,, \tag{3.22}$$

defining the pressure field from the velocity field. By using (3.22) to eliminate the pressure in (3.12), the 3D incompressible Navier-Stokes equations in Fourier space reads

$$\frac{\partial \boldsymbol{u_k}}{\partial t} = \left(I - \frac{\boldsymbol{kk}}{k^2} \right) \sum_{p+q=\boldsymbol{k}} i(\boldsymbol{k} \cdot \boldsymbol{u}_p)\boldsymbol{u}_q - \nu k^2 \boldsymbol{u}_k + \boldsymbol{F}_k \,, \tag{3.23}$$

with

$$\boldsymbol{k} \cdot \boldsymbol{u_k} = 0 \,. \tag{3.24}$$

3.6 Shell models of turbulence

Shell models of turbulence have attracted interest as useful phenomenological models that retain certain features and simplified representative versions of the Navier-Stokes equations and Euler equations, but they do retain enough of the flavor of the parent equations making themselves handy testing grounds for many statistical properties of fluid turbulence. In fact, shell models have been used to study statistical properties of turbulence in the past [26,32] with a fair degree of success. The popularity of shell models is due to their usefulness in modeling this very energy-cascade mechanism. The other advantage of using shell models is that, being deterministic dynamical models, they can be studied because the fast and accurate numerical simulations.

In addition, shell models for the energy cascade go back to the pioneering works of Obukhov [116], Lorenz [101], Densnyansky and Novikov [60], and Gledzer [75]. At the beginning, the idea was to find a particular closure scheme which is able to reproduce the Kolmogorov spectrum in terms of an attractive fixed point of appropriate differential equations for the velocity field averaged over shells in Fourier space, and to mimic the Navier-Stokes equations by a dynamical system with N variables u_1, u_2, ..., u_N each representing the typical magnitude of the velocity field on a certain length scale [32].

Moreover, shell models are a set of coupled nonlinear ordinary differential equations (ODEs) each one labeled by index n, where the Fourier space (the spectral space) is divided into concentric spheres N shells in each shell $n = 1, 2, \ldots, N$, called the shell index. These shells are shown in Figure 3.3.

Shell models are purely spectral models with a complex dynamical variables u_n representing a typical modal amplitude for all modes $\boldsymbol{u_k}$ such that $|\boldsymbol{k}| \in [k_n, k_{n+1})$, with $k_n = k_0 q^n$, where q, called the geometric shell spacing factor, usually set to 2, and k_0 is the amplitude of the zeroth mode. The modes u_n interact via a quadratic nonlinearity, (chosen so that the total energy, helicity and phase space volume are invisced conserved quantities like the nonlinear terms in the invisced Navier-Stokes equations), which has the general form

$$k_n \sum_{i,j} G_{i,j} u_i^* u_j^* \;, \tag{3.25}$$

where the sum is restricted to the modes of the nearest and next nearest shells, in shell (Fourier) space, of mode n. The shells are damped by the viscous term $-\nu k_n^2 u_n$, and forced with force f_n . The general evolution equation for shell models is

$$\left(\frac{d}{dt} + \nu k_n^2\right) u_n = k_n \sum_{i,j} G_{i,j} u_i^* u_j^* + f_n \,. \tag{3.26}$$

The energy of such models is defined as

$$E = \frac{1}{2} \sum_n |u_n|^2 \,. \tag{3.27}$$

Higher-order moments of shell models of turbulence are also available, with the p^{th} moment defined as

$$S_p(n) = \langle |u_n|^p \rangle, \tag{3.28}$$

where $\langle \cdot \rangle$ indicates averaging in time.

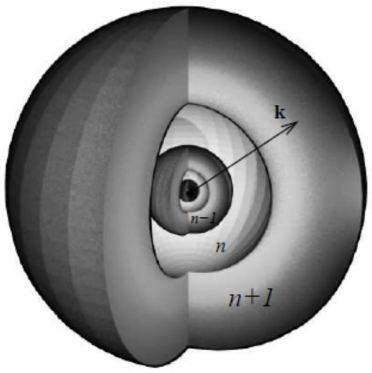

Figure 3.3: The spectral space is divided into spherical shells, each assigned a wave number which is the radius of the outer sphere.

In the next subsections, we present four models, namely the Obukhov model (Section 3.6.1), the DN model (Section 3.6.2), the GOY model (Section 3.6.3), and the Sabra model (Section 3.6.4).

3.6.1 The Obukhov model

Obukhov [116] was the first who proposed a shell model having in mind to find a simple nonlinear dynamic system capable of preserving the volume invariance in the phase space. Although structurally similar, this model is not inspired directly from the Navier-Stokes equations. It possesses quadratic nonlinear terms and linear dissipative terms. If one restricts the nonlinear term in Equation (3.26) to nearest-neighbor interactions, then the time evaluation equation is

$$\left(\frac{d}{dt}+\nu k_n^2\right)u_n = a_{n-1}u_{n-1}u_n - a_n u_{n+1}^2 + f_n\,, \tag{3.29}$$

where a_n's are the nonlinear interaction coefficients, which are typically constant with respect to n, ν is the viscosity, where the dissipation term on the left-hand side is active for large wave numbers, and only f_1 is nonzero, that is,

$$f_n = f\,\delta_{n,1}\,, \tag{3.30}$$

where δ is a Kronecker symbol. In order for the model to display an energy cascade from large to small scales, the energy must be injected at the large scales (small wave-numbers), flow through an inertial range, and be dissipated at the small scales (large wave-numbers).

3.6.2 The Desnyansky-Novikov model

The Desnyansky-Novikov (DN) model was proposed by by Desnyansky and Novikov [60]. Like the Navier-Stokes equations, the DN model has a conserved quadratic invariant, namely energy E. In this model, the evolution equation is

$$\left(\frac{d}{dt}+\nu k_n^2\right)u_n = ik_n\left[a\left(u_{n-1}^2 - qu_nu_{n+1}\right) + b\left(u_{n-1}u_n - qu_{n+1}^2\right)\right]^* + f_n\,, \tag{3.31}$$

where (*) denotes the complex conjugation, a and b are the nonlinear interaction coefficients, being the external forcing term f_n prescribed, time-independent and restricted usually to a single shell:

$$f_n = f\,\delta_{n,1}\,, \tag{3.32}$$

where δ is a Kronecker symbol.

3.6.3 The Gledzer-Okhitani-Yamada model

The Gledzer-Okhitani-Yamada (GOY) model was first proposed as a model with u_n real-valued by Gledzer [75]. He proposed the following equations

$$\left(\frac{d}{dt}+\nu k_n^2\right)u_n = (a_nu_{n+1}u_{n+2} + b_nu_{n-1}u_{n+1} + c_nu_{n-2}u_{n-1}) + f_n \quad (n=1,\cdots,N), \tag{3.33}$$

where a_n, b_n and c_n are the nonlinear interaction coefficients defined by

$$a_n = \alpha k_n = \alpha k_0 q^n, \quad b_n = \beta k_{n-1} = \frac{\beta}{q}k_n, \quad c_n = \gamma k_{n-2} = \frac{\gamma}{q^2}k_n, \tag{3.34}$$

with the lower boundary conditions $u_{-1} = u_0 = 0$, and the upper boundary conditions $u_{N+1} = u_{N+2} = 0$. The interaction coefficients α, β, and γ are chosen such that the energy, $E = \sum_n u_n^2/2$, and enstrophy, $Z = \sum_n k_n u_n^2/2$, are inviscid invariants.

This shell model, proposed by Gledzer, was investigated numerically by Yamada and Okhitani [159], 15 years after it was proposed by Gledzer. Their simulations showed that the model display an enstrophy cascade and chaotic dynamics. Interest in shell models grew rapidly after that and, since then, many papers investigating shell models have been published. The most well studied model is that proposed by Gledzer and investigated by Yamada and Okhitani [117]. It is now in a complex version referred to as the Gledzer–Okhitani–Yamada (GOY) model. The GOY model, just like other shell models, possesses a rich multiscale and temporal statistics and shares many striking similarities with real turbulent flows (see e.g., [104], [26], [73], and [31]). The evolution equation is

$$\left(\frac{d}{dt}+\nu k_n^2\right)u_n = ik_n\left(\alpha u_{n+1}u_{n+2}+\frac{\beta}{q}u_{n-1}u_{n+1}+\frac{\gamma}{q^2}u_{n-2}u_{n-1}\right)^* + f_n\,, \tag{3.35}$$

where α, β, and γ ($\alpha+\beta+\gamma=0$) are the nonlinear interaction coefficients ($u_{-1}=u_0=u_{N+1}=u_{N+2}=0$). Moreover, the external forcing, f_n, is usually applied to the fourth shell and is given by

$$f_n = f\delta_{4,n}\,. \tag{3.36}$$

3.6.4 The Sabra model

The Sabra model, introduced by L'vov *et. al.* [104], is a next-nearest neighbour model. The evolution equation of the Sabra model is

$$\left(\frac{d}{dt}+\nu k_n^2\right)u_n = ik_n\left(\alpha u_{n+1}^* u_{n+2}+\frac{\beta}{q}u_{n-1}^* u_{n+1}-\frac{\gamma}{q^2}u_{n-2}u_{n-1}\right)+f_n\,, \tag{3.37}$$

where (*) denotes complex conjugation, α, β, and γ are the nonlinear interaction coefficients, with boundary conditions $u_{-1}=u_0=u_{N+1}=u_{N+2}=0$ and the external forcing, f_n. Moreover, Sabra model displays a Kolmogorov spectrum in forced dissipative simulations. By following the same steps above for Goy model, we can rewrite the Sabra model in this form

$$\left(\frac{d}{dt}+\nu k_n^2\right)u_n = ik_n\left(u_{n+1}^* u_{n+2}+\frac{-\epsilon}{q}u_{n-1}^* u_{n+1}+\frac{1-\epsilon}{q^2}u_{n-2}u_{n-1}\right)+f_n\,, \tag{3.38}$$

to satisfy the condition that ensures the conservation of the energy.

3.6.5 Properties of the shell models

Shell models sharing some properties conserving the energy when the forcing f and viscosity ν are zero and is defined as

$$E = \frac{1}{2}\sum_n |u_n|^2\,. \tag{3.39}$$

Now, let us prove that the energy is conserved for example Gledzer shell model (3.33) by taking the time derivative of the energy with respect to time, then we have

$$
\begin{aligned}
\dot{E} &= \frac{1}{2}\frac{d}{dt}\sum_n |u_n|^2 \\
&= \sum_n k_n \left(\alpha u_n u_{n+1} u_{n+2} + \frac{\beta}{q} u_{n-1} u_n u_{n+1} + \frac{\gamma}{q^2} u_{n-2} u_{n-1} u_n\right) \\
&= \sum_n \left(\alpha k_n + \frac{\beta}{q} k_{n+1} + \frac{\gamma}{q^2} k_{n+2}\right) u_n u_{n+1} u_{n+2}\,.
\end{aligned}
$$

where we have changed just the summation label in the last two terms and used the boundary conditions. Since we may have any set of initial velocities, we must have the following condition for E to be an inviscid invariant

$$
\alpha k_n + \frac{\beta}{q} k_{n+1} + \frac{\gamma}{q^2} k_{n+2} = 0\,, \tag{3.40}
$$

then we have

$$
\alpha + \beta + \gamma = 0\,. \tag{3.41}
$$

Now, with a simple change of the units, we can eliminate one of the three constants, say α, by dividing the equation by α and absorbing it in the unit of time. Let define $\beta = -\epsilon$ and by using Eq. (3.41), we have $\gamma = \epsilon - 1$, and the Gledzer model equation is written in the form

$$
\left(\frac{d}{dt} + \nu k_n^2\right) u_n = i k_n \left(u_{n+1} u_{n+2} + \frac{-\epsilon}{q} u_{n-1} u_{n+1} + \frac{\epsilon - 1}{q^2} u_{n-2} u_{n-1}\right) + f_n\,. \tag{3.42}
$$

Similary, we may rewrite GOY model in the form

$$
\left(\frac{d}{dt} + \nu k_n^2\right) u_n = i k_n \left(u_{n+1} u_{n+2} + \frac{-\epsilon}{q} u_{n-1} u_{n+1} + \frac{\epsilon - 1}{q^2} u_{n-2} u_{n-1}\right)^* + f_n\,, \tag{3.43}
$$

The GOY model has another conserved quantity besides the energy which can be determined by the pth power of the wave number:

$$
\frac{1}{2}\sum_n k_n^p |u_n|^2\,, \tag{3.44}
$$

where p, ϵ, and q are related through $q^p = |\epsilon - 1|^{-1}$, i.e., through the relation

$$
\log q = -\frac{1}{p}\log|\epsilon - 1|\,. \tag{3.45}
$$

For $\epsilon < 1$, (e.g., $\epsilon = 1/2$), and $q = 2$, the second invariant is not positive, and it can be written as

$$
H = \frac{1}{2}\sum_n (-1)^n k_n |u_n|^2\,, \tag{3.46}
$$

which we call the *shell-model helicity*. Like helicity in 3D turbulence, this quantity is not

positive definite. For $\epsilon > 1$, (e.g., $\epsilon = 5/4$), and $q = 2$, the second conserved invariant is always positive, and it can be written as

$$Z = \frac{1}{2}\sum_n k_n^2 |u_n|^2 \,, \tag{3.47}$$

which we call the *enstrophy*. Like enstrophy in 2D turbulence.

3.6.6 2D and 3D shell models

For $\epsilon < 1$, the second invariant is given as $H = (1/2)\sum_n H_n$, where $H_n = (-1)^n k_n^p |u_n|^2$ so the shell helicity is dimensionally the same as the helicity when $p = 1$. In this case, the shell model is said to be of the 3D turbulence. Then, the common choice of parameters for the 3D type shell model is $(\epsilon, q) = (1/2, 2)$ [87], where $p = 1$ and the shell spacing is an octave [61].

In 2D flow, the vorticity is always perpendicular to the plane of the flow, implying that the helicity H is identically zero. The enstrophy is also an inviscid invariant. The spectral density of the enstrophy $Z(k)$ is simply related to the spectral density of energy, $E(k)$, by $Z(k) = k^2 E(k)$. Then, for $\epsilon > 1$, the second invariant is given as $Z = (1/2)\sum_n Z_n$, where $Z_n = k_n^p |u_n|^2 = k_n^2 E_n$. So, for $p = 2$, this corresponds to the enstrophy in 2D flow. Thus, the canonical choice in the 2D case is $(\epsilon, q) = (5/4, 2)$ [75], where $p = 2$, and it is referred to as a 2D type shell model.

To summarize, for $\epsilon < 1$, the model is of the 3D type, for $\epsilon > 1$, the model is of 2D turbulence type, and for $\epsilon = 1$ occurs the transition of these two type models.

3.7 Introduction to optimal control theory

3.7.1 Formulation of the optimal control problem and general considerations

The optimal control theory was established in the middle of 20th to address optimization problems featuring constraints defined by differential equations which depend on a parameter called control that takes values on a closed set and, since then, did not stop growing continuously, having become a very sophisticated scientific area. In fact, what distinguishes calculus of variations from optimal control is that while the constraint on the time derivative of the trajectory is open on the former, it is closed on the later, [49].

The rapid development of optimal control theory resides on the very wide range of applications in which optimal control problems (OCPs) play a key role that arise in engineering, economics, management, science, health, mobility, industrial processes, navigation, robotics, data gathering systems, among many other fields, [36]. This is not surprising given the tremendous versatility of the optimal control paradigm which not only

encompasses a wide range of constraints types on the two key variables - state and control - such as, constraints on the state, control, mixed state and control, on the endpoints and intermediate points of the state variable, isoperimetric constraints, [113, 126, 148, 154], but also appears in multiple types of formulations, [36, 49].

The objective of an OCP is to determine the control strategy that optimizes (minimizes or maximizes) a given optimality criterion or performance index usually denoted by $J(\cdot)$. The performance index may be very general. It may simply be a function depending on the state and/or time endpoints, or also involve an integral whose integrand may be a function of the values of both the state and the control variables. One common, relatively general, formulation of the optimal control problem defined on a given time interval $[t_a, t_b]$ where either or both t_a and t_b may be either fixed or decision variables is as follows:

$$
\begin{aligned}
(P)\ \text{Minimize} \quad & J(x,u) && (3.48)\\
\text{subject to} \quad & \dot{x}(t) = f(t, x(t), u(t)) \qquad \mathcal{L}\text{-a.e. in } [t_a, t_b] && (3.49)\\
& u(t) \in \Omega \qquad \mathcal{L}\text{-a.e. in } [t_a, t_b] && (3.50)\\
& (x(t_a), x(t_b)) \in C && (3.51)\\
& h(t, x(t)) \leq 0 && (3.52)\\
& m(t, x(t), u(t)) \leq 0 && (3.53)
\end{aligned}
$$

Here, $x : [t_a, t_b] \to \mathbb{R}^n$ is the state variable which is absolutely continuous, $u \in \mathcal{U}$ is the control function where $\mathcal{U} = \{u \in L^\infty([t_a, t_b]; \mathbb{R}^m) : u(t) \in \Omega\}$. The functional

$$J[x,u] = \int_{t_a}^{t_b} L(t, x(t), u(t))dt\,,$$

is the cost functional, being the function

$$L : [t_a, t_b] \times \mathbb{R}^n \times \mathbb{R}^m \to \mathbb{R}$$

called the integrand. The dynamics of the system for the case where the first-order derivative of the state variable x is considered is defined by the function

$$f : [t_a, t_b] \times \mathbb{R}^n \times \mathbb{R}^m \to \mathbb{R}^n,$$

while the maps

$$h : [t_a, t_b] \times \mathbb{R}^n \to \mathbb{R}^k$$

and

$$m : [t_a, t_b] \times \mathbb{R}^n \times \mathbb{R}^m \to \mathbb{R}^l$$

define, respectively, inequality state constraints, and inequality mixed constraints. While the set $C \subset \mathbb{R}^{n \times n}$ defines the state variable endpoint constraints, the set $\Omega \subset \mathbb{R}^m$ specifies the constraints on the control function values. Notice that endpoint state constraints above generalize the usual equality and inequality type of constraints.

The pair (x, u) is designated as control process. The control process (x, u) is said to be feasible if it satisfies all the constraints of the OCP. The control process (x^*, u^*) is a solution to the OCP if it yields the smallest value of the cost functional among all feasible control processes (x, u).

It is worth to point out that there are several types of minimum that depend on the topology chosen for the underlying control space which, in turn, is linked to the class of admissible perturbations that are considered. The smaller the class of control processes considered for comparison the weaker type of minimum. Besides the usual topologies induced by the underlying normed spaces (strong, weak, and weak star), we would like to emphasize the Pontryagin type of minimum in which the so-called "needle" variations are considered, [5, 109, 110, 126, 148]. The relevance of type of minimum is great since it should reflect the requirements of the specific application of interest.

The emphasis of this overview will be on the necessary conditions of optimality where the maximum principle attracted most of the attention. Necessary conditions of optimality are particularly important as they allow the restriction of the class of control processes which are potential candidates to the solution to the OCP. Under some suitable assumptions, locally these conditions might also be sufficient and, thus, solving the solution to the OCP is reduced to the comparison among a relatively small, possibly finite, set of control processes.

It is important to note that a solution to the OCP must exist in order to guarantee that the application of the necessary conditions of optimality yield a meaningful result. There are several sets of conditions which are sufficient to ensure the existence of solution to the OCP. We are not going to dwell on this topic but simply mention that, by and large these ensure that the cost functional is lower semi-continuous on the set of feasible control processes which should be compact in a compatible topology. For more details, see, for example, [39, 113, 148]. Thus, from now on, we assume that there exists a solution to the OCP.

Typical assumptions on the data of $(\bar{P})$, a simplified version of the OCP (P) in order to enable the derivation of necessary conditions of optimality are listed below. $(\bar{P})$ coincides with (P) but without state and mixed constraints. The presence of these constraints would make the formulation too complex for this general introduction and will imply a cumbersome discussion of the required underlying assumptions.

1. The functions $L(t, x, u)$ and $f(t, x, u)$ are Lipschitz continuous in x with constant K_f, for all $(t, u) \in \mathbb{R} \times \mathbb{R}^m$.

2. The functions $L(t,x,u)$ and $f(t,x,u)$ are Lebesgue $\times$ Borel measurable in (t,u), for all $x \in \mathbb{R}^n$.

3. The set valued map $(t,x) \to f(t,x,\Omega)$ is compact-valued.

4. The map $L(t,x,u)$ is bounded from below for all $(t,x,u) \in [t_a,t_b] \times \mathbb{R}^n \times \Omega$

5. The set C is compact.

6. The set Ω is compact.

It is worth to remark that some of these assumptions require the usage of methods of nonsmooth analysis able to handle non-differentiable functions. If one does not need to enter in the real of nonsmooth analysis, then the above assumptions 1. and 2. could be replaced by the following appropriate smoother data:

1'. The functions $L(t,x,u)$ and $f(t,x,u)$ are differentiable in x and continuous in x and u, for all $(t,x,u) \in \mathbb{R} \times \mathbb{R}^n \times \mathbb{R}^m$.

2'. The gradient of $L(t,x,u)$ with respect to x and the Jacobian of $f(t,x,u)$ with respect to x are bounded on bounded sets for all $(t,u) \in [t_a,t_b] \times \Omega$.

These are by no means the weakest set of assumptions that one is able to impose on the assumptions on the data of the OCP in order to be able to derive necessary conditions of optimality. However, these are simpler to express and more intuitive to grasp.

It is also important to remark that these conditions do not suffice to ensure that the derived necessary conditions of optimality are informative in the sense that they enable the successful reduction of the number of candidates to the solution of the problem. Additional assumptions are required in order to make sure that the optimality conditions do not degenerate.

Depending on the type of cost functional, the optimal control problem may be designated by Mayer (function of the state variable at endpoints), Lagrange (integral of a function of time, state and control variables), and Bolza (combining both costs of Mayer and Lagrange types of problems), that is

1. Bolza formulation

$$J(x,u) = g(t_a, x(t_a), t_b, x(t_b)) + \int_{t_a}^{t_b} L(t, x(t), u(t))dt,$$

2. Lagrange formulation

$$J(x,u) = \int_{t_a}^{t_b} L(t, x(t), u(t))dt,$$

3. Mayer formulation

$$J(x,u) = g(t_a, x(t_a), t_b, x(t_b)).$$

There are other vaster set of formulations of the OCP that is impossible to cover in such a short overview:

- Free time, [148]
- Infinite time horizon, [18, 121]
- Multi-processes OCP, [51, 52]
- Unbounded controls or velocity sets (sets of feasible derivatives of the state variable), [154]
- Impulsive control, [149]
- Minimax optimal control, [88]

In what concerns the range of issues and problems that, over the years, have been subject of intense research in the construction of the body of Optimal Control theory, one can consider the three main pillars:

- Higher-order necessary conditions of optimality.
- Sufficient conditions of optimality under convexity and in the absence of convexity assumptions.
- Existence theory under a wide variety of the so-called growth conditions.

In what concerns necessary conditions of optimality, intense research has been devoted to many classes of challenges that arise when attempting to solve concrete problems with results and methods from optimal control theory: (i) the best assumptions required to ensure the non-degeneracy of the conditions, and even, on formulation of nondegenerate conditions that do not require a priori normality assumptions; (ii) results on sensitivity of the multiplier associated with optimality conditions; (iii) robustness to perturbations and to unknown model parameters; among many other that we cannot accommodate in this short overview.

For a sample, by no means exhaustive, of the vast literature in optimal control theory, check the following:

- Set of monographs: [5, 19, 39, 49, 62, 74, 109, 110, 113, 126, 148]
- Set of articles and references therein: [15, 16], [8, 17], [9], [11–13], [10], [7, 14], [67], [77],[89], [120].

3.7.2 Necessary conditions optimality

In this subsection, we present a brief discussion on the necessary conditions of optimality in order to provide a flavor on the multipliers and conditions that can be used. Let us consider the simplified version of problem (P), $(\tilde{P})$ with smooth data, in which neither state nor mixed constraints are present, and formulated in the context of fixed time interval, i.e. t_a and t_b are not decision variables, and with a Bolza cost functional, i.e.,

$$J(x,u) = g(x(t_a), x(t_b) + \int_{t_a}^{t_b} L(t, x(t), u(t))dt\,.$$

In what follows, $N_C(c)$ denotes the limiting normal cone to the closed set C at the point $c \in C$ [109] and $H(t,x,p,u,\lambda)$ denotes the so-called Pontryagin function defined by

$$H(t,x,p,u,\lambda) = p^T f(t,x,u) - \lambda L(t,x,u)\,.$$

Then, the necessary conditions of optimality in the form of a Maximum Principle of Pontryagin for $(\tilde{P})$ can be stated as follows, [5, 126],

Let the control process (x^*, u^*) be a solution to $(\tilde{P})$. Then, there exists a multiplier (p,λ) with $p \in AC([t_a,t_b];\mathbb{R}^n)$ and $\lambda \geq 0$ that satisfies the following conditions

1. Nontriviality
$$\|p\| + \lambda \neq 0\,,$$

2. Adjoint equation
$$-\dot{p}(t) = \nabla_x H(t, x^*(t), p(t), u^*(t), \lambda)\,,$$

3. Boundary conditions:
$$(p(t_a), -p(t_b)) \in \lambda\, \nabla g(x^*(t_a), x^*(t_a)) + N_C(x^*(t_a), x^*(t_a))\,,$$

4. Maximum condition: For almost all $t \in [t_a, t_b]$, $u^*(t)$ maximizes in Ω the map
$$v \to H(t, x^*(t), p(t), v, \lambda)\,.$$

Notice that it may well happen that these conditions hold with $\lambda = 0$. In this case, it is clear that the cost functional plays no role in the characterization of the solution to the problem $(\tilde{P})$ and the conditions are said to degenerate. This phenomenon has been noted early on, but significant progress in understanding the various conditions under which this arises has been achieved only recently. We would like to say that, under less general constraints on the endpoint of the state variable, this result has been proved for the first time by Lev Semenovich Pontryagin and his co-workers, [126]. As it is clear from the above, this spurred a huge research effort that still goes on currently. Some observations concerning the usage of these conditions are in order:

- For time invariant systems, i.e., the data of the problem does not depend on time, the Pontryagin function along the optimal control process $H(x^*(t), p(t), u^*(t), \lambda)$ is constant. Moreover, if the final time is free, then, we have that $H(t, x^*(t), p(t), u^*(t), \lambda) = 0$.

- Clearly, these conditions transform the original functional optimization problem into a collection of finite dimensional optimization problems formulated for almost all $t \in [t_a, t_b]$.

- It is also clear from the Maximum Principle that the optimal control function is eliminated by the maximum condition and, the use of the conditions is reduced to solve a two-point boundary value differential problem.

- Finally, it is important to note the fact that if, on the one hand, the computation of the adjoint variable requires the knowledge of the optimal control process, then, on the other hand, the computation of the optimal control function requires the knowledge of the optimal state variable and associated adjoint vvariable. This calls for a recursive procedure that is embedded in both the analysis and numerical schemes that used these conditions. This will be briefly outlined next.

Let us expand the last item above a little more by providing an abstract algorithm. For the sake of simplicity of the presentation let us consider the set $C = \{x_0\} \times \mathbb{R}^n$ and the cost functional given by

$$J(x, u) = g(x(t_b)) + \int_{t_a}^{t_b} L(t, x(t), u(t))dt\,.$$

Assume also that Ω is a convex set. In this case, it is well known that the Maximum Principle does not degenerate and, thus, we may set $\lambda = 1$ and, thus, we omit it from the arguments of the Pontryagin function.

1. Initialization. Set $i = 0$ and let $u_i \in L^\infty([t_a, t_b]; \Omega)$ be the initial optimal control estimate, and take some constant $\delta_i > 0$ small (to be tuned).

2. Compute the pair (x_i, p_i) by solving

$$\begin{aligned} \dot{x} &= f(t, x, u_i(t)), \quad x(t_a) = x_0 \\ -\dot{p}^T &= p^T D_x f(t, x_i(t), u_i(t)) - L(t, x_i(t), u_i(t)), \quad -p^T(t_b) = \nabla_x g(x_i(t_b)) \end{aligned}$$

3. Check whether $u_i(t)$ maximizes, Lebesgue a.e. in $[t_a, t_b]$ in Ω the map

$$v \to H(t, x_i(t), p_i(t), v).$$

   If that is the case, the algorithm should stop as the current control satisfies the Maximum Principle. Otherwise, pursue to the next step.

4. Compute the new control strategy u_{i+1} satisfying $\bar{u}_{i+1}(t) \in \Omega$ such that, Lebesgue a.e. in $[t_a, t_b]$,

$$H(t, x_i(t), p_i(t), \bar{u}_{i+1}(t)) \geq H(t, x_i(t), p_i(t), v) \quad \forall v \in \Omega.$$

   For a.a. $t \in [t_a, t_b]$, let $u_{i+1}(t) = \bar{u}_i(t)) + \delta_i(u_{i+1}(t) - u_i(t))$.

5. Let $i = i + 1$ and go to step 2.

Observation: the constant δ_i should be tuned as the iterations proceed in order to ensure a smooth convergence of the procedure.

We conclude this section by establishing the key relation with the first order necessary conditions of optimality in the context of Calculus of Variations, and more precisely, the Euler-Lagrange conditions. Now we assume that both f and L are differentiable in u and that Ω is an open set with nonempty interior.

We remark that the conditions stated above for the Maximum Principle remain except that, now, the maximum condition, item 4. defining the value of the optimal control $u^*(t) \in \Omega$ at time t is replaced by

$$\frac{\partial}{\partial u} H(t, x^*(t), p(t), u, \lambda) = 0.$$

Chapter 4

Optimization problem for shell models of turbulence

As we mentioned earlier, shell models of turbulence were introduced by Obukhov and Gledzer (see [61, 75, 116]). The original purpose was to find a particular closure scheme which is able to reproduce the Kolmogorov spectrum [91–93] in terms of an attractive fixed point of an appropriate set of differential equations for the velocity field averaged over shells in Fourier space, while mimicking the Navier-Stokes equations, in the sense of preserving some invariants (energy, enstrophy, ...), by a dynamical system of dimension N, $u_1, u_2, \cdots, u_N$, each representing the typical magnitude of a velocity field on a certain length scale.

These models consist of a set of coupled nonlinear ordinary differential equations structurally similar to the Navier-Stokes equation written in the Fourier space. For these models, a scaling theory identical to the Kolmogorov theory [91–93] has been developed, and they show the same kind of deviation from the Kolmogorov scaling as real turbulent systems do. Understanding the behavior of shell models in their own right is one of the keys to understand the systems governed by the Navier-Stokes equations. The shell models are constructed to obey the same conservation laws and symmetries as the Navier-Stokes equations.

In this chapter, we develop a theoretical methodology based on an optimization approach in order to optimize the forcing of turbulence. By fixing a cost function, we want to tune the force so as to minimize the cost function. Following the ideas of [65], we want to reach the statistical regime observed in the structure functions within a certain given and fixed time interval $[0, T]$.

In the next section, we summarized the ideas of [65] and the next sections are devoted to the mathematical formulation of the optimization problem for the GOY, Sabra and DN models.

4.1 Control of the dual cascade model of two-dimensional turbulence

Farazmand *et. al.* [65] use and develop an optimization theory approach to find a forcing that produces the dual scaling ranges predicted by KLB theory. However, they consider the 2D incompressible NSEs on a 2D box with periodic boundary condition,

$$\mathcal{L}\boldsymbol{q} \triangleq \partial_t \boldsymbol{u} + \boldsymbol{u}\cdot\nabla\boldsymbol{u} + \nabla p - \nu\Delta\boldsymbol{u} = \boldsymbol{f}, \tag{4.1a}$$

$$\nabla\cdot\boldsymbol{u} = 0, \tag{4.1b}$$

$$\boldsymbol{u}(t=0,x) = \boldsymbol{u}_0(x), \tag{4.1c}$$

where $\boldsymbol{u}(t,\cdot) : [0,2\pi]^2 \to \mathbb{R}^2$ is the velocity field, $p(t,\cdot) : [0,2\pi]^2 \to \mathbb{R}$ is the pressure, ν is the coefficient of kinematic viscosity, and $\boldsymbol{f}(t,\cdot) : [0,2\pi]^2 \to \mathbb{R}^2$ is the external forcing. The vector function $\boldsymbol{q} = [\boldsymbol{u} \quad p]^T$ contains the two components of velocity field $\boldsymbol{u}$ and the pressure field p. However, for any solution of (4.1a), we define the energy spectrum as

$$E(t,k) = \frac{1}{2}\int_{C(k)} |\hat{\boldsymbol{u}}(t,\boldsymbol{k})|^2 \, dS(\boldsymbol{k}), \tag{4.2}$$

where $\hat{\boldsymbol{u}}$ is the Fourier transform of $\boldsymbol{u}$ and $\boldsymbol{k}$ is the wave vector. $C(k)$ is a circle with radius k in the 2D plane, $C(k) = \{\boldsymbol{k} \in \mathbb{R}^2 : |\boldsymbol{k}| = k\}$. Let $E_0(k)$ be the energy spectrum predicted by KLB theory, i.e.

$$E_0(k) = \begin{cases} C_1 k^{-5/3}, & k_1^e \leqslant k \leqslant k_2^e, \\ C_2\, k^{-3}, & k_1^z \leqslant k \leqslant k_2^z, \end{cases} \tag{4.3}$$

where $[k_1^e, k_2^e]$ and $[k_1^z, k_2^z]$ are the energy and enstrophy inertial ranges, respectively (see Fig. 4.1). Here, C_1 and C_2 are constants, where C_1 depends only on the energy dissipation rate (ε) and C_2 depends only on the enstrophy dissipation rate (η). The goal is to find a forcing, $\boldsymbol{f}$, which results in a solution of NSEs (4.1a) with the KLB energy spectrum $E_0(k)$. Define the following cost functional:

$$\mathcal{J}(\boldsymbol{f}) \triangleq \frac{1}{2}\int_0^T \int_I w(t,k)\, |E(t,k) - E_0(k)|^2 \, dk dt, \tag{4.4}$$

where $I = [k_1^e, k_2^e] \cup [k_1^z, k_2^z]$. The function $w(t,k)$ is a positive weight function which normalizes the error $|E(t,k) - E_0(k)|^2$ to get a uniform error distribution over all wavenumbers. Now, we may formulate our problem as follows:

$$\min_{f\in\mathcal{U}} \mathcal{J}(\boldsymbol{f}), \tag{4.5}$$

where $\mathcal{U}$ is a suitable function space with Hilbert structure. The cost functional $\mathcal{J}$ depends

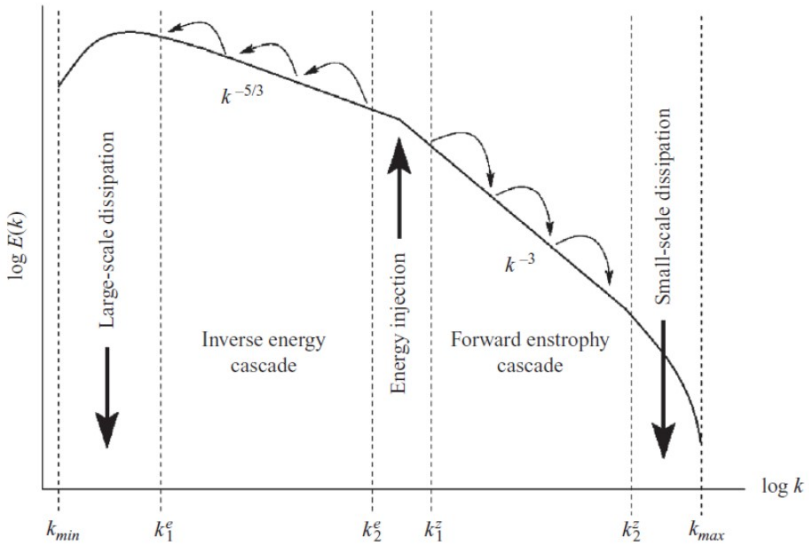

Figure 4.1: Schematic representation of the KLB theory, [65]. Energy and enstrophy are injected by the external forcing over the range (k_2^e, k_1^z). Energy and estrophy inertial ranges are $[k_1^e, k_2^e]$ and (k_1^z, k_2^z), respectively. The smallest wavenumber is $k_{min} = 1$ (if the domain is unbounded $k_{min} = 0$ and the large-scale dissipation is not necessary), while the largest available wavenumber k_{max} depends on the numerical resolution.

on $\boldsymbol{f}$ through (4.1a). This type of cost functional is called a reduced cost functional. Our goal is to find a forcing $\boldsymbol{f}_{opt} \in \mathcal{U}$ that minimizes the cost functional $\mathcal{J}$. A set of optimization techniques are used to compute the minimum of the cost functional based on a gradient descent method. In addition, this control method is used to study the effect of forcing on the scaling properties of the energy spectrum in forced 2D turbulence.

4.2 General formulation of an optimization problem

In our strategy, we will follow the same ideas, but we use the shell models instead of Navier-Stokes equations. The models are truncated to a finite number of shells, with the number n of shells typically running from 1 to N ($N = 22$ or 25 are the typical values found in the literature) and the boundary conditions given by $u_{-1} = u_0 = u_{N+1} = u_{N+2} = 0$.

We consider a target energy spectrum, and, then, find the forcing. The target energy spectrum in our study follows, for instance, the KLB energy spectrum for 2D turbulence, or the K41 energy spectrum for 3D turbulence (or some reference energy spectrum given in the literature). The problem is to minimize the difference between the energy spectrum obtained from solving the shell model equations, with some particular forcing, and the target energy spectrum.

Start with an arbitrary forcing, and, then, calculate the difference between the resulting

spectrum, and the target spectrum. The next choice of the forcing should be one that results in a smaller difference between these spectra. The criterion for updating the forcing comes from an idea in multivariable calculus, where the multivariable function decreases in the opposite direction of its gradient. If this gradient direction is known, then the forcing can be updated by moving from the previous forcing in the opposite direction of that of the gradient by some appropriate increment. By continuing the same procedure from the new forcing, a closer spectrum to the target will be found. After a sufficient number of iterations, the difference between the spectra will be minimized. If all goes well, this minimum is zero (or below some prescribed tolerance) and the calculated spectrum is the target spectrum.

Before formulating the optimization problem, we present some fundamental definitions and theorems of functional analysis.

Definition 4.1. *(Dual Space). Consider a Banach space X. A map $\mathcal{M} : X \to \mathbb{R}$ is called a functional on X. The set of all continuous linear functionals on X is called the dual space of X and is denoted by $X^\dagger$.*

Definition 4.2. *(Gâteaux Derivative). Consider a Banach space X and let $f, f' \in X$. The Gâteaux differential of a functional $\mathcal{M} \in X^\dagger$ at f in direction f' is defined as*

$$\mathcal{M}'(f;\, f') \triangleq \lim_{\delta \to 0} \frac{\mathcal{M}(f + \delta f') - \mathcal{M}(f)}{\delta}\,, \tag{4.6}$$

if the limit exists. If the limit exists for all $f' \in X$, then $\mathcal{M}$ is Gâteaux differentiable at f.

Theorem 4.1. *(Riesz Representation Theorem). Consider a Hilbert space X with the inner product $(\cdot,\cdot)_X$. Let $\mathcal{M}$ be a continuous linear functional on X, i.e. $\mathcal{M} \in X^\dagger$. Then there is a unique element $u^\dagger \in X$ such that*

$$\mathcal{M}(f) = (f, u^\dagger)_X\,, \tag{4.7}$$

for all $f \in X$.

4.3 Application to the GOY model

Write the GOY shell model as

$$\mathcal{L}\boldsymbol{u} = \frac{du_n}{dt} - ik_n \left(u_{n+1}u_{n+2} - \frac{\epsilon}{q} u_{n-1}u_{n+1} + \frac{\epsilon - 1}{q^2} u_{n-2}u_{n-1} \right)^* + \nu k_n^2 u_n = f_n\,. \tag{4.8}$$

For any solution of GOY model, we define the structure function [26],

$$S_p(k_n) \equiv \langle |u_n|^p \rangle = C_0 k_n^{\zeta(p)},$$

where $\zeta(p) = p/3$ according to the K41 theory (i.e., without energy-cascade intermittency) and C_0 a non-dimensional constant of order of unity [55]. Here, $\langle |u_n|^p \rangle$ is defined as an average over time, i.e., $\langle |u_n|^p \rangle = (1/T) \int_0^T |u_n(t)|^p dt$. Long numerical runs (hundreds of millions of time steps), with parameter values $N = 25$, $\nu = 5 \times 10^{-7}$, $k_0 = 0.05$, and $q = 2$, and with $f_n = 0.1(1+i)\delta_{n,0}$, the numerical values $\zeta^{\mathrm{NV}}(4) = 1.26(3)$, and $\zeta^{\mathrm{NV}}(6) = 1.76(5)$ are obtained. Other values for different p's can be found in [26].

Our goal is to characterize the forcing, f_n, which results in a solution of the GOY with these scaling exponents, but in a much shorter time interval, say $[0, T]$. With this in mind, consider the following cost functional

$$\mathcal{M}(\boldsymbol{f}) \triangleq \frac{1}{2\,T} \int_0^T \sum_{n=1}^{N} w(t, k_n) \left| S_p(k_n) - S_p^{\mathrm{NV}}(k_n) \right|^2 dt \,,$$

The function $w(t, k_n)$ is a positive weight function which normalizes the error

$$\left| S_p(k_n) - S_p^{\mathrm{NV}}(k_n) \right|^2 \,,$$

to get a uniform error distribution over all wave numbers. We may now formulate the following optimization problem:

$$\min_{f \in \mathcal{U}} \mathcal{M}(f) \,,$$

where $\mathcal{U}$ is a suitable function space with a Hilbert structure. The cost functional $\mathcal{M}$ depends on f through the system of ODE (4.8). From now on, we will consider $p = 2$, since it corresponds to the energy spectrum case.

4.3.1 Mathematical formulation of an optimization problem for the GOY model

The necessary condition characterizing the minimizer f_{opt} of the cost functional is the vanishing of Gâteaux differential $\mathcal{M}'$, i.e.,

$$\mathcal{M}'(f_{opt}, f') = 0, \tag{4.9}$$

for all $f' \in \mathcal{U}$. After some calculations, it can be shown that

$$\mathcal{M}'(f; f') = \frac{1}{T} \int_0^T \sum_{n=1}^{N} w(t, k_n)(S_{2p}(k_n) - S_2^{\mathrm{NV}}(k_n)) \times (u_n u_n'^* + u_n' u_n^*)\, dt \,, \tag{4.10}$$

that is

$$\mathcal{M}'(f; f') = \sum_{n=1}^{N} \int_0^T S(t, n) \mathrm{Re}(u_n' u_n^*)\, dt \; = \mathrm{Re} \sum_{n=1}^{N} \int_0^T S(t, n) u_n^*(t) u_n'(t)\, dt \,, \tag{4.11}$$

where

$$S(t,n) = \frac{2}{T} w(t,k_n)[S_2(k_n) - S_2^{\mathrm{NV}}(k_n)],$$

and u'_n is the solution of the GOY model equation linearized around the state u_n , i.e.,

$$\begin{aligned} Lu' &\triangleq \frac{du'_n}{dt} - ik_n((u_{n+1}u'_{n+2} + u'_{n+1}u_{n+2}) + \frac{-\epsilon}{q}(u_{n-1}u'_{n+1} + u'_{n-1}u_{n+1}))^* \\ &- i\frac{(\epsilon-1)}{q^2} k_n(u_{n-1}u'_{n-2} + u'_{n-1}u_{n-2})^* + \nu k_n^2 u'_n = f'_n. \end{aligned}$$

On the other hand, the Riesz representation theorem, [94], guarantees the existence of a unique element $\nabla\mathcal{M}$ which satisfies the identity

$$\mathcal{M}'(f; f') = \langle \nabla\mathcal{J}, f' \rangle ,$$

where $\langle \cdot, \cdot \rangle$ is the L^2 inner product. By using a suitably defined adjoint variable $u^\dagger$, we have

$$\langle u^\dagger, f' \rangle = \langle u^\dagger, Lu' \rangle = \langle L^\dagger u^\dagger, u' \rangle,$$

where the adjoint operator $L^\dagger$ and the adjoint variable are interconnected by

$$L^\dagger u^\dagger = \begin{bmatrix} w(t,k_1)(S_1(k_1) - S_1^{\mathrm{NV}}(k_1))u_1 \\ w(t,k_2)(S_2(k_2) - S_2^{\mathrm{NV}}(k_2))u_2 \\ w(t,k_3)(S_2(k_3) - S_2^{\mathrm{NV}}(k_3))u_3 \\ \vdots \\ w(t,k_N)(S_2(k_N) - S_2^{\mathrm{NV}}(k_N))u_N \end{bmatrix}.$$

The determination of the analytical expression for $L^\dagger$ is done as follows. Consider the decomposition

$$Lu' = \left(\frac{d}{dt} - iAC + \nu B \right) u' ,$$

where we use the notation

$$u' = \begin{bmatrix} u'_1 \\ u'_2 \\ u'_3 \\ \vdots \\ u'_N \end{bmatrix},$$

and

$$A^* = \begin{bmatrix} 0 & a_{1,2} & a_{1,3} & 0 & \cdots & 0 & 0 & 0 & 0 \\ a_{2,1} & 0 & a_{2,3} & a_{2,4} & \cdots & 0 & 0 & 0 & 0 \\ a_{3,1} & a_{3,2} & 0 & a_{3,4} & \cdots & 0 & 0 & 0 & 0 \\ 0 & a_{4,2} & a_{4,3} & 0 & \cdots & 0 & 0 & 0 & 0 \\ \vdots & \vdots & \vdots & \vdots & \ddots & \vdots & \vdots & \vdots & \vdots \\ 0 & 0 & 0 & 0 & \cdots & 0 & a_{N-3,N-2} & a_{N-3,N-1} & 0 \\ 0 & 0 & 0 & 0 & \cdots & a_{N-2,N-3} & 0 & a_{N-2,N-1} & a_{N-2,N} \\ 0 & 0 & 0 & 0 & \cdots & a_{N-1,N-3} & a_{N-1,N-2} & 0 & a_{N-1,N} \\ 0 & 0 & 0 & 0 & \cdots & 0 & a_{N,N-2} & a_{N,N-1} & 0 \end{bmatrix},$$

being the coefficients of the matrix given by

$$\begin{aligned}
&a_{1,2} = k_1(u_3 + bu_0), \quad a_{1,3} = k_1 u_2 \\
&a_{2,1} = k_2(bu_3 + cu_0), \quad a_{2,3} = k_2(u_4 + bu_1), \quad a_{2,4} = k_2 u_3 \\
&a_{3,1} = ck_3 u_2, \quad a_{3,2} = k_3(bu_4 + cu_1), \quad a_{3,4} = k_3(u_5 + bu_2) \\
&a_{4,2} = ck_4 u_3, \quad a_{4,3} = k_4(bu_5 + cu_2) \\
&a_{N-3,N-2} = k_{N-3}(u_{N-1} + bu_{N-4}), \quad a_{N-3,N-1} = k_{N-3} u_{N-2} \\
&a_{N-2,N-3} = k_{N-2}(bu_{N-1} + cu_{N-4}), \quad a_{N-2,N-1} = k_{N-2}(u_N + bu_{N-3}) \\
&a_{N-2,N} = k_{N-2} u_{N-1}, \quad a_{N-1,N-3} = ck_{N-1} u_{N-2} \\
&a_{N-1,N-2} = k_{N-1}(bu_N + cu_{N-3}), \quad a_{N-1,N} = k_{N-1}(u_{N+1} + bu_{N-2}) \\
&a_{N,N-2} = ck_N u_{N-1}, \quad a_{N,N-1} = k_N(bu_{N+1} + cu_{N-2})
\end{aligned}$$

with the boundary conditions

$$u_{-1} = u_0 = u_{N+1} = u_{N+2} = 0\,,$$

and

$$Cu' = u'^*\,,$$

$$B = \begin{bmatrix} k_1^2 & 0 & 0 & \dots & 0 \\ 0 & k_2^2 & 0 & \dots & 0 \\ 0 & 0 & k_3^2 & \dots & 0 \\ \vdots & \vdots & \vdots & \ddots & \vdots \\ 0 & 0 & 0 & \dots & k_N^2 \end{bmatrix}.$$

Let us define the operator L in the form

$$L = \frac{d}{dt} + \mathbb{A}\,,$$

where

$$\mathbb{A} = -iAC + \nu B.$$

We have

$$\begin{aligned}
\langle f, Lg\rangle &= \int_a^b f(t)(Lg)^* dt \\
&= \int_a^b f(t)\left[\frac{dg^*(t)}{dt} + \mathbb{A}^* g^*(t)\right] dt \\
&= \int_a^b f(t)\frac{dg^*(t)}{dt} dt + \int_a^b f(t)\mathbb{A}^* g^*(t) dt \\
&= -\int_a^b \frac{df(t)}{dt} g^*(t) dt + \int_a^b f(t)\mathbb{A}^* g^*(t) dt \\
&= \int_a^b g^*(t)\left[-\frac{df(t)}{dt} + \mathbb{A}^H f(t)\right] dt \\
&= \left\langle g^*, (-\frac{df(t)}{dt} + \mathbb{A}^H f(t))^* \right\rangle \\
&= \left\langle g, -\frac{df(t)}{dt} + \mathbb{A}^H f(t) \right\rangle^* \\
&= \left\langle -\frac{df(t)}{dt} + \mathbb{A}^H f(t),\, g \right\rangle \\
&= \left\langle \left(-\frac{d}{dt} + \mathbb{A}^H\right) f,\, g \right\rangle,
\end{aligned}$$

where $\mathbb{A}^H = \mathbb{A}^{*\dagger}$ and the fact that $[f(t)g^*(t)]_{t=a}^b$ vanishes due to the boundary conditions was used. Then, the Gâteaux derivative can be rewritten as $\mathcal{M}'(f;\, f') = \langle L^\dagger u^\dagger, u'\rangle$. Therefore,

$$\nabla \mathcal{M} = u^\dagger.$$

Hence, the gradient direction $\nabla\mathcal{M}$ can be conveniently expressed in terms of the solution to the following adjoint system:

$$\begin{aligned}
L^\dagger u^\dagger &= \left(-\frac{d}{dt} + \mathbb{A}^H\right) u^\dagger \\
&= -\frac{d}{dt} u^\dagger + \mathbb{A}^H u^\dagger \\
&= -\frac{d}{dt} u^\dagger + (-iAC + \nu B)^H u^\dagger \\
&= \begin{bmatrix} w(t,k_1)\left(S_p(k_1) - S_p^{\mathrm{NV}}(k_1)\right) u_1 \\ w(t,k_2)\left(S_p(k_2) - S_p^{\mathrm{NV}}(k_2)\right) u_2 \\ w(t,k_3)\left(S_p(k_3) - S_p^{\mathrm{NV}}(k_3)\right) u_3 \\ \vdots \\ w(t,k_N)\left(S_p(k_N) - S_p^{\mathrm{NV}}(k_N)\right) u_N \end{bmatrix}.
\end{aligned} \tag{4.12}$$

4.3.2 Numerical strategy

By using the results from the previous section, we can now delineate a recursive algorithm that generates successive updates of the force so that the cost function $\mathcal{M}$ decreases monotonically. Our goal is to find a forcing f_{opt} that minimizes the cost functional $\mathcal{M}$. By starting with an initial guess $f^{(0)}$, an approximation of the minimizer can be found by using a gradient-based descent method of the form

$$f^{(n+1)} = f^{(n)} + \tau^{(n)} \mathcal{A}\nabla\mathcal{M}(f^{(n)}),\ n = 1, 2, \cdots \tag{4.13}$$

such that $\lim_{n\to\infty} f^{(n)} = f_{opt}$, where n is the iteration count and $\tau^{(n)} \in \mathbb{R}^-$ is a constant to be determined at each iteration (for instance, by the search line method [127]. At each iteration, the descent direction $\mathcal{A}\nabla\mathcal{M}$ is computed based on the gradient of cost functional $\nabla\mathcal{M}$.

To summarize, the optimization process can be expressed in the following algorithm.

1. Choose an initial guess $f^{(0)}$; $n = 0$.
2. Solve GOY model equation with $f = f^{(n)}$.
3. Solve adjoint equation (4.12).
4. Obtain the cost functional gradient as $\nabla\mathcal{M} = u^\dagger$.
5. Find parameter $\tau^{(n)}$ through line minimization.
6. Update the control variable through (4.13); $n = n + 1$.
7. Go back to step 2.

The loop continues until the optimality condition is approximately satisfied, i.e.,

$$\nabla\mathcal{M}(f^{(n)}) \approx 0\,.$$

4.4 Application to the Sabra model

Now consider the Sabra model

$$\mathcal{S}\boldsymbol{u} \triangleq \frac{du_n}{dt} - ik_n\left(u^*_{n+1}u_{n+2} - \frac{\epsilon}{q}\,u^*_{n-1}u_{n+1} + \frac{1-\epsilon}{q^2}\,u_{n-2}u_{n-1}\right) + \nu k_n^2 u_n = f_n\,, \tag{4.14}$$

where ν is the coefficient of kinematic viscosity, ϵ is the 3D/2D selector (3D, for $\epsilon = 1/2$) and f_n is the external forcing. For any solution of Sabra model, we define the energy spectrum as

$$E(t, k_n) = \frac{1}{2}\sum_n |u_n(t)|^2\,, \tag{4.15}$$

Let $E_0(k_n)$ be the energy spectrum predicted by K41 theory, i.e.,

$$E_0(k_n) = Ck_n^{-5/3}\,, \tag{4.16}$$

where C is a constant depends only on the energy dissipation rate ε. The goal is to find a forcing f which results in a solution of the Sabra model equation (4.14) with the K41 energy spectrum $E_0(k_n)$. Define the following cost functional:

$$\mathcal{M}(f_n) \triangleq \frac{1}{2\,T}\int_0^T \sum_{n=1}^{N} w(t,k_n)\left(E(t,k_n) - E_0(k_n)\right)^2 dt\,. \tag{4.17}$$

where $w(t,k_n)$ is a positive weight function. We may state our optimization problem as follows:

$$\min_f \mathcal{M}(f)\,, \tag{4.18}$$

Now, we are ready to formulate the optimization problem for the Sabra model. The goal is to find a forcing $f_{\rm opt}$ that minimizes the cost functional $\mathcal{M}$. Starting with an initial guess $f^{(0)}$, an approximation of the minimizer can be found using a gradient-based descent method (4.13). The necessary condition characterizing the minimizer f_{opt} of the cost functional is defined in (4.9), where the Gâteaux differential is defined in (4.6). By substituting from (4.15) and (4.17) into (4.6), we have

$$\mathcal{M}'(f;f') = \frac{1}{T}\int_0^T \sum_{n=1}^{N} w(t,k_n)\left(E(t,k_n) - E_0(k_n)\right)\left(u_n.u_n'^{*} + u_n'.u_n^{*}\right) dt\,, \tag{4.19}$$

where u_n' is the solution of the Sabra model equation linearized around the state u_n , i.e.,

$$\begin{aligned} S\boldsymbol{u'} \;\triangleq\; & \frac{du_n'}{dt} - ik_n((u_{n+2}u_{n+1}'^{*} + u_{n+2}'u_{n+1}^{*}) - \frac{\epsilon}{q}(u_{n+1}u_{n-1}'^{*} + u_{n+1}'u_{n-1}^{*})) \\ & -i\,\frac{1-\epsilon}{q^2}\,k_n\left(u_{n-1}u_{n-2}' + u_{n-1}'u_{n-2}\right) + \nu k_n^2 u_n' = f_n'\,. \end{aligned} \tag{4.20}$$

Also, the Riesz representation theorem guarantees the existence of a unique element $\nabla\mathcal{M}$ which satisfies the identity

$$\mathcal{M}'(f;f') = (\nabla\mathcal{M}, f')\,. \tag{4.21}$$

The Gâteaux differential (4.6) can be transformed to the Riesz form using a suitably defined adjoint variable $u^\dagger$. We have

$$(u^\dagger, f') = (u^\dagger, Su') = (S^\dagger u^\dagger, u')\,, \tag{4.22}$$

where the adjoint matrix $S^\dagger$ is

$$S^\dagger u^\dagger = \begin{bmatrix} w(t,k_1)(E(t,k_1)-E_0(k_1))u_1 \\ w(t,k_2)(E(t,k_2)-E_0(k_2))u_2 \\ w(t,k_3)(E(t,k_3)-E_0(k_3))u_3 \\ \vdots \\ w(t,k_N)(E(t,k_N)-E_0(k_N))u_N \end{bmatrix} \tag{4.23}$$

We can rewrite the equation (4.20) in the block form

$$S\boldsymbol{u}' = \left(\frac{d}{dt} - iA_1 - iA_2C + \nu B\right)\boldsymbol{u}', \tag{4.24}$$

where

$$\boldsymbol{u}' = \begin{bmatrix} u_1' \\ u_2' \\ u_3' \\ \vdots \\ u_N' \end{bmatrix}, \tag{4.25}$$

$$A_1 = \begin{bmatrix} 0 & 0 & k_1u_2^* & 0 & \cdots & 0 & 0 & 0 & 0 \\ 0 & 0 & bk_2u_1^* & k_2u_3^* & \cdots & 0 & 0 & 0 & 0 \\ ck_3u_2 & ck_3u_1 & 0 & bk_3u_2^* & \cdots & 0 & 0 & 0 & 0 \\ 0 & ck_4u_3 & ck_4u_2 & 0 & \cdots & 0 & 0 & 0 & 0 \\ \vdots & \vdots & \vdots & \vdots & \ddots & \vdots & \vdots & \vdots & \vdots \\ 0 & 0 & 0 & 0 & \cdots & 0 & bk_{N-3}u_{N-4}^* & k_{N-3}u_{N-2}^* & 0 \\ 0 & 0 & 0 & 0 & \cdots & ck_{N-2}u_{N-4} & 0 & bk_{N-2}u_{N-3}^* & k_{N-2}u_{N-1}^* \\ 0 & 0 & 0 & 0 & \cdots & ck_{N-1}u_{N-2} & ck_{N-1}u_{N-3} & 0 & bk_{N-1}u_{N-2}^* \\ 0 & 0 & 0 & 0 & \cdots & 0 & ck_Nu_{N-1} & ck_Nu_{N-2} & 0 \end{bmatrix} \tag{4.26}$$

$$A_2 = \begin{bmatrix} 0 & k_1u_3 & 0 & 0 & \cdots & 0 & 0 & 0 & 0 \\ bk_2u_3 & 0 & k_2u_4 & 0 & \cdots & 0 & 0 & 0 & 0 \\ 0 & bk_3u_4 & 0 & k_3u_5 & \cdots & 0 & 0 & 0 & 0 \\ 0 & 0 & bk_4u_5 & 0 & \cdots & 0 & 0 & 0 & 0 \\ \vdots & \vdots & \vdots & \vdots & \ddots & \vdots & \vdots & \vdots & \vdots \\ 0 & 0 & 0 & 0 & \cdots & 0 & k_{N-3}u_{N-1} & 0 & 0 \\ 0 & 0 & 0 & 0 & \cdots & bk_{N-2}u_{N-1} & 0 & k_{N-2}u_N & 0 \\ 0 & 0 & 0 & 0 & \cdots & 0 & bk_{N-1}u_N & 0 & 0 \\ 0 & 0 & 0 & 0 & \cdots & 0 & 0 & 0 & 0 \end{bmatrix} \tag{4.27}$$

with the boundary conditions $u_{-1} = u_0 = u_{N+1} = u_{N+2} = 0$, and

$$C\boldsymbol{u}' = \boldsymbol{u}'^{*}, \tag{4.28}$$

$$B = \begin{bmatrix} k_1^2 & 0 & 0 & \dots & 0 \\ 0 & k_2^2 & 0 & \dots & 0 \\ 0 & 0 & k_3^2 & \dots & 0 \\ \vdots & \vdots & \vdots & \ddots & \vdots \\ 0 & 0 & 0 & \dots & k_N^2 \end{bmatrix} \tag{4.29}$$

Let us define the operator S in this form

$$S = \frac{d}{dt} + \mathbb{A}\,, \tag{4.30}$$

where

$$\mathbb{A} = -iA_1 - iA_2C + \nu B\,. \tag{4.31}$$

We have, as mentioned above, that

$$(f, Sg) = \left(\left(-\frac{d}{dt} + \mathbb{A}^H\right) f,\, g\right) = \left(S^\dagger f,\, g\right)\,.$$

Now, we have the adjoint of the operator S

$$S^\dagger = -\frac{d}{dt} + \mathbb{A}^H, \tag{4.32}$$

where $\mathbb{A}^H = \mathbb{A}^{*\dagger}$ and $[f(t)g^*(t)]_{t=a}^b$ vanishes by using integration by parts and due to the boundary conditions. Then, the adjoint operator can be used to reexpress the Gâteaux differential (4.19) as $\mathcal{M}'(f;\, f') = (S^\dagger u^\dagger, u')$. This, together with the Riesz identity (4.21), and the duality expression (4.22), implies that $\mathcal{M}'(f;\, f') = (u^\dagger, f') = (\nabla\mathcal{M}, f')$. Therefore,

$$\nabla\mathcal{M} = u^\dagger\,. \tag{4.33}$$

Hence, the gradient direction $\nabla\mathcal{M}$ can be conveniently expressed in terms of the solution of the following adjoint system:

$$\begin{aligned} S^* u^* &= \left(-\frac{d}{dt} + \mathbb{A}^H\right) u^\dagger \\ &= \left(-\frac{d}{dt} u^\dagger + \mathbb{A}^H u^\dagger\right) \\ &= \left(-\frac{d}{dt} u^\dagger + \left(-iA_1 - iA_2C + \nu B\right)^H u^\dagger\right) \end{aligned}$$

$$= \begin{bmatrix} w(t,k_1)\left(E(t,k_1)-E_0(k_1)\right)u_1 \\ w(t,k_2)\left(E(t,k_2)-E_0(k_2)\right)u_2 \\ w(t,k_3)\left(E(t,k_3)-E_0(k_3)\right)u_3 \\ \vdots \\ w(t,k_N)\left(E(t,k_N)-E_0(k_N)\right)u_N \end{bmatrix} . \tag{4.34}$$

By solving the adjoint system to compute the gradient $\nabla\mathcal{M}$, and by using the iterative process (4.13), one can find an approximation of the minimizer f_{opt}. Then, we follow the same optimization process as we mentioned above in the subsection (4.3.2).

4.5 Application to the DN model

Now consider the DN model in this form

$$\mathcal{D}\boldsymbol{u} \triangleq \frac{du_n}{dt} - ik_n\left[a\left(u_{n-1}^2 - qu_nu_{n+1}\right) + b\left(u_{n-1}u_n - qu_{n+1}^2\right)\right]^* + \nu k_n^2 u_n = f_n\,, \tag{4.35}$$

where the (*) mean the complex conjugation, ν is the coefficient of kinematic viscosity, a and b are the nonlinear interaction coefficients, and f_n is the external forcing. For any solution of DN model, we define the energy spectrum as

$$E(t,k_n) = \frac{1}{2}\sum_n |u_n(t)|^2\,, \tag{4.36}$$

Let $E_0(k_n)$ be the energy spectrum predicted by K41 theory, i.e.,

$$E_0(k_n) = Ck_n^{-5/3}\,, \tag{4.37}$$

where C is a constant that depends only on the energy dissipation rate ε. The goal is to find a forcing f which results in a solution to the DN model equation (4.35) with the K41 energy spectrum $E_0(k_n)$. Define the following cost functional:

$$\mathcal{M}(f_n) \triangleq \frac{1}{2\,T}\int_0^T \sum_{n=1}^{N} w(t,k_n)\left(E(t,k_n)-E_0(k_n)\right)^2 dt\,. \tag{4.38}$$

where $w(t,k_n)$ is a positive weight function. We may be state our optimization problem as follows:

$$\min_f \mathcal{M}(f)\,, \tag{4.39}$$

Like for previous models, we also formulate the optimization problem for the DN model. The same strategy will be used to find a forcing f_{opt} that minimizes the cost functional $\mathcal{M}$. Starting with an initial guess $f^{(0)}$, an approximation of the minimizer can be found by using a gradient-based descent method (4.13). The necessary condition characterizing

the minimizer f_{opt} of the cost functional is defined in (4.9), where the Gâteaux differential is defined in (4.6). By substituting from (4.36), and (4.38) into (4.6), we have

$$\mathcal{M}'(f;f') = \frac{1}{T}\int_0^T \sum_{n=1}^{N} w(t,k_n)\left(E(t,k_n) - E_0(k_n)\right)\left(u_n.u_n'^{*} + u_n'.u_n^{*}\right)dt\,, \tag{4.40}$$

where u_n' is the solution of the Sabra model equation linearized around the state u_n , i.e.,

$$\begin{aligned} D\boldsymbol{u}' &\triangleq \frac{du_n'}{dt} - iak_n\left(2u_{n-1}u_{n-1}' - q(u_n'u_{n+1} + u_nu_{n+1}')\right)^{*} \\ &- ibk_n\left((u_nu_{n-1}' + u_{n-1}u_n') - 2qu_{n+1}u_{n+1}'\right)^{*} + \nu k_n^2 u_n' = f_n'\,. \end{aligned} \tag{4.41}$$

The Riesz representation theorem guarantees the existence of a unique element $\nabla\mathcal{M}$ which satisfies the identity

$$\mathcal{M}'(f;f') = (\nabla\mathcal{M}, f')\,. \tag{4.42}$$

The Gâteaux differential (4.6) can be transformed in order to enable the use of the Riesz form representation. By introducing a suitably defined adjoint variable $u^{\dagger}$, we have

$$(u^{\dagger}, f') = (u^{\dagger}, Du') = (D^{\dagger}u^{\dagger}, u')\,, \tag{4.43}$$

where the adjoint matrix $D^{\dagger}$ is

$$D^{\dagger}u^{\dagger} = \begin{bmatrix} w(t,k_1)(E(t,k_1) - E_0(k_1))u_1 \\ w(t,k_2)(E(t,k_2) - E_0(k_2))u_2 \\ w(t,k_3)(E(t,k_3) - E_0(k_3))u_3 \\ \vdots \\ w(t,k_N)(E(t,k_N) - E_0(k_N))u_N \end{bmatrix}. \tag{4.44}$$

We can rewrite the equation (4.41) as a matrix,

$$D\boldsymbol{u}' = \left(\frac{d}{dt} - iAC + \nu B\right)\boldsymbol{u}' \tag{4.45}$$

where

$$\boldsymbol{u}' = \begin{bmatrix} u_1' \\ u_2' \\ u_3' \\ \vdots \\ u_N' \end{bmatrix}, \tag{4.46}$$

$$A^* = \begin{bmatrix} a_{1,1} & a_{1,2} & 0 & 0 & \cdots & 0 & 0 & 0 & 0 \\ a_{2,1} & a_{2,2} & a_{2,3} & 0 & \cdots & 0 & 0 & 0 & 0 \\ 0 & a_{3,2} & a_{3,3} & a_{3,4} & \cdots & 0 & 0 & 0 & 0 \\ 0 & 0 & a_{4,3} & a_{4,4} & \cdots & 0 & 0 & 0 & 0 \\ \vdots & \vdots & \vdots & \vdots & \ddots & \vdots & \vdots & \vdots & \vdots \\ 0 & 0 & 0 & 0 & \cdots & a_{N-3,N-3} & a_{N-3,N-2} & 0 & 0 \\ 0 & 0 & 0 & 0 & \cdots & a_{N-2,N-3} & a_{N-2,N-2} & a_{N-2,N-1} & 0 \\ 0 & 0 & 0 & 0 & \cdots & 0 & a_{N-1,N-2} & a_{N-1,N-1} & a_{N-1,N} \\ 0 & 0 & 0 & 0 & \cdots & 0 & 0 & a_{N,N-1} & a_{N,N} \end{bmatrix} \tag{4.47}$$

where the coefficients of the matrix are

$$\begin{aligned} a_{1,1} &= k_1(-aqu_2 + bu_0), \quad a_{1,2} = -qk_1(au_1 + 2bu_2) \\ a_{2,1} &= k_2(2au_1 + bu_2), \quad a_{2,2} = k_2(-aqu_3 + bu_1), \quad a_{2,3} = -qk_2(au_2 + 2bu_3) \\ a_{3,2} &= k_3(2au_2 + bu_3), \quad a_{3,3} = k_3(-aqu_4 + bu_2), \quad a_{3,4} = -qk_3(au_3 + 2bu_4) \\ a_{4,3} &= k_4(2au_3 + bu_4), \quad a_{4,4} = k_4(-aqu_5 + bu_3) \\ a_{N-3,N-3} &= k_{N-3}(-aqu_{N-2} + bu_{N-4}), \quad a_{N-3,N-2} = -qk_{N-3}(au_{N-3} + 2bu_{N-2}) \\ a_{N-2,N-3} &= k_{N-2}(2au_{N-3} + bu_{N-2}), \quad a_{N-2,N-2} = k_{N-2}(-aqu_{N-1} + bu_{N-3}) \\ a_{N-2,N-1} &= -qk_{N-2}(au_{N-2} + 2bu_{N-1}), \quad a_{N-1,N-2} = k_{N-1}(2au_{N-2} + bu_{N-1}) \\ a_{N-1,N-1} &= k_{N-1}(-aqu_N + bu_{N-2}), \quad a_{N-1,N} = -qk_{N-1}(au_{N-1} + 2bu_N) \\ a_{N,N-1} &= k_N(2au_{N-1} + bu_N), \quad a_{N,N} = k_N(-aqu_{N+1} + bu_{N-1}) \end{aligned} \tag{4.48}$$

with the boundary conditions $u_{-1} = u_0 = u_{N+1} = u_{N+2} = 0$, and

$$C\boldsymbol{u}' = \boldsymbol{u}'^*, \tag{4.49}$$

$$B = \begin{bmatrix} k_1^2 & 0 & 0 & \dots & 0 \\ 0 & k_2^2 & 0 & \dots & 0 \\ 0 & 0 & k_3^2 & \dots & 0 \\ \vdots & \vdots & \vdots & \ddots & \vdots \\ 0 & 0 & 0 & \dots & k_N^2 \end{bmatrix}. \tag{4.50}$$

Let define the operator D in this form

$$D = \frac{d}{dt} + \mathbb{A}\,, \tag{4.51}$$

where

$$\mathbb{A} = -iAC + \nu B\,. \tag{4.52}$$

We have, as mentioned above, that

$$(f, Dg) = \left(\left(-\frac{d}{dt} + \mathbb{A}^H\right) f,\, g\right) = \left(D^\dagger f,\, g\right) .$$

Now, we have the adjoint of the operator D

$$D^\dagger = -\frac{d}{dt} + \mathbb{A}^H , \tag{4.53}$$

where $\mathbb{A}^H = \mathbb{A}^{*\dagger}$ and $[f(t)g^*(t)]_{t=a}^b$ vanishes by using integration by parts, and due to the boundary conditions. Then, the adjoint operator can be used to reexpress Gâteaux differential (4.40) as $\mathcal{M}'(f;\, f') = (D^\dagger u^\dagger, u')$. This, together with the Riesz identity (4.42), and the duality expression (4.43) implies that $\mathcal{M}'(f;\, f') = (u^\dagger, f') = (\nabla\mathcal{M}, f')$. Therefore,

$$\nabla\mathcal{M} = u^\dagger . \tag{4.54}$$

Hence, the gradient direction $\nabla\mathcal{M}$ can be conveniently expressed in terms of the solution of the following adjoint system:

$$\begin{aligned} D^* u^* &= \left(-\frac{d}{dt} + \mathbb{A}^H\right) u^\dagger \\ &= \left(-\frac{d}{dt} u^\dagger + \mathbb{A}^H u^\dagger\right) \\ &= \left(-\frac{d}{dt} u^\dagger + \left(-iAC + \nu B\right)^H u^\dagger\right) \\ &= \begin{bmatrix} w(t,k_1)\left(E(t,k_1) - E_0(k_1)\right) u_1 \\ w(t,k_2)\left(E(t,k_2) - E_0(k_2)\right) u_2 \\ w(t,k_3)\left(E(t,k_3) - E_0(k_3)\right) u_3 \\ \vdots \\ w(t,k_N)\left(E(t,k_N) - E_0(k_N)\right) u_N \end{bmatrix} . \end{aligned} \tag{4.55}$$

By solving the adjoint system to compute the gradient $\nabla\mathcal{M}$, and by using the iterative process (4.13), one can find an approximation of the minimizer f_{opt}. Then, we follow the same optimization process as we mentioned above in the subsection (4.3.2).

4.6 The adjoint of linear and antilinear operators

In this section, we will discuss a central issue for this work related to the adjoint operator of an operator which is the sum of a linear operator with an antilinear operator. This scenario arises, for example, in (4.12).

4.6.1 Basic constructs

In this section, we present the building blocks required to address the challenge of this section. Although, we are focused in the context of the main problem of this work, these results are of independent interest. To the best of our knowledge, they have not been reported in the literature.

4.6.1.1 The Hermitien transpose of matrix with complex entries

Let A be a m-by-n matrix with complex entries. The transpose of A, denoted by A^T, is the matrix defined by $\left(A^T\right)_{ij} = A_{ji}$, where $(A)_{ij}$ represents the $(i,j)-$th entry of A ($i = 1, 2, \cdots, m$; $j = 1, 2, \cdots, n$). By taking the complex conjugate of each entry in A^T, we obtain the so-called Hermitien transpose or adjoint of A, i.e., $A^H = \overline{A^T}$. Of course, $A^H = \left(\overline{A}\right)^T$, and $\left(A^H\right)_{ij} = \overline{A_{ji}}$.

4.6.1.2 The inner product of two complex vectors

The complex inner product of two complex vectors $v = (v_1, \cdots, v_n) \in \mathbf{C}^n$, and $w = (w_1, \cdots, w_n) \in \mathbf{C}^n$ is defined by

$$\langle v, w \rangle = \sum_{i=1}^{n} v_i \overline{w}_i \, .$$

The following algebraic properties,one has:

- $\langle v, w + u \rangle = \langle v, w \rangle + \langle v, u \rangle \ , \quad \forall v, w, u \in \mathbf{C}^n$
- $\langle v, w \rangle = \overline{\langle w, v \rangle} \, , \quad \forall v, w \in \mathbf{C}^n$
- $\langle cv, w + u \rangle = c \, \langle v, w \rangle \ , \quad \forall c \in \mathbf{C} \quad \forall v, w, u \in \mathbf{C}^n$
- $\langle v, cu \rangle = \overline{c} \, \langle v, w \rangle \ , \quad \forall c \in \mathbf{C} \quad \forall v, w \in \mathbf{C}^n$

By using Einstein's summation notation (repeated indices are summed over), from the previous definitions, we concluded that

$$\langle Av, w \rangle = (Av)_i \overline{w}_i = A_{ij} v_j \overline{w}_i = v_j A_{ij} \overline{w}_i = v_i A_{ji} \overline{w}_j = v_i \overline{(A^H)_{ij}} \overline{w}_j = \left\langle v, A^H w \right\rangle \, ,$$

i.e.

$$\langle Av, w \rangle = \left\langle v, A^H w \right\rangle \, , \forall v, w \in \mathbf{C}^n .$$

For the derivation of this equality, it was important the linearity (here, implicitly assumed) of A :

$$A(v + w) = Av + Aw, \quad \forall v, w \in \mathbf{C}^n,$$

and

$$A(cv) = cAv, \quad \forall c \in \mathbf{C} \quad \forall v \in \mathbf{C}^n.$$

4.6.1.3 Antilinear operators

The previous developments becomes quite different, if the operator A is antilinear. An antilinear operator is defined by $A(v + w) = Av + Aw$, and $A(cv) = \overline{c}Av$, $\forall c \in \mathbf{C}$ $\forall v, w \in \mathbf{C}^n$. An example of an antilinear operator is $\mathcal{C}z = \overline{z}$ (complex conjugate). In fact, $\mathcal{C}(z + w) = \overline{z} + \overline{w} = \mathcal{C}z + \mathcal{C}w$, and $\mathcal{C}(cz) = \overline{c}\,\overline{z} = \overline{c}\mathcal{C}z$.

4.6.1.4 Adjoint of antilinear operators

The definition of Hermitien transpose or adjoint, A^H, for an antilinear operator, A, is defined by

$$\langle Av, w\rangle = \overline{\langle v, A^H w\rangle}\,, \quad \forall v, w \in \mathbf{C}^n.$$

Here, the complex conjugation on the r.h.s. is present in order to compensate the complex conjugation of scalar c.

4.6.1.5 Adjoint of the sum of a linear operator with an antilinear operator

Consider the operator $M = A + B$, where A is a linear operator and B is an antilinear operator. Of course, we have

$$M(v + w) = A(v + w) + B(v + w) = Av + Aw + Bv + Bw = M(v) + M(w),$$

but

$$M(cv) = A(cv) + B(cv) = cA(v) + \overline{c}B(v).$$

So, if we want to define the adjoinct operator for M, we must have

$$\langle Mv, w\rangle = \langle Av + Bv, w\rangle = \langle Av, w\rangle + \langle Bv, w\rangle = \left\langle v, A^H w\right\rangle + \overline{\langle v, B^H w\rangle}\,.$$

Due to the complex conjugation that appears in the rightmost term in this last equality, we can not write an equality of type

$$\langle Mv, w\rangle = \langle v, \bigstar\rangle\ ,$$

where the object "$\bigstar$" would serve to define the adjoint operator of M. Not being the case, the alternative we have for determining the adjoint operator of the linearized GOY model (for example) is to write the linearized operator in its real form, that is, to obtain the equations for the temporal evolution of its real and imaginary parts.

4.7 Application to the real GOY model

Here, we start with the GOY model (4.8) and write its real and its imaginary parts. For this, we introduce the notation $u_n = a_n + ib_n$, with $a_n, b_n \in \mathbb{R}$. Then, the equation (4.8) is equivalent to the pair ($f_n = f_n^r + i\, f_n^i$, $f_n^r, f_n^i \in \mathbb{R}$):

$$\begin{cases} \frac{da_n}{dt} = k_n \left[a_{n+1}b_{n+2} + a_{n+2}b_{n+1} + A\left(a_{n+1}b_{n-1} + a_{n-1}b_{n+1}\right) + B\left(a_{n-1}b_{n-2} + Ba_{n-2}b_{n-1}\right)\right] - \nu k_n^2 + f_n^r\,, \\ \\ \frac{db_n}{dt} = k_n \left[\left(a_{n+1}a_{n+2} - b_{n+1}b_{n+2}\right) + A\left(a_{n-1}a_{n+1} - b_{n-1}b_{n+1}\right) + B\left(a_{n-2}a_{n-1} - b_{n-2}b_{n-1}\right)\right] + f_n^i\,, \end{cases}$$

where we put $A = -\epsilon/q$, and $B = (\epsilon - 1)/q^2$. In the pair of real variables (a_n, b_n), the Gâteaux derivative of the objective functions (4.11) is written down as follows:

$$\mathcal{M}'(f; f') = \frac{1}{T}\sum_{n=1}^{N} S(n) \int_0^T \left(a_n a_n' + b_n b_n'\right) dt\,, \tag{4.56}$$

where $u_n' = a_n' + ib_n'$ is the solution of the linearization of the GOY model around the state $u_n = a_n + ib_n$, and their temporal dynamics is given by the following equations

$$\begin{cases} \frac{da_n^{'}}{dt} &= k_n[\mathrm{a}_{n+2}^{'}b_{n+1} + \mathrm{a}_{n+1}^{'}b_{n+2} + a_{n+2}\mathrm{b}_{n+1}^{'} + a_{n+1}b_{n+2}^{'} + \\ & \quad A(a_{n+1}\mathrm{b}_{n-1}^{'} + a_{n-1}\mathrm{b}_{n+1}^{'} + \mathrm{a}_{n+1}^{'}b_{n-1} + \mathrm{a}_{n-1}^{'}b_{n+1}) \\ & \quad B(a_{n-1}\mathrm{b}_{n-2}^{'} + a_{n-2}\mathrm{b}_{n-1}^{'} + \mathrm{a}_{n-1}^{'}b_{n-2} + \mathrm{a}_{n-2}^{'}b_{n-1})] - \nu k_n^2 + f_n^{'r} \\ \\ \frac{db_n^{'}}{dt} &= k_n[a_{n+2}\mathrm{a}_{n+1}^{'} + a_{n+1}\mathrm{a}_{n+2}^{'} - b_{n+2}\mathrm{b}_{n+1}^{'} - b_{n+1}\mathrm{b}_{n+2}^{'} + \\ & \quad A(a_{n+1}\mathrm{a}_{n-1}^{'} + a_{n-1}\mathrm{a}_{n+1}^{'} - b_{n+1}\mathrm{b}_{n-1}^{'} - b_{n-1}\mathrm{b}_{n+1}^{'}) \\ & \quad B(a_{n-1}\mathrm{a}_{n-2}^{'} + a_{n-2}\mathrm{a}_{n-1}^{'} - b_{n-1}\mathrm{b}_{n-2}^{'} - b_{n-2}\mathrm{b}_{n-1}^{'})] + f_n^{'i} \end{cases}$$

With the GOY model written in these real variables, the difficulty of the definition of the adjoint operator disappears. It is worth noting here that, since the usual internal products in $\mathbb{R}^n$, and $\mathbb{C}^n$ are intrinsically distinct, these two problems, with respect to the adjoint operator, are not comparable.

Chapter 5

Maximum principle for the optimal control of the Obukhov model

In this chapter, we discuss and prove a Pontryagin maximum principle for the simplest Obukhov shell model with the state constraints restricted to $N = 3$.

The aim of this chapter is to obtain the optimal solution for an optimal-control problem in which the dynamics are given by the Obukhov model with a given initial value for the state variable by using the necessary conditions of optimality in the form of a Maximum Principle.

As it will be seen below, the complexity inherent to the use of these optimality conditions depends strongly on the initial conditions of the state variable. For some sets of conditions, it is not difficult to simplify the resulting equations so that we may arrive to the optimal solution analytically. However, for other classes of values, this is not possible and we have to resort to numerical methods. In a first instance, we consider an algorithm of the shooting-type to solve the problem. In a second instance, we consider a relaxed version of the problem equivalent to a optimum control process to which we formulate an algorithm of the steepest descent type.

5.1 Problem formulation

In this section, we state the optimal-control problem for which the dynamics takes the form of Obukhov shell model restricted to $N = 3$ with a given initial condition for the state variable.

We consider the following optimal-control problem

$$(P) \quad \text{Minimize} \qquad J[x,u] \equiv \frac{1}{2}\int_0^T \left[(x_1(t)-1)^2 + (x_2(t)-1)^2 + (x_3(t)-1)^2\right] dt \tag{5.1}$$

$$\text{subject to} \quad \begin{cases} \dot{x} = F(x) + u, \\ u \in \Omega, \\ x(0) = x_0 \end{cases} \tag{5.2}$$

where $\Omega = col([-M, M], \{0\}, \{0\})$, and

$$F(x) = \begin{bmatrix} 2\rho x_2 x_3 - \lambda x_1 \\ -\rho x_1 x_3 - \lambda x_2 \\ -\rho x_1 x_2 - \lambda x_3 \end{bmatrix}. \tag{5.3}$$

Here, J is a cost function, u is a measurable control, $M > 0$, $x(0)$ is the initial point, and $t \in [0, T]$.

5.2 Application of the maximum principle

Let us first state the necessary conditions of optimality in the form of a maximum principle of Pontryagin for this problem. If (x^*, u^*) is an optimal control process for (P), then, there is a nontrivial multiplier specified by the adjoint function p, $p = col(p_1, p_2, p_3)$, satisfying $\mathcal{L}$-a.e. the adjoint differential equation

$$-\dot{p}^T(t) = \frac{\partial H}{\partial x}(x^*(t), p(t), u^*(t)) = p^T D_x F(x^*(t)) - (x^*(t) - \mathbf{1})^T, \tag{5.4}$$

with the transversality condition

$$p(T) = 0, \tag{5.5}$$

and the optimal control u^* satisfies the maximum condition $\mathcal{L}$-a.e.

$$H\left(x^*(t), p(t), u^*(t)\right) = \max_{u \in \Omega} \left\{H\left(x^*(t), p(t), u\right)\right\}. \tag{5.6}$$

Here, $\mathbf{1}^T = (1, 1, 1)$, and $D_x F(x)$ the Jacobian of the function $F(x)$ is defined as

$$D_x F(x) = \begin{bmatrix} -\lambda & 2\rho x_3 & 2\rho x_2 \\ -\rho x_3 & -\lambda & -\rho x_1 \\ -\rho x_2 & -\rho x_1 & -\lambda \end{bmatrix}, \tag{5.7}$$

and H is designated the Pontryagin function defined by

$$H(x, p, u) = p^T \left[F(x) + u\right] - \frac{1}{2} \sum_{i=1}^{3} (x_i - 1)^2. \tag{5.8}$$

From the maximum condition, we conclude that the control u^* that maximizes (5.6) is given by

$$u^*(t) = M\, col(\text{sign}(p_1(t)), 0, 0)\,, \tag{5.9}$$

where

$$sign(a) = \begin{cases} -1 & \text{if} \quad a < 0\,, \\ 1 & \text{if} \quad a > 0\,, \\ 0 & \text{if} \quad a = 0\,, \end{cases} \tag{5.10}$$

Since the system is time invariant, the Pontryagin function is constant along the optimal control process, that is

$$H(x^*, p^*, u^*) = \text{constant}, \text{ for all } t \in [0, T]. \tag{5.11}$$

Let us confirm this fact. We have, Lebesgue a.e.,

$$\begin{aligned} 0 &= \frac{dH}{dt}(x^*(t), p^*(t), u^*(t)) \\ &= \dot{p}^T(t)[F(x^*(t)) + u^*(t)] + p^T(t)\frac{d}{dt}[F(x^*(t)) + u^*(t)] - (x^*(t) - \mathbf{1})^T[F(x^*(t)) + u^*(t)] \\ &= [-p^T(t)D_xF(x^*(t)) + (x^*(t) - \mathbf{1})][F(x^*(t)) + u^*(t)] \\ &\qquad + p^T(t)\,[D_xF(x^*(t))[F(x^*(t)) + u^*(t)] + \dot{u}^*(\,t)] \\ &\qquad - (x^*(t) - \mathbf{1})^T[F(x^*(t)) + u^*(t)] \\ &= p^T(t)\dot{u}^*(t)\,, \end{aligned}$$

which confirms the constancy $\mathcal{L}$-a.e. of the Pontryagin function since u^* is segmentwise constant.

In the next subsections, we will use these conditions in order to derive the solution analytically for two examples of initial conditions of increasing complexity.

5.2.1 The case of $x_2(0) = x_3(0) = 0$

In this section, we apply the results of the previous section for the case $x_2(0) = x_3(0) = 0$. We clearly have $x_2(t) \equiv x_3(t)$ and, as a consequence, the dynamics will depend linearly on either of these variables, which, given the initial condition will be $x_2(t) = x_3(t) \equiv 0$. Thus, the optimal control problem becomes

$$\begin{aligned} \text{Minimize} \qquad & J\,[x, u] \equiv \frac{1}{2}\int_0^T (x_1(t) - 1)^2 dt \\ \text{subject to} \qquad & \dot{x}_1 = -\lambda x_1 + u \;\; \mathcal{L} - \text{-a.e.}, \qquad (5.12) \\ & x_1(0) = x_{1,0}, \quad u(t) \in [-M, M] \; \mathcal{L} - \text{-a.e.} \qquad (5.13) \end{aligned}$$

For this case, the Pontryagin function becomes

$$H(x, p, u) = p_1(-\lambda x_1 + u) - \frac{1}{2}(x_1 - 1)^2, \tag{5.14}$$

The maximum condition states that $u^*(t)$ maximizes the map

$$u \to p_1(t)u\,,$$

on $[-M, M]$ $\mathcal{L}$-a.e., where p_1 satisfies the adjoint system

$$\dot{p}_1 = \lambda p_1 + x_1^* - 1, \quad \text{with} \quad p_1(T) = 0. \tag{5.15}$$

Now, let us consider that the time interval is $[\tau, t]$, and compute the solution to the adjoint system. We have

$$p_1(t) = e^{\lambda(t-\tau)}p_1(\tau) + \int_\tau^t e^{\lambda(t-s)}(x_1^*(s) - 1)ds, \tag{5.16}$$

and, from the transversality condition, we obtain

$$0 = p_1(T) = e^{\lambda(T-\tau)}p_1(\tau) + \int_\tau^T e^{\lambda(T-s)}(x_1^*(s) - 1)ds, \tag{5.17}$$

Then, by eliminating the initial condition, we conclude that

$$p_1(t) = -\int_t^T e^{\lambda(t-s)}(x_1^*(s) - 1)ds. \tag{5.18}$$

Let us now use these conditions to solve the optimal control problem. First, note that, by solving (5.12) on $[t_1, t_2] \subset [0, T]$ $(t_2 \geq t_1)$ with $u(t) \equiv \beta$, we obtain

$$x_1(t_2) = e^{-\lambda(t_2-t_1)}\left(x_1(t_1) - \frac{\beta}{\lambda}\right) + \frac{\beta}{\lambda} \tag{5.19}$$

In what follows, let $\varepsilon > 0$ sufficiently small and consider $\forall \tau \in (T - \varepsilon, T]$. Take some τ_2 and τ_1 such that $T \geq \tau_2 \geq \tau_1 \geq T - \varepsilon$.

Now, we may consider three possibilities:

1) $x_1^*(T) = 1$. In this case, we conclude that $\dot{p}_1(t)_{|t=T} = 0$ and no information is provided concerning the sign of p_1 in a close neighborhood of T. By definition of the function *sign*, we have $u^*(t)_{|t=T} = 0$, and, hence, $\dot{x}_1^*(t) = -\lambda x_1^*(t)$ for $t = T$. This leads to the fact that, for values of t arbitrarily close to T, we have $x_1^*(t) = e^{\lambda(T-t)}x_1^*(T) > 1$. This is precisely the next case.

2) $\forall\ x_1^*(\tau) > 1$ (by this, it is meant that, for τ arbitrarily close to T, we may have $x_1^*(\tau) > 1$, and τ may also be arbitrarily close to T).

   We have $p_1(\tau) < 0$ and, thus, $u^*(\tau) = -M$. Then, by (5.19) with $\beta = -M$, $\forall \tau_2 > \tau_1 > \tau$, we have

$$x_1^*(\tau_2) = -\frac{M}{\lambda} + e^{-\lambda(\tau_2-\tau_1)}\left(x_1^*(\tau_1) + \frac{M}{\lambda}\right). \tag{5.20}$$

Since $x_1^*(\cdot)$ is decreasing, and noting that

$$x_1^*(\tau_2) - x_1^*(\tau_1) = \left(e^{-\lambda(\tau_2-\tau_1)} - 1\right)\left(x_1^*(\tau_1) + \frac{M}{\lambda}\right) < 0\,,$$

we conclude that $x^*(t) > 1\ \forall t$. This implies that $p(t) < 0\ \forall t \in [0,T)$, and hence $u^*(t) = -M$ for all $t \in [0,T)$.

3) $\forall\ x_1^*(\tau) < 1$ (by this, it is meant that, for τ arbitrarily close to T, we have $x_1^*(\tau) < 1$, and τ may also be arbitrarily close to T).

We have $p_1(\tau) > 0$ and the control $u^*(\tau) = M$. Now, similarly to the previous case, we have by (5.19) with $\beta = M$, that $\forall \tau_2 > \tau_1 > \tau$,

$$x_1^*(\tau_2) - x_1^*(\tau_1) = \left(e^{-\lambda(\tau_2-\tau_1)} - 1\right)\left(x_1^*(\tau_1) - \frac{M}{\lambda}\right). \tag{5.21}$$

Now, we have may consider two possibilities:

a) If $M\lambda^{-1} > 1$, then, since for $x_1^*(\tau) < 1$, but arbitrarily close to 1, we have $1 > x_1^*(\tau_2) > x_1^*(\tau_1)$. Thus, $x_1^*(t) \le 1$, and $u^*(t) = M$, $\forall\ t \in [0,T]$. The optimal trajectory is

$$x_1^*(t) = e^{-\lambda t}x_1^*(0) + \left(1 - e^{-\lambda t}\right)\frac{M}{\lambda},\ \text{where } x_1^*(0) = x_{1,0}. \tag{5.22}$$

b) If $M\lambda^{-1} < 1$, then, since $M\lambda^{-1} < x_1^*(\tau) < 1\ \forall\ \tau \in (T-\epsilon, T]$, we have, for $\tau_2 > \tau_1 > \tau$,

$$\begin{aligned} x_1^*(\tau_2) - x_1^*(\tau_1) &= \frac{M}{\lambda}\left(1 - e^{-\lambda(\tau_2-\tau_1)}\right) - x_1^*(\tau_1)\left(1 - e^{-\lambda(\tau_2-\tau_1)}\right), \\ &= \left(\frac{M}{\lambda} - x_1^*(\tau_1)\right)\left(1 - e^{-\lambda(\tau_2-\tau_1)}\right) < 0. \end{aligned} \tag{5.23}$$

Since $x_1^*(\tau_1) > x_1^*(\tau_2)$, we will try to assert the existence of $t^* \in (0,T)$ for which $x_1^*(t^*) = 1$. Let us assume that such t^* exists. Since $u^*(t) = M\ \forall\, t \in (t^*, T)$, we have

$$x_1^*(T) = \frac{M}{\lambda} + e^{-\lambda(T-t^*)}\left(x_1^*(t^*) - \frac{M}{\lambda}\right) = \frac{M}{\lambda} + e^{-\lambda(T-t^*)}\left(1 - \frac{M}{\lambda}\right).$$

From here, we conclude that

$$t^* = T - \frac{1}{\lambda}\ln\left(\frac{1 - \frac{M}{\lambda}}{x_1^*(T) - \frac{M}{\lambda}}\right) < T. \tag{5.24}$$

Then, we conclude that, if $u^*(t) = M\ \forall\ t \in (t^* - \epsilon, t^*)$, $x_1^*(t) > 1$. However, this contradicts the maximum condition. Thus, we should have a control switch,

i.e., $u^*(t) = -M$ for $t < t^*$. It is straightforward to conclude that $t^* > 0$ if and only if

$$x_1^*(T) > \frac{M}{\lambda} + e^{-\lambda T}\left(1 - \frac{M}{\lambda}\right).$$

Let us assume that this inequality holds. Then, by solving the state differential equation in $[0, t^*)$, we obtain

$$x_1^*(t) = e^{\lambda(t^*-t)} + \frac{M}{\lambda}\left(e^{\lambda(t^*-t)} - 1\right) > 1.$$

This implies that, under the considered conditions and assumptions, the maximum condition holds in $[0, t^*)$ with $u^*(t) = -M$ and the optimal control is given by $u^*(t) = -M$ in $[0, t^*)$ and $u^*(t) = M$ in $[t^*, T]$.

5.3 The case $x_2(0) = x_3(0) \neq 0$

By inspection of the control system dynamic, we conclude that $x_2(t) = x_3(t)$ for all $t \in [0, T]$, independently of the control function and of the value of $x_1(0)$. Thus, the optimal control problem can be reduced to the following

$$\begin{aligned}
\text{Minimize} \quad & \frac{1}{2}\int_0^T \left[(x_1(t)-1)^2 + 2(x_2(t)-1)^2\right] dt \\
\text{subject to} \quad & \dot{x}_1 = 2\rho x_2^2 - \lambda x_1 + u, \quad x_1(0) = x_{1,0} \in (0, 1] \\
& \dot{x}_2 = -(\rho x_1 + \lambda)x_2, \quad x_2(0) = x_{2,0} \in (0, 1] \\
& u(t) \in [-M, M].
\end{aligned}$$

In this discussion, we consider $M > 0$ sufficiently large to ensure the system's controllability, $\lambda > 0$ small to ensure low dissipativity, and $\rho > \lambda$. These relations will be detailed later in the course of the analysis required to characterize the solution with the help of the maximum principle.

As we shall see, given the number of parameters and the nonlinearities of the differential equations, the complexity of the analysis for this example is significantly greater than that for the previous example. Since the type of arguments are similar in nature, our analysis of this example will be much less detailed in terms of specifying estimates and of a more qualitative nature in the determination of the features of an extremal which is a plausible candidate to solve the optimal control problem.

For later convenience, we obtain the state trajectories by integrating the dynamics

$$x_1(t) = e^{-\lambda(t-\tau)}x_1(\tau) + \int_\tau^t e^{-\lambda(t-s)}\left[2\rho x_2^2(s) + u(s)\right] ds, \quad \forall \tau \in [0, T] \tag{5.25}$$

$$x_2(t) = x_2(\tau)e^{-\int_\tau^t (\rho x_1(s) + \lambda) ds}, \quad \forall \tau \in [0, T] \tag{5.26}$$

$$x_1(t) = e^{\lambda(T-t)}x_1(T) - \int_t^T e^{\lambda(s-t)}\left[2\rho x_2^2(s) + u(s)\right] ds, \quad \forall t \in [0,T] \tag{5.27}$$

$$x_2(t) = x_2(T)e^{\int_t^T(\rho x_1(s)+\lambda)ds}, \quad \forall t \in [0,T]. \tag{5.28}$$

By examining the cost functional, and the dynamics, we see that a candidate to solution should take on positive values. Moreover, by considering (5.28), we conclude that x_2 is strictly decreasing. We observe also that the monotonicity of x_1 depends on u. If $u(t) = M$ in a certain interval, then x_1 is strictly increasing in that interval.

Let us now write down the conditions of the maximum principle. We have the Pontryagin function

$$H(x,u,p) = p_1[2\rho x_2^2 - \lambda x_1 + u] - p_2[(\rho x_1 + \lambda)x_2] - \frac{1}{2}(x_1-1)^2 - (x_2-1)^2,$$

the adjoint system

$$\dot{p}_1 = \lambda p_1 + \rho p_2 + (x_1 - 1), \quad p_1(T) = 0 \tag{5.29}$$

$$\dot{p}_2 = (\rho x_1 + \lambda)p_2 - 4\rho p_1 x_2 + 2x_2 - 2, \quad p_2(T) = 0, \tag{5.30}$$

and the optimal control u^* maximizes the map $v \to H(x^*(t), v, p(t))$ $[0,T] - \mathcal{L}$-a.e.. The later condition means that $u^*(t) = col(M\text{sgn}(p_1(t)), 0, 0)$. Again, for later convenience, we compute the adjoint functions

$$p_1(t) = -\int_t^T e^{-\lambda(s-t)}[\rho p_2(s) + x_1(s) - 1]ds, \tag{5.31}$$

$$p_2(t) = -\int_t^T e^{-\int_t^s(\rho x_1(\sigma)+\lambda)d\sigma}[4\rho p_1(s)x_2(s) + 2x_2(s) - 2]ds. \tag{5.32}$$

Consider some $\varepsilon > 0$ arbitrarily small and any $\tau \in (T-\varepsilon, T]$. It is clear that for ε sufficiently small, we have $\dot{p}_1(\tau) < 0$, and, thus, $p_1(\tau) > 0$ on $(T-\varepsilon, T]$. Then, by the maximum condition, $u(\tau) = M$. From the observations above just before the statement of the maximum principle, we conclude that x_1 is strongly increasing, while x_2 is strongly decreasing. This leads us to seek solutions for which $x_1(T)$ is close to 1, while $x_2(T)$ is close to 0.

By inspecting (5.32), we conclude that p_2 is strongly decreasing in $(T-\varepsilon, T]$. This, together with the analysis of (5.31), leads to the conclusion that, there are relations between parameters λ and ρ for which the following statements are consistent:

- Although, possibly not monotonic, p_1 is always bounded by a small value on $[0,T]$.
- Both p_1 and p_2 are always positive.

In this scenario, there exists some t_s for which the pair (x^*, u^*) with $u^*(t) = M$ for all $t \in (t_s, T]$ is an extremal control process on this time interval. Since all the functions

involved are continuous, smooth and locally monotonous, there exists an infimum value for t_s, for which p_1 becomes negative for $t < t_s$. From now on, such a value is denoted by t_s. Depending on the initial condition $x_{1,0}$, we may have $t_s^- = 0$

However, $x_{1,0}$ may also be such that $\exists \delta > 0$ small for which $\forall \bar{t} \in (t_s - \delta, t_s)$, $x_1(\bar{t})$ computed with (5.25) with $u(\bar{t}) = M$, and p_1, p_2, and x_2 prolonged backwards from the point t_s with $u(\bar{t}) = M$ is such that $p_1(\bar{t}) < 0$ and $\dot{p}_1(\bar{t}) < 0$. This situation means that the initial condition of x_1 is too large in order to ensure the consistency of the maximum principle with $u(\bar{t}) = M$ in the interval $(t_s - \delta, t_s)$ and, thus, a control switch, i.e., $u_1^*(\bar{t}) = -M$ on $\forall \bar{t} \in (t_s - \delta, t_s)$, will have to occur in order to preserve the validity of the maximum principle conditions.

By noting that p_2 at t_s has to be sufficiently large in order to force $p_1(t_s)$ for the given value of $x_1(t_s)$, we have that, since $u^*(t) = -M$ and, in the light of the controllability assumption, x_1^* decreases. Thus, from

$$p_1(\bar{t}) = -\int_{\bar{t}}^{t_s} [\rho p_2(s) + x_1(s) - 1] ds\,, \quad \bar{t} \in (t_s - \delta, t_s),$$

we conclude that $p_1(\bar{t}) < 0$ in that interval, and, thus, $\dot{p}_1(\bar{t}) > 0$. Now, from the increasing monotonicity of p_2 for $t < t_s$ that can be inferred from (5.32) with the fact that p_1 is negative, we conclude $\dot{p}_1(t) > 0$ for $t < t_s$, and it becomes obvious that the maximum condition is satisfied on $[0, t_s)$.

Finally, we have that (x^*, u^*) with $u^*(t) = -M$ on $[0, t_s)$ and $u^*(t) = M$ on $[t_s, T]$ for some $t_s \in [0, T)$ satisfies the conditions of the maximum principle, and, by examining the cost functional, it is, in fact the solution to the stated optimal control problem.

Clearly, this analysis of the problem is a very soft. More precise estimates backing the above statements can be computed but the details are cumbersome and the reasoning very intricate. However, the methodology is the same as the one for the previous example, and, thus, the reader was spared to this effort.

The relevance of this example is to show that, on the one hand, a lot of information can be extracted by simply reasoning with the conditions of the maximum principle, and, on the other hand, that this effort can become cumbersome, and, thus, there are limits to what can be achieved in an efficient way in terms of computing the solution to the optimal control problem. This points out to the need of using computational procedures for more complex problems. This is path taken in the next subsection.

5.4 Numerical computation of solutions to the optimal control problem

In this sub-section, we resort to a numerical procedure in order to overcome the very significant difficulties arising in carrying out the analysis of the maximum principle

conditions to compute the solution. Below, we outline a general numerical procedure based on a "brute-force" type of shooting method. This method is justified by the fact that the boundary conditions of the dynamic system and of the associated adjoint system are specified at different time endpoints.

Given the initial conditions for the state variables $x_1(0)$, $x_2(0)$ and $x_3(0)$, we consider the following recursive numerical scheme:

1. Step 0. Assume a terminal values for the state variables x_1, x_2 and x_3 by scanning a given region of the state space, and set the iteration counter $k = 1$.

2. Step 1. Given that, from the maximum principle, we know the terminal conditions for the adjoint variables $p_i(T) = 0$, $i = 1, 2, 3$, we solve the two systems (5.2) and (5.4) by integrating backwards in time with the Runge-Kutta scheme with the control value being chosen as the "argmax" of the Pontryagin function.

3. Step 2. Check weather the obtained initial conditions in the previous step coincide with the ones given a priori in the problem statement. If the answer is positive, the recursive process stops since the extremal process has been found and go to Step 4. Otherwise proceed to the next step.

4. Step 3. Change the value of the final conditions interval if the initial conditions for the state variables did not converge. Increase the iteration counter and go to Step 1.

5. Step 4. Plot the data of the state and adjoint variables $x_1(t)$, $x_2(t)$, $x_3(t)$, $p_1(t)$, $p_2(t)$, $p_3(t)$ and $t \in [0, T]$.

This scheme was implemented in FORTRAN program to solve the two point boundary value problem (5.2), and (5.4) by backward integration with a Runge-Kutta scheme (**??**). We found the best solutions for the state and adjoint variables by successively refining the interval of values for the state variable x at final time.

We consider the search interval for each one of the state variable components at the final time, $x_1(T)$, $x_2(T)$, and $x_3(T)$ to be $[-10, 10]$. From the transversality conditions of the maximum principle, we have the final value for adjoint variable $p(T) = 0$.

For convenience, we recall the dynamics of both the state controlled and of the adjoint systems, and of the Pontryagin function. They are given, respectively, by

$$\begin{aligned} \dot{x}_1 &= 2\rho x_2 x_3 - \lambda x_1 + u \\ \dot{x}_2 &= -\rho x_1 x_3 - \lambda x_2 \\ \dot{x}_3 &= -\rho x_1 x_2 - \lambda x_3, \end{aligned}$$

$$\begin{aligned} \dot{p}_1 &= \lambda p_1 + \rho p_2 x_3 + \rho p_3 x_2 + x_1 - 1 \\ \dot{p}_2 &= -2\rho p_1 x_3 + \lambda p_2 + \rho p_3 x_1 + x_2 - 1 \end{aligned}$$

$$\dot{p}_3 \quad = \quad -2\rho p_1 x_2 + \rho p_2 x_1 + \lambda p_3 + x_3 - 1,$$

and

$$H(x,u,p) = p_1[2\rho x_2 x_3 - \lambda x_1 + u] + p_2[-\rho x_1 x_3 - \lambda x_2] + p_3[-\rho x_1 x_2 - \lambda x_3] - \frac{1}{2}\sum_{i=1}^{3}(x_i - 1)^2.$$

Given the computational complexity of the above described scheme, we will deal only with examples for which $x_2(0) = x_3(0)$. As we have seen before, this yields $x_2(t) = x_3(t)$ for all $t \in [0,t]$ and, as a consequence $p_2 \equiv p_3$. In other words, there is a reduction of dimension of the problem from 3 to 2 to which there corresponds a significant decrease in the complexity of the optimum search procedure without loosing its essence. Nevertheless, the procedure was applied to the system with full dimension 3 in order to assess the impact of numeric "perturbations". However, in the graphical representation of the obtained results for the different cases presented below, we only consider the first and the second components of x and of p. In all examples, we consider $T = 5$, and $\lambda = \rho = M = 1$.

1) $x(0) = 0$.

As expected, we obtain $x^*(T) = (0.993, 0, 0)$ (notice that $1 - e^{-5} \simeq 0.993$).

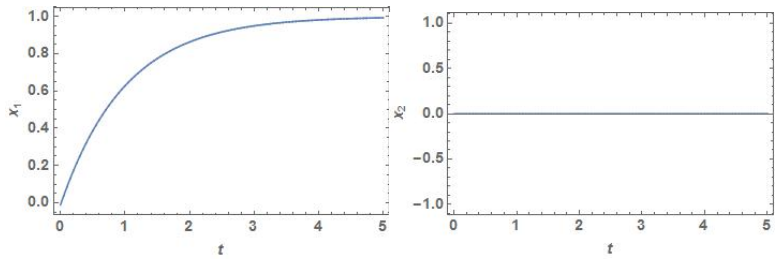

Figure 5.1: Optimal state trajectory

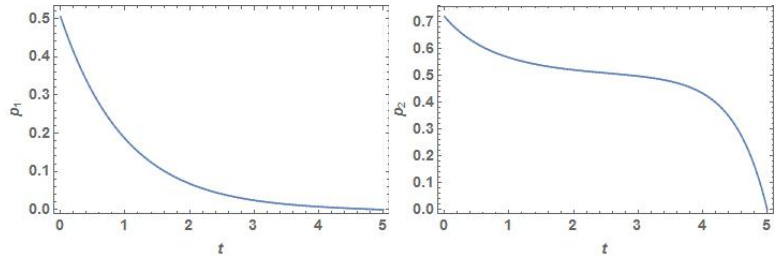

Figure 5.2: Adjoint function

2) $x(0) = col(0.0, 0.5, 0.5)$.

In this case, we obtain $x^*(T) \simeq (0.995, 0.472 \times 10^{-4}, 0.539 \times 10^{-4})$.

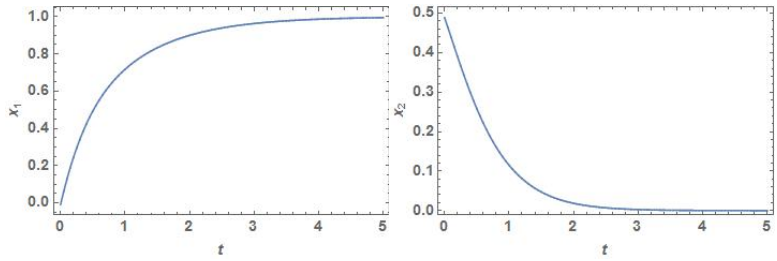

Figure 5.3: Optimal state trajectory

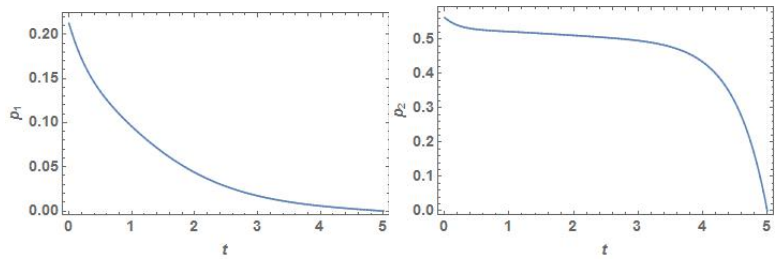

Figure 5.4: Adjoint function

3) $x(0) = col(1, 0.5, 0.5)$.

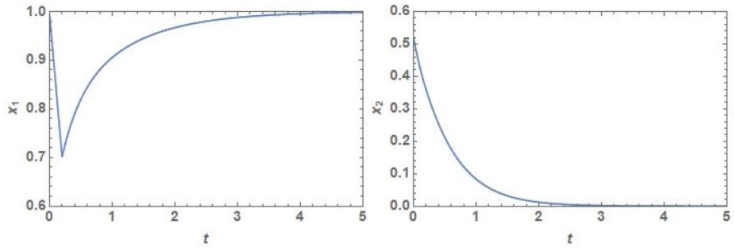

Figure 5.5: Optimal state trajectory

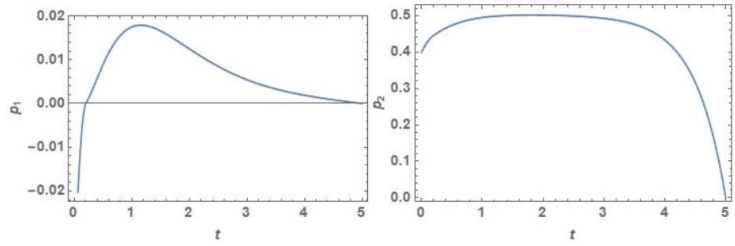

Figure 5.6: Adjoint function

4) $x(0) = col(2.5, 1.0, 1.0)$.

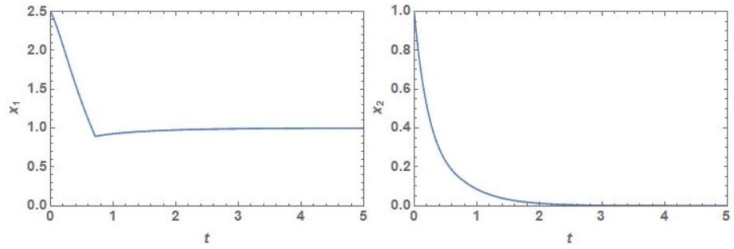

Figure 5.7: Optimal state trajectory

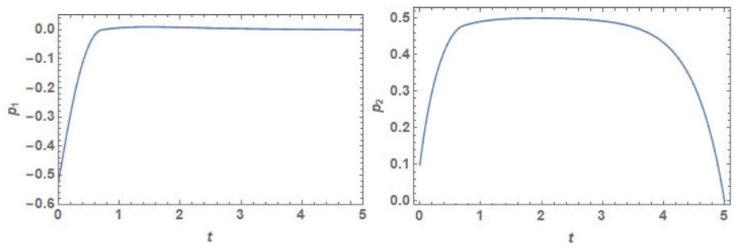

Figure 5.8: Adjoint function

It must be stressed that this approach of exhaustively searching the possibilities of the optimal values of the trajectory in a given region is extremely time consuming. This motivated the investigation of optimization algorithms for optimal control problems that, by taking advantage of the properties of the specific dynamic control systems addressed in this thesis, are sufficiently efficient to enable the scaling of the dimension of the state variable that ideally should be above 20. An investigation of a conceptual algorithm is the subject of the next section.

5.5 A recursive algorithm based on the maximum principle

In this section, we present an algorithm that attempts to improve the performance, notably, to decrease the number of iterations, by formulating an equivalent auxiliary optimal control problem such that the application of the maximum principle to the later yields a two boundary value problem with the boundary conditions in the same endpoint.

The intensive computational character of the two point boundary value problems used to solve the pertinent optimal control problems in order to obtain the results presented until now were due to the fact that the adjoint and primal differential systems of equations were solved for all elements of a sequence of increasingly refined grids of state initial conditions.

In order to significantly decrease the computational complexity, we propose a new algorithm for a related sequence of optimal control problems whose terms are extensions of

the original problem constructed to allow a relaxation of the boundary conditions which, as the iterations increase, are progressively tightened. This relaxation provides the ground for an increased efficiency of the descent direction algorithm.

In the next subsection, we provide the basis for the control problem relaxation mechanism.

5.5.1 The relaxation mechanism

Let us consider the following general optimal control problem with sufficiently smooth data as stated in Chapter 4 together with the Lipschitz continuity of the maps $x \to f(x,u)$ and $x \to h(x)$ with Lipschitz constants, respectively, K_f for all $u \in \Omega$, and K_h, and where $\Omega \subset \mathbb{R}^m$ is a compact set.

$$\begin{aligned} (P)\ \text{Minimize} \quad & \int_0^1 h(x(t))dt \\ \text{subject to} \quad & \dot{x}(t) = f(x(t),u(t)) \\ & x(0) = x_0 \in \mathbb{R}^n \\ & u(t) \in \Omega \subset \mathbb{R}^m \end{aligned}$$

Let us assume that the solution to (P) is unique. This hypothesis may look restrictive, but, since we will be dealing with a given solution, it is not difficult to modify the problem so that this assumption holds.

Consider also the following auxiliary optimal control problem that results from the previous one by omitting the initial value of the state variable

$$\begin{aligned} (P_{aux})\ \text{Minimize} \quad & \int_0^1 h(x(t))dt + K\|x(0) - x_0\| \\ \text{subject to} \quad & \dot{x}(t) = f(x(t),u(t)) \\ & u(t) \in \Omega \subset \mathbb{R}^m \end{aligned}$$

where K is a given constant whose estimate will be determined next in the context of the proof of the following Proposition.

Proposition 1. There exists some constant $K > 0$ for which problems (P) and (P_{aux}) are equivalent.

Proof. Let

$$\mathcal{Z} := \{(x,u) \in AC([0,1];\mathbb{R}^n \times L^\infty([0,1];\mathbb{R}^m) : \dot{x} = f(x,u),\ u \in \Omega\},$$

$$Z := \{(x,u) \in \mathcal{Z} : x(0) = x_0\},$$

$$d_Z(x,u) : \mathcal{Z} \to \mathbb{R}$$

defined by $d_Z(x,u) = ||x(0) - x_0||$, and

$$J(x,u) = \int_0^1 h(x(t))dt\,.$$

To estimate the above constant K, let us compute $\nabla_{x(0)}J(x,u)$. Let $\Phi(t,0;u)$ be the state transition matrix of the linearized system

$$\dot{y} = D_x f(x(t),u(t))y\,,$$

with the initial condition $y(0) = y_0$. Notice that, because of the compactness on the velocity set, we have that there exists $M_f(u) > 0$ such that $|\Phi(t,0;u)| \leq M_f(u)$. Denote by $\bar{M}_f = \sup_{u\in\mathcal{U}}\{M_f(u)\}$ and let $K = K_h\bar{M}_f$. Since we have

$$\begin{aligned}\nabla_{x(0)}J(x,u) &= \int_0^1 \nabla_{x(t)}h(x(t))D_{x(0)}x(t)dt \\ &= \int_0^1 \nabla_{x(t)}h(x(t))\Phi(t,0;u)dt,\end{aligned}$$

we readily conclude that

$$|\nabla_{x(0)}J(x,u)| \leq K\,.$$

Thus, the constant K can be regarded as a Lipschitz constant of the functional J with respect to the initial value of the state variable. Let

$$(x^*,u^*) = arg\min_{(x,u)\in Z}\{J(x,u)\}\ .$$

Take any $(\tilde{x},\tilde{u}) \in \mathcal{Z}$, and let $(\bar{x},\bar{u}) \in Z$ such that

$$|(\bar{x},\bar{u}) - (\tilde{x},\tilde{u})| = d_Z(\tilde{x},\tilde{u}).$$

Then,

$$\begin{aligned}J(x^*,u^*) - J(\tilde{x},\tilde{u}) &\leq J(\bar{x},\bar{u}) - J(\tilde{x},\tilde{u}) \\ &\leq K|(\bar{x},\bar{u}) - (\tilde{x},\tilde{u})| \\ &= Kd_Z(\tilde{x},\tilde{u}).\end{aligned}$$

Thus, we have that

$$\min_{(x,u)\in Z}\{J(x,u)\} \Leftrightarrow \min_{(x,u)\in\mathcal{Z}}\{J(x,u) + Kd_Z(x,u)\}.$$

By expressing this conclusion in terms of the original data, we conclude the proof.

Now, let us embed the OCP (P_{aux}) in an extended family of problems $(P_{aux}^{\varepsilon_i})$, where $\{\varepsilon_i\}$ is a sequence of positive numbers converging to zero, defined as follows

$$\begin{aligned}
(P_{aux}^{\varepsilon_i}) \text{ Minimize} \quad & \int_0^1 h(x(t))dt + K\|y(1) - x_0\| \\
\text{subject to} \quad & \dot{x}(t) = f(x(t), u(t)) \\
& \dot{y}(t) = v(t) \\
& x(0) = y(0) \in \mathbb{R}^n \\
& u(t) \in \Omega \subset \mathbb{R}^m, \quad v(t) \in \varepsilon_i B_1(0),
\end{aligned}$$

where $B_1(0)$ is the closed unit ball centered at zero. Let us show the following Proposition.

Proposition 2. $\lim_{i\to\infty}(P_{aux}^{\varepsilon_i}) = (P)$ in the sense that the sequence of solutions $\{(x^i, y^i, u^i, v^i)\}$ to $\{(P_{aux}^{\varepsilon_i})\}$ are such that $(x^i, u^i) \to (x^*, u^*)$ as $i \to \infty$ in some natural sense, where (x^*, u^*) is the solution to (P).

Proof. First, observe that

$$\int_0^1 h(x^i(t))dt + K\|y^i(1) - x_0\| \leq \int_0^1 h(x^*(t))dt\,,$$

since the control process $(x^*, x_0, 0, u^*))$ is feasible for $(P_{aux}^{\varepsilon_i})$. Second, we have that, as $i \to +\infty$, $\varepsilon_i \to 0^+$, this implies that

$$\dot{y}^i \to 0\,,$$

and, as a consequence, that

$$y^i(0) - y^i(1) = x^i(0) - y^i(1) \to 0\,.$$

Thus, in the limit, the problem $(P_{aux}^{\varepsilon_i})$ becomes

$$\begin{aligned}
(P_{aux}^{0}) \text{ Minimize} \quad & \int_0^1 h(\bar{x}(t))dt + K\|\bar{x}(0) - x_0\| \\
\text{subject to} \quad & \dot{\bar{x}}(t) = f(\bar{x}(t), \bar{u}(t)), \qquad \bar{x}(0) = y(0) \in \mathbb{R}^n \\
& u(t) \in \Omega \subset \mathbb{R}^m,
\end{aligned}$$

where $(\bar{x}, y(0), \bar{u}, 0) = \lim_{i\to\infty}(x^i, y^i, u^i, v^i)$.

Observe that (P_{aux}^0) is precisely (P_{aux}) which, from Proposition 1, we have that (P_{aux}^0) is equivalent to (P) in the sense that they have the same solution, that is

$$\bar{x}(0) = x_0\,.$$

Thus, by the above observation, we have that $(\bar{x}, \bar{u})$ is such that

$$\int_0^1 h(\bar{x}(t))dt \leq \int_0^1 h(x^*(t))dt\,,$$

being (x^*, u^*) the solution to (P). However, since (P) has a unique solution, we have that $(\bar{x}, \bar{u}) = (x^*, u^*)$ in some appropriate sense. Thus, by solving (P^0_{aux}), we solve (P) and vice-versa.

Since we are going to using the maximum principle in our algorithm, let us check whether these conditions are preserved under the limiting operation. Thus we need the following Proposition.

Proposition 3. The conditions of the maximum principle conditions (P) are obtained as a limit of a subsequence of the ones for $(P^{\varepsilon_i}_{aux})$ as $i \to \infty$.

Proof. Let us consider (x^i, y^i, u^i, v^i) to be the solution to $(P^{\varepsilon_i}_{aux})$ whose Pontryagin function is

$$H_i(x^i, y^i, p^i, q^i, u, v, \lambda^i) = p^{i,T} f(x^i, u) + p^{i,T} v - \lambda^i h(x^i).$$

The maximum principle of Pontryagin states that there exists a nontrivial multiplier (p^i, q^i, λ^i) with $\lambda^i \geq 0$, satisfying

$$\begin{aligned}
-\dot{p}^{i,T} &= p^{i,T} f_x(x^i, u^i) + q^{i,T} v^i - \lambda^i h_x(x^i), \qquad -p^i(1) = 0 \\
-\dot{q}^{i,T} &= 0, \qquad -q^i(1) = \lambda^i K \frac{y^i(1) - x_0}{\|y^i(1) - x_0\|}, \qquad q^i(0) = -p^i(0) \\
&\quad u^i(t) \text{ maximizes the map } u \to p^{i,T} f_x(x^i, u), \text{ and} \\
&\quad v^i(t) \text{ maximizes the map } v \to q^{i,T} v.
\end{aligned}$$

Note that, $\forall i \in \mathbb{N}$, we have that $\lambda_i > 0$. Otherwise, $q^i(1) = q^i(0) = -p^i(0) = 0$, and, in fact, $p^i(t) \equiv 0$ and $q^i(t) \equiv 0$. This fact contradicts the nontriviality of the multiplier. Moreover, for an infinite subsequence of multipliers, $\exists \lambda_0 > 0$ such that $\lambda^i > \lambda_0$. If this were not the case, the limiting problem (P) would have to be abnormal which is clearly false due to the absence of state constraints and endpoint state constraints. From now on, we consider $\lambda^i > 0$ such that $\lambda^i \to \bar{\lambda} > 0$ as $i \to \infty$.

Since

$$q^i(t) = -\lambda^i K \frac{y^i(1) - x_0}{\|y^i(1) - x_0\|} \neq 0\,,$$

we have that

$$v^i(t) = \varepsilon^i \frac{q^i(t)}{|q^i(t)|}\,.$$

Thus, $v^i(t) \to 0$ as $i \to \infty$.

By extracting subsequences (if necessary) from $\{(x^i, y^i, u^i, v^i)\}$ considered above,

by using the uniqueness of the solution to (P), and the assumptions on its data, we readily conclude that

- $\lim_{i\to\infty} q^i(t) = -\bar{K}\zeta$ where $\bar{K} = \bar{\lambda}K$, $\zeta = \lim_{i\to\infty} \dfrac{y^i(1) - x_0}{\|y^i(1) - x_0\|}$, for some ζ with $|\zeta| = 1$,
- $\lim_{i\to\infty} p^i(0) = -\bar{K}\zeta$ and $\lim_{i\to\infty} p^i(t) = \bar{p}(t)$,

satisfying

$$-\dot{\bar{p}}^T = \bar{p}^T f_x(x^*, u^*) - \bar{\lambda} h_x(x^*), \quad -\bar{p}(1) = 0.$$

It is clear that $\bar{p}(t) \equiv p(t)$, where p is the adjoint function in the maximum principle for (P). By scaling down (permitted by the linearity of the adjoint differential system), we may have $\bar{\lambda} = 1$ and we consider so in the limit.

Clearly, the maximum condition of the maximum principle applied to (P) follows from the limiting operation of the maximum condition of the maximum principle applied to $(P^{\varepsilon_i}_{aux})$. Just notice that

$$\lim_{i\to\infty} H_i(x^i, y^i, p^i, q^i, u^i, v^i, \lambda^i) = H(x^*, p^*, u^*).$$

Now, we will present the proposed recursive algorithm.

5.5.2 A steepest descent algorithm

Let us now consider an iterative optimization algorithm to find an optimal control process to (P) based on the maximum principle of Pontryagin which takes advantages of the embedding results proved above in order to increase its convergence efficiency. We point out that this is a "conceptual" algorithm in the sense that no numerical issues are taken into account.

As it is inferred from the previous subsection, the optimization process requires that the relaxation of the original optimal control problem is progressively tightened in each iteration. Thus, we consider the following "running" optimal control problem.

$$\begin{aligned} (P_i)\ \text{Minimize} \quad & \int_0^1 g(x(t))dt + K\|y(1) - x_0\| \\ \text{subject to} \quad & \dot{x} = F(x) + u, \quad \dot{y} = v \\ & x(0) = y(0) \\ & u \in \mathcal{U}, \quad v \in \mathcal{V}^i, \end{aligned}$$

where

$$\mathcal{U} = \{u \in L^1 : u_1(t) \in [-M, M], u_2(t) = u_3(t) = 0\},$$

and

$$\mathcal{V}^i = \{v \in L^1 : v(t) \in \varepsilon^i B_1(0)\},$$

being $B_1(0)$ a closed unit ball centered at the origin, and ε^i a positive number that will decrease from one iteration to the next.

For convenience, let us write down the maximum principle for this problem. First, let us shorten the notation by considering $z = col(x, y)$, $w = col(u, v)$, and $r = col(p, q)$ and define

- Pontryagin function: $H(z, w, r) = p^T(F(x) + u) + q^T v - g(x)$,
- Extended Pontryagin function $H^i(z, w, r; \bar{K}^i, \bar{w}) = H(z, w, r) + (w - \bar{w})^T \bar{K}^i (w - \bar{w})$.

Here, $\bar{K}^i$ is a square matrix of appropriate dimensions that may increase as the iterations progress.

Let $(\bar{z}^i, \bar{w}^i)$ be an optimal control process for (P_i), then there exists a nontrivial multiplier $r^i = col(p^i, q^i)$ satisfying

- The adjoint equations and transversality conditions

  $-\dot{p}^i = p^{i,T} D_x F(\bar{x}^i) - \nabla_x h(\bar{x}^i)$, $-p^i(1) = 0$. Here, $D_x F$ and $\nabla_x h$ denote, respectively the Jacobian of F and the gradient of h w.r.t. x.

  $$-\dot{q}^i = 0, \quad -q^i(1) \in K\partial_y \|\bar{y}^i - x_0\| := \begin{cases} K\frac{\bar{y}^i(1) - x_0}{\|\bar{y}^i(1) - x_0\|} & \text{if } \bar{y}^i(1) \neq x_0 \\ KB_1(0) & \text{if } \bar{y}^i(1) = x_0 \end{cases}.$$

- The maximum condition:

  The control function $\bar{w}^i$ is such that $w^i(t)$ maximizes $\mathcal{L}$-a.e. the map

  $$w \to H(\bar{x}^i(t), w, r^i(t)),$$

  on $\mathcal{U} \times \mathcal{V}^i$.

Here, $\partial_x f(x)$ is the generalized gradient of the map f w.r.t. x which, for the specific case at hand is defined above.

Now, let us present the iterative algorithm that generates a minimizing sequence converging to a control process that satisfies the conditions of the maximum principle. This algorithm depends on four parameters, two of which are constant, $\gamma_1 \in (0, 1)$ and $\gamma_2 > 1$, and have to be tuned to properly update the other two parameters $\varepsilon^i > 0$ and $\bar{K}^i$ which is a diagonal matrix in $\mathbb{R}^{(n+m)\times(n+m)}$, respectively, as follows $\varepsilon^{i+1} = \gamma_1 \varepsilon^i$, and $\bar{K}^{i+1} = \gamma_2 \bar{K}^i$.

The proposed optimization conceptual algorithm consists in the following steps:

1. Initialization. Set iterations counter i to 0, and choose the initial values:

   $$w^i = (u^i, v^i),\ K^i = 1,\ \text{and } \varepsilon^i = \frac{1}{2}$$

2. Computation of

   2.1 State Trajectory by forward integrating the state dynamics:

$$\begin{aligned} \dot{x}^i &= F(x^i) + u^i, & x^i(0) &= x_0 \\ \dot{y}^i &= v^i, & y^i(0) &= x_0 \end{aligned}$$

   2.2 Adjoint Function by backward integrating the adjoint differential equations:

$$\begin{aligned} -\dot{p}^{i,T} &= p^{i,T} D_x F(x^i) - \nabla_x h(x^i), & -p^i(1) &= 0 \\ -\dot{q}^i &= 0, & -q^i(1) &= K\partial_y \|\bar{y}^i - x_0\| \end{aligned}$$

   2.3 The Cost Functional

$$J(w^i) = \int_0^1 g(x^i(t))dt + \bar{K}\varepsilon^i$$

3. Testing of the Maximum Condition

   If u^i is such that $u^i(t)$ maximizes $[0,1]$ $\mathcal{L}$-a.e. the map $u \to p^{i,T}(t)u$ on $\mathcal{U}$ and $\varepsilon^i = 0$, then stop. Otherwise proceed to Step 4.

4. Update of the next Control Estimate.

   4.1 Computation of w_{i+1} as follows:

$$w_{i+1}(t) = \arg\max_{w \in \mathcal{U}\times\mathcal{V}^i} \left\{ H^i(z^{i+1}(t), w, r^i(t); w^i(t), \bar{K}^i) \right\},$$

   where z^{i+1} is obtained by integrating forward the dynamics with just the computed value of w_{i+1}.

   4.2 Compute the cost $J(w_{i+1})$ associated with (z_{i+1}, w_{i+1}):

$$J(w_{i+1}) = \int_0^1 g(x_{i+1}(t))dt + K\|y_{i+1} - x_0\|.$$

   4.3 If $J(w_{i+1}) \geq J(w_i)$, let $\bar{K}^{i+1} = \gamma_2 \bar{K}^i$ and go to Step 4.. Otherwise, proceed to Step 5.

5. Preparation of the new iteration.

   Let $\varepsilon^{i+1} = \gamma_1 \varepsilon^i$, $i = i + 1$, and go to Step 2.

This algorithm is designed having in mind strong assumptions on the data of the optimal control problem which are afforded by its specific structure: dynamics bilinear on the state variable an affine in the control. Moreover, it has to be considered in the light of the results of the previous subsection that show that the sequence of relaxed control

problems converge (in the sense made clear there) to the original problem as the parameter $\varepsilon^i \to 0$.

It is clearly a maximum descent direction type of algorithm in the space of the feasible controls. The maximum descent direction is specified by the maximization of the Pontryagin function in each direction, being the step length determined in the step 4. of the algorithm.

We are not going into details of the proof which are relatively straightforward to prove but rather list a number of facts which constitute the dorsal spine of the proof of convergence to a control process that satisfies the conditions of the maximum principle and, at the same time, is a local minimum.

First, let us focus on the assumptions on the data of the problem. Besides the strong smooth assumptions satisfied by F due to its structure, we assume that h is C_2 and that its first and second order derivatives are bounded. Notice also that the control constraints are strongly compact. From these assumptions, it follows that both the state and the adjoint variables take on values on compact sets at each point in time, and that the attainable set of the considered dynamic control system is compact.

Second, let us observe that $\mathcal{U} \times \mathcal{V}^i$ endowed with the metric

$$\Delta(w_a, w_b) := \max \quad \begin{array}{l} \{M\mathcal{L}\text{-a.e.}\,(\{t \in [0,1] : u_a(t) \neq u_b(t)\}), \\ \int_0^1 |u_a(t) - u_b(t)|dt, \int_0^1 |v_a(t) - v_b(t)|dt \end{array} \Big\}$$

becomes a complete metric space.

From here, we will provide a number of hints of the proof. It is straightforward to show that:

1 The map $w \to J(w)$ is bounded from below and continuous in the topology induced by the norm Δ.

2 The mechanism of the algorithm generates a sequence of extremal control estimates w^i satisfying:

- $\lim_{i\to\infty} \Delta(w^{i+1}, w^i) = 0$.
- $\exists M > 0$ independent of i (iteration counter) such that

$$J(w^{i+1}) - J(w^i) < M\Delta(w^{i+1}, w^i).$$

3 From 1. and 2., one concludes that the sequence $J(w^i)$ is such that $\lim_{i\to\infty} J(w^i) = J^*$.

4 From the convexity w.r.t. to the control of H^i, for i sufficiently large, together with the fact that $\varepsilon^i \to 0$, as $i \to \infty$, one concludes that, there exists some $\bar{u}$, such that, for a subsequence of $\{w^i\}$, $\lim_{i\to\infty} w^i = (\bar{u}, 0)$ satisfying $J((\bar{u}, 0)) = J^*$.

5 Finally the fact that, as $i \to \infty$, (P_i) converges to the original optimal control problem, and that H^i converges to H, we conclude that, together with the decreasing monotonicity of $\{J(w^i)\}$, $\bar{u} = u^*$, i.e., the limiting control process (x^*, u^*) is a local minimum to the given optimal control problem.

We would like to emphasize that this is just a conceptual algorithm and that many very important issues, chiefly among them, the algorithm's nature and rate of convergence, and the characterization of the region of the attraction to support the initialization step, were left out of the discussion. Moreover, all numerical issues were left out of the discussion. These are particularly important when the dimension and nature of the optimal control problem is such that the numeric sensitivity becomes a critical issue.

In the next section, some results will be presented. These were obtained by procedures that are of similar nature in the sense that are dominantly of maximum-descent type but for which the numerical aspects were properly taken care of by using algorithms well established in the literature.

5.6 Computation of the optimal control problem with the Gledzer model

The key objectives of this section is to show that first order algorithms for optimal control based on the Maximum Principle are effective in solving the class of problems considered in this thesis. It should be stressed out that, in this class of infinite dimensional problems, numerical issues play a critical role due to the required fine numerical sampling to ensure accuracy, notably in the case in which long integration time horizons are defined. On the other hand, the complexity also increases enormously. Thus, it is important to figure out the optimal trade-off between selecting a detailed sampling scheme and mitigating the effect of accumulating numerical errors. Another important issue concerns the scalability of the dimension of the problem, that is, the number of shells increases to values of practical interest, say, between 22 and 24. Here, we provide an illustration that the above issues are properly handled by the used algorithms.

In this section, we consider the shell-model introduced by Gledzer to model two-dimensional turbulence [76]:

$$\dot{x}_n = k_n \left(a x_{n-2} x_{n-1} + b x_{n-1} x_{n+1} + c x_{n+1} x_{n+2}\right) - \nu k_n^2 x_n,$$

where $x_n = x_n(t)$, $n = 1, \ldots, N$, and $k_n = k_0 2^n$. All variables with indices $n < 1$ or $n > N$ are assumed to be zero by definition.

We consider the following optimal control problem:

$$\text{minimize } J[\mathbf{x},u]=\frac{1}{2}\int_0^1\sum_{n=1}^{N}(x_n-\alpha_n)^2\mathrm{dt} \tag{5.33}$$

subject to

$$\dot{x}_n=k_0 2^n\left(ax_{n-2}x_{n-1}+bx_{n-1}x_{n+1}+cx_{n+1}x_{n+2}\right)-\nu k_0^2 4^n x_n+u_n, \tag{5.34}$$

$$x_n(0)=x_n^0, \tag{5.35}$$

where $u_n=\delta_{n,1}u(t)$, $u\in[-M,M]$, and $M>0$, $N>0$, $\nu>0$, $k_0>0$, x_n^0, α_n are given constants.

The Pontryagin maximum principle gives rise to the following two-point boundary value problem involving: *i*) the final-value problem for the adjoint system

$$\begin{aligned}-\dot{p}_n &= k_0 2^n[4ap_{n+2}x_{n+1}+2p_{n+1}(ax_{n-1}+bx_{n+2})-\nu k_0 2^n p_n \\ &\quad +\frac{1}{2}p_{n-1}(bx_{n-2}+cx_{n+1})+\frac{1}{4}cp_{n-2}x_{n-1}]-(x_n-\alpha_n), \qquad (5.36)\\ p_n(1) &= 0, \qquad (5.37)\end{aligned}$$

and *ii*) the initial-value problem for the original system, (5.34)–(5.35), with $u=M\mathrm{sign}(p_1)$.

The problem (5.34)–(5.37) was solved numerically using MATLAB `bvp5c` solver, implementing the implicit four-stage fifth-order accurate Lobatto collocation method (see [85] for further details) with direct error control.

In computations we used the following values of the parameters: $N=10$, $M=1$, $\nu=0.01$, $k_0=0.1$, $\alpha_n=2^{-n/3}$; the initial values, x_n^0 in (5.35), were computed (using the MATLAB `random` function) as a realization of a random variable distributed uniformly in interval $(-5,5)$:

$$\mathbf{x}^0=(1.312,-1.449,4.970,-2.758,1.525,1.050,-1.128,-3.578,-4.749,-0.789). \tag{5.38}$$

Values of the model parameters were taken to be $a=1/16$, $b=-5/8$, and $c=1$, implying conservation of energy and enstrophy for $\nu=0$.

Numerical solution to the problem (5.34)–(5.37) with initial condition (5.38) is presented in fig. 5.9. The computed control function, $u(t)$, displays two "switches" at $t\approx 0.37$ and at $t\approx 0.96$, responsible for non-smoothness of $x_1(t)$ at these points.

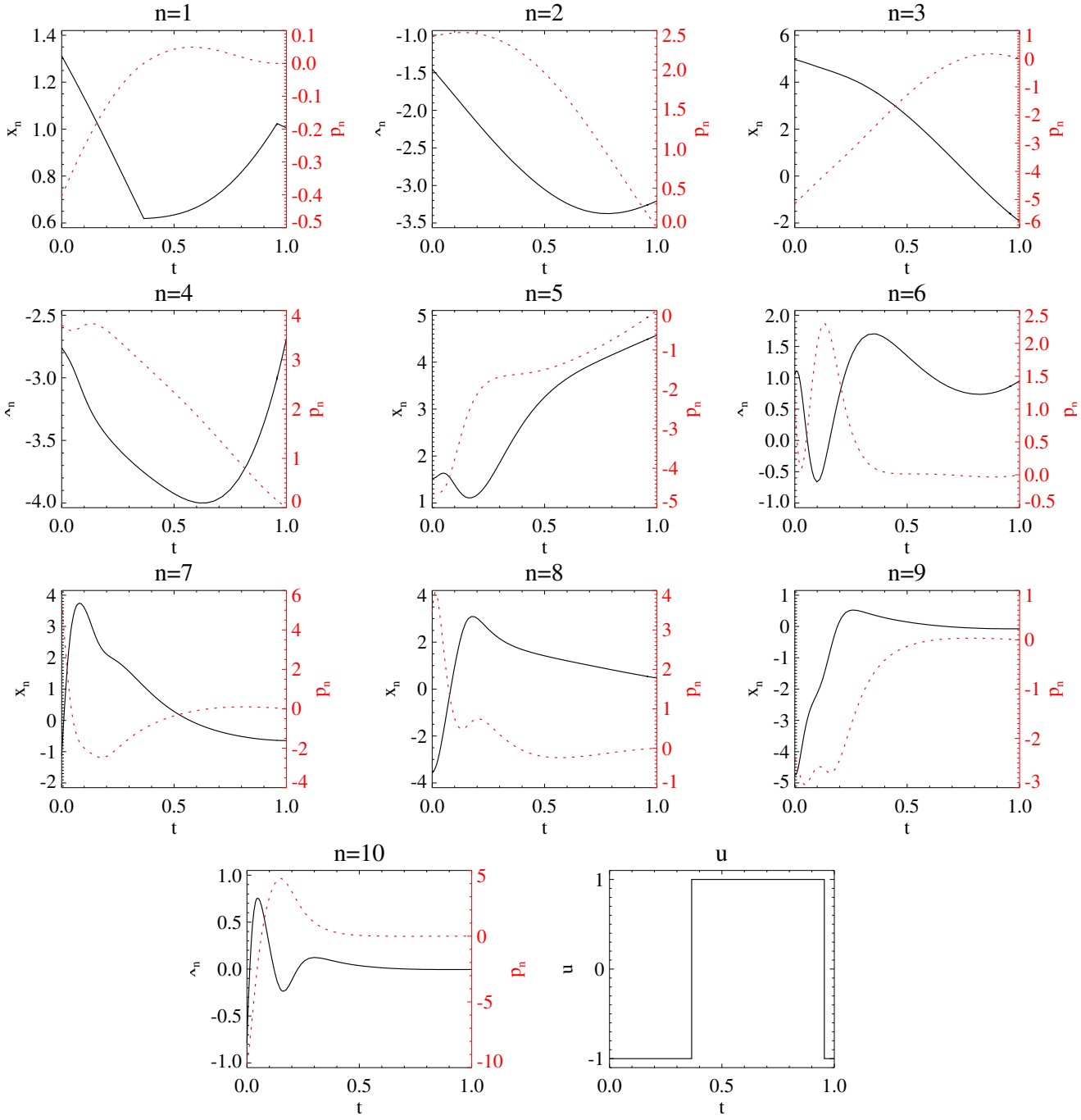

Figure 5.9: Numerical solution to the two-point boundary problem (5.34)–(5.37) given by the Pontryagin maximum principle for the Gledzer model. $x_n(t)$ (black solid line, left vertical axis) and $p_n(t)$ (dotted red line, right vertical axis) are shown for $n = 1, \ldots, 10$ as well as the control $u(t)$.

Chapter 6

Conclusions and future work

In this work, we present the development of a theoretical methodology based on optimization schemes and on optimal and control approaches, in order to optimize and control the forcing of turbulence, and we applied this methodology to the shell models of turbulence.

The approach of exhaustively searching the possibilities of the optimal values of the trajectory in a given region is extremely time consuming. This motivates the investigation of optimization algorithms for optimal control problems that, by taking advantage of the properties of the specific dynamic control systems addressed in this work, are sufficiently efficient to enable the scaling of the dimension of the state variable.

This is a preliminary investigation to novel iterative algorithm for nonlinear optimal control problems in which the specific structure of the problem is exploited in order to initiate the optimization process with an easier related problem. By easier, we mean that cost descent directions enabling an efficient progress towards the solution of the original problem can be found. Then, as iterations progress, the structure of the sequence of auxiliary easier problems converge to that of the original problem. At this point, we consider only control problems whose dynamics are given by the Gledzer model. Future work consists in extending the results obtained so far to more control problems with more general data characterized by assumptions that enable the success of the approach introduced here.

As a general conclusion, we note that the theoretical results reported here point for the possibility of reducing the computation time so that the systems defined by shell models of turbulence rapidly attain the steady state regime in the phase space, where the structure functions are characterized by power laws.

Bibliography

[1] C. Abbe, *The physical basis of long-range weather forecasts 1*, Month. Weath. Rev. **29** (1901), no. 12, 551–561.

[2] J. Abello, P. M. Pardalos, and M. G. Resende, *Handbook of massive data sets*, Vol. 4, Springer, 2013.

[3] B. Anderson, J. Tinapple, and L. Surber, *Optimal control of shock wave turbulent boundary layer interactions using micro-array actuation*, 3rd aiaa flow control conference, 2006, pp. 3197.

[4] R. A. Antonia, A. Prabhu, and S. E. Stephenson, *Conditionally sampled measurements in a heated turbulent jet*, J. Fluid Mech. **72** (1975), no. 03, 455–480.

[5] A. Arutyunov, *Optimality conditions. abnormal and degenerate problems*, Vol. 526, Springer, 2000.

[6] ———, *Optimality conditions: Abnormal and degenerate problems*, Vol. 526, Springer Science & Business Media, 2013.

[7] A. Arutyunov, V. Jaćimović, and F. L. Pereira, *Second order necessary conditions for optimal impulsive control problems*, J. dynamical and control sys. **9** (2003), no. 1, 131–153.

[8] A. Arutyunov, D. Karamzin, and F. L. Pereira, *On a generalization of the impulsive control concept: controlling system jumps*, Discrete Contin. Dyn. Syst **29** (2011), no. 2, 403–415.

[9] A. Arutyunov, D. Y. Karamzin, and F. L. Pereira, *Rv gamkrelidze?s maximum principle for optimal control problems with bounded phase coordinates and its relation to other optimality conditions*, Doklady Mathematics **83** (2011), no. 1, 131–135.

[10] ———, *Pontryagin maximum principle for constrained impulsive control problems*, Nonlinear Analysis: Theory, Methods & Applications **75** (2012), no. 3, 1045–1057.

[11] ———, *State constraints in impulsive control problems: Gamkrelidze-like conditions of optimality*, J. Optimization Theo. Appli. **166** (2015), no. 2, 440–459.

[12] ———, *Conditions for the absence of jumps of the solution to the adjoint system of the maximum principle for optimal control problems with state constraints*, Proc. Steklov Instit. Math. **292** (2016), no. 1, 27–35.

[13] A. Arutyunov, D. Y. Karamzin, F. L. Pereira, and G. N. Silva, *Investigation of regularity conditions in optimal control problems with geometric mixed constraints*, J. Optimization **65** (2016), no. 1, 185–206.

[14] A. Arutyunov and F. L. Pereira, *Second-order necessary optimality conditions for problems without a priori normality assumptions*, Math. Operations Research **31** (2006), no. 1, 1–12.

[15] A. V. Arutyunov, V. Dykhta, and F. L. Pereira, *Necessary conditions for impulsive nonlinear optimal control problems without a priori normality assumptions*, J. Optimization Theo. appli. **124** (2005), no. 1, 55–77.

[16] A. V. Arutyunov, D. Y. Karamzin, and F. L. Pereira, *Maximum principle in problems with mixed constraints under weak assumptions of regularity*, J. Optimization **59** (2010), no. 7, 1067–1083.

[17] ———, *The maximum principle for optimal control problems with state constraints by rv gamkrelidze: revisited*, Journal of Optimization Theory and Applications **149** (2011), no. 3, 474–493.

[18] S. M. Aseev and A. V. Kryazhimskiy, *The pontryagin maximum principle for infinite-horizon optimal controls*, Iiasa interim report, 2003.

[19] Martino Bardi and Italo Capuzzo-Dolcetta, *Optimal control and viscosity solutions of hamilton-jacobi-bellman equations*, Springer Science & Business Media, 1997.

[20] C. Basdevant, B. Legras, and R. Sadourny, *A study of barotropic model flows: Intermittency, waves and predictability*, J. Atmos. Sci. **38**, no. 11.

[21] G. K. Batchelor, *Computation of the energy spectrum in homogeneous two-dimensional turbulence*, Phys. Fluids Suppl. **12**, no. 12.

[22] ———, *Energy decay and self-preserving correlation functions in isotropic turbulence*, Quart. Appl. Math. **6** (1948), no. 2, 97–116.

[23] H. Behncke, *Optimal control of deterministic epidemics*, Optimal control applications and methods **21** (2000), no. 6, 269–285.

[24] A. F. Bennett, L. M. Leslie, C. R. Hagelberg, and P. E. Powers, *Tropical cyclone prediction using a barotropic model initialized by a generalized inverse method*, Monthly Weather Rev. **121** (1993), no. 6, 1714–1729.

[25] T. Bewley and P. Moin, *Optimal control of turbulent channel flows*, Active Control of Vibration and Noise **75** (1994), 221–227.

[26] Luca Biferale, *Shell models of energy cascade in turbulence*, Annual review of fluid mechanics **35** (2003), no. 1, 441–468.

[27] Vilhelm Bjerknes, *Das problem der wettervorhersage: betrachtet vom standpunkte der mechanik und der physik*, 1904.

[28] R. F. Blackwelder and L. S. G. Kovasznay, *Time scales and correlations in a turbulent boundary layer*, Phys. Fluids **15** (1972), 1545–1554.

[29] G. Boffetta, *Energy and enstrophy fluxes in the double cascade of two dimensional turbulence*, J. Fluid Mech. **589** (2007), 253–260.

[30] G. Boffetta, A. Celani, and M. Vergassola, *Inverse energy cascade in two-dimensional turbulence: Deviations from gaussian behavior*, Phys. Rev. E **61** (2000), no. 1, R29.

[31] G. Boffetta, F. De Lillo, and S. Musacchio, *Shell model for quasi-two-dimensional turbulence*, Phys. Rev. E **83** (2011), no. 6, 066302.

[32] T. Bohr, M. H. Jensen, G. Paladin, and A. Vulpiani, *Dynamical systems approach to turbulence*, Cambridge University Press, 1998.

[33] R. Boudarel, J. Delmas, and P. Guichet, *Dynamic programming and its application to optimal control*, Vol. 81, Elsevier, 1971.

[34] P. D. Bromirski, O. V. Sergienko, and D. R. MacAyeal, *Transoceanic infragravity waves impacting antarctic ice shelves*, Geophysical Research Letters **37** (2010), no. 2.

[35] Ch. H. Bruneau and H. Kellay, *Experiments and direct numerical simulations of two-dimensional turbulence*, Phys. Rev. E **71** (2005), no. 4, 046305.

[36] A. E. Bryson and Y. C. Ho, *Applied optimal control*, John Wiley & Sons, New York, 1975.

[37] J. M. Burgers, *A mathematical model illustrating the theory of turbulence*, Adv. appl. mech. **1** (1948), 171–199.

[38] R. W. Burpee, *The sanders barotropic tropical cyclone track prediction model (sanbar)*, Synoptic-dynamic meteorology and weather analysis and forecasting, 2008, pp. 233–240.

[39] L. Cesari, *Optimization—theory and applications: problems with ordinary differential equations*, Vol. 17, Springer Science & Business Media, 2012.

[40] G. T. Chapman and M. Tobak, *Observations, theoretical ideas, and modeling of turbulent flows ? past, present and future, in theoretical approaches to turbulence*, Springer-Verlag, New York **pp** (1985), 19–49.

[41] J. Charney, *The use of the primitive equations of motion in numerical prediction*, Tellus **7** (1955), no. 1, 22–26.

[42] J. G. Charney, *The dynamics of long waves in a baroclinic westerly current*, J. of Meteorology **4** (1947), no. 5, 136–162.

[43] ———, *On the scale of atmospheric motions*, Cammermeyer in Komm., 1948.

[44] J. G. Charney, A. Arakawa, D. J. Baker, B. Bolin, R. E. Dickinson, R. M. Goody, C. E. Leith, H. M. Stommel, and C. I. Wunsch, *Carbon dioxide and climate: a scientific assessment*, National Academy of Sciences, Washington, DC, 1979.

[45] J. G. Charney, R. Fjörtoft, and J. v. Neumann, *Numerical integration of the barotropic vorticity equation*, Tellus **2** (1950), no. 4, 237–254.

[46] P. Chen and S. M. Islam, *Optimal control models in finance*, Springer, 2005.

[47] C. W. Clark, *Mathematical bioeconomics: The optimal management of sustainable resources*, Wiley-Interscience, New York, 1990.

[48] F. Clarke, *The maximum principle in optimal control, then and now*, Control and Cybernetics **34** (2005), no. 3, 709.

[49] F. H. Clarke, *Optimization and nonsmooth analysis*, Wiley, New York, 1983.

[50] F. H. Clarke, Y. S. Ledyaev, R. J. Stern, and P. R. Wolenski, *Nonsmooth analysis and control theory*, Vol. 178, Springer Science & Business Media, 2008.

[51] F. H. Clarke and R. B. Vinter, *Applications of optimal multiprocesses*, SIAM Journal on Control and Optimization **27** (1989), no. 5, 1048–1071.

[52] ———, *Optimal multiprocesses*, SIAM Journal on Control and Optimization **27** (1989), no. 5, 1072–1091.

[53] Y. Cohen, *Applications of control theory in ecology: Proceedings of the symposium on optimal control theory held at the state university of new york, syracuse, new york, august 10–16, 1986*, Vol. 73, Springer Science & Business Media, 2013.

[54] G. Comte-Bellot and S. Corrsin, *The use of a contraction to improve the isotropy of grid-generated turbulence*, J. Fluid Mech. **25** (1966), no. 04, 657–682.

[55] P. Constantin, C. Foias, and O. P. Manley, *Effects of the forcing function spectrum on the energy spectrum in 2-d turbulence*, Phys. of Fluids **6** (1994), no. 1, 427–429.

[56] S. Corrsin, *An experimental verification of local isotropy*, J. Aero. Sci. **16** (1949), no. 12, 757–758.

[57] B. E. Davis and D. J. Elzinga, *The solution of an optimal control problem in financial modeling*, Operations Research **19** (1971), no. 6, 1419–1433.

[58] R. E. Davis, *Lagrangian ocean studies*, Annual Review of Fluid Mechanics **23** (1991), no. 1, 43–64.

[59] J. W. Deardorff, *A numerical study of three-dimensional turbulent channel flow at large reynolds numbers*, J. Fluid Mech. **41** (1970), no. 02, 453–480.

[60] V. N. Desnyansky and E. A. Novikov, *Evolution of turbulence spectra to similarity regime*, IZV. AKAD. NAUK SSSR FIZ. ATMOS. OKEANA **10** (1974), no. 2, 127–136.

[61] P. D. Ditlevsen, *Turbulence and shell models*, Cambridge University Press, 2010.

[62] A. Ya. Dubovitskiy and A. A. Milyutin, *Necessary conditions of extremum in a general optimal control problem*, Nauka, Moscow, 1971.

[63] I. Esau, *Large-eddy simulations of geophysical turbulent flows with applications to planetary boundary layer research*, arXiv preprint arXiv:0907.0103 (2009).

[64] J. Extermann, P. Béjot, L. Bonacina, P. Billaud, J. Kasparian, and J.-P. Wolf, *Effects of atmospheric turbulence on remote optimal control experiments*, Appl. Phys. Lett. **92** (2008), no. 4, 041103.

[65] M. M. Farazmand, NK-R. Kevlahan, and B. Protas, *Controlling the dual cascade of two-dimensional turbulence*, J. Fluid Mech. **668** (2011), 202–222.

[66] R. Fjørtoft, *On the changes in the spectral distribution of kinetic energy for two dimensional, nondivergent flow*, Tellus **5** (1953), no. 3, 225–230.

[67] S. L. Fraga and F. L. Pereira, *Hamilton-jacobi-bellman equation and feedback synthesis for impulsive control*, IEEE Transactions on Automatic Control **57** (2012), no. 1, 244–249.

[68] U. Frisch, *Turbulence: the legacy of an kolmogorov*, Cambridge university press, 1995.

[69] A. E. Gargett, *"Theories" and techniques for observing turbulence in the ocean euphotic zone*, Oceanographic Literature Rev. **3** (1998), no. 45, 598.

[70] C. Garrett, *Turbulent dispersion in the ocean*, Prog. in Oceanography **70** (2006), no. 2, 113–125.

[71] C. H. Gibson, *Fine structure of scalar fields mixed by turbulence. i. zero-gradient points and minimal gradient surfaces*, Phys. Fluids **11** (1968), no. 11, 2305–2315.

[72] F. Gifford Jr, *Relative atmospheric diffusion of smoke puffs*, J. of Meteorology **14** (1957), no. 5, 410–414.

[73] T. Gilbert, V. S. L'vov, A. Pomyalov, and I. Procaccia, *Inverse cascade regime in shell models of two-dimensional turbulence*, Phys. Rev. Lett. **89** (2002), no. 7, 074501.

[74] I. V. Girsanov, *Lectures on mathematical theory of extremum problems*, Vol. 67, Springer Science & Business Media, 1972.

[75] E. B. Gledzer, *System of hydrodynamic type admitting two quadratic integrals of motion*, Sov. Phys. Dokl. SSSR **18** (1973), 216.

[76] E. B. Gledzer and A. L. Makarov, *On construction of a shell modell for two-dimensional turbulence*, Notices of the USSR Academy of Sciences: Physics of Atmosphere and Ocean **9(7)** (1979), 899–906.

[77] J. Gregory and C. Lin, *Constrained optimization in the calculus of variations and optimal control theory*, Springer, 2007.

[78] E. V. Grigorieva, E. N. Khailov, and E. Kharitonova, *Optimal control of pollution stock through ecological interaction of the manufacturer and the state*, Revista de Matemática Teoría y Aplicaciones **18** (2011), no. 1, 77–109.

[79] B. A. Hawkins and H. V. Cornell, *Theoretical approaches to biological control*, Cambridge University Press, 1999.

[80] W Heisenberg, *On the theory of statistical and isotropic turbulence*, Proc. Roy. Soc. A **195**.

[81] K. Hinkelmann, *Der mechanismus des meteorologischen lärmes*, Tellus **3** (1951), no. 4, 285–296.

[82] J. O. Hinze, *Turbulence*, McGraw-Hill, New York, 1959.

[83] R. Honnert, *Representation of the grey zone of turbulence in the atmospheric boundary layer*, Adv. in Science and Research **13** (2016), 63–67.

[84] M. M. Hoque, M. J. Sathe, J. B. Joshi, and G. M. Evans, *Analysis of turbulence energy spectrum by using particle image velocimetry*, Procedia Engineering **90** (2014), 320–326.

[85] Kierzenka J. and Shampine L.F., *A bvp solver based on residual control and the matlab pse*, ACM Transactions on Mathematical Software **27(3)** (2001), 299–316.

[86] E. Jung, S. Lenhart, and Z. Feng, *Optimal control of treatments in a two-strain tuberculosis model*, Discrete and Continuous Dynamical Systems Series B **2** (2002), no. 4, 473–482.

[87] L. Kadanoff, D. Lohse, J. Wang, and R. Benzi, *Scaling and dissipation in the GOY shell model*, Phys. Fluids **7** (1995), no. 3, 617–629.

[88] D. Karamzin, V. de Oliveira, F. L. Pereira, and G. Silva, *Minimax optimal control problem with state constraints*, European Journal of Control **32** (2016), 24–31.

[89] D. Y. Karamzin, V. A. de Oliveira, F. L. Pereira, and G. N. Silva, *On some extension of optimal control theory*, European J. Control **20** (2014), no. 6, 284–291.

[90] H. Kellay and W. I. Goldburg, *Two-dimensional turbulence: a review of some recent experiments*, Rep. Prog. Phys. **65** (2002), no. 5, 845.

[91] A. N. Kolmogorov, *Dissipation of energy in locally isotropic turbulence*, Dokl. Akad. Nauk SSSR **32** (1941), 16–18.

[92] ———, *The local structure of turbulence in incompressible viscous fluid for very large Reynolds numbers*, Dokl. Akad. Nauk SSSR **30** (1941), 301–305.

[93] ———, *On degeneration (decay) of isotropic turbulence in an incompressible viscous liquid*, Dokl. Akad. Nauk SSSR **31** (1941), 538–540.

[94] A. N. Kolmogorov and S. V. Fomin, *Elements of the theory of functions and functional analysis*, Vol. 1, Dover Books on Mathematics, 1999.

[95] R. H. Kraichnan, *Inertial ranges in two-dimensional turbulence*, Phys. Fluids **10** (1967), 1417–1423.

[96] B. E. Launder and D. B. Spalding, *Mathematical models of turbulence*, Academic press (1972).

[97] BE Launder, G Jr Reece, and W Rodi, *Progress in the development of a reynolds-stress turbulence closure*, J. fluid mech. **68** (1975), no. 03, 537–566.

[98] C. E. Leith, *Diffusion approximation for two-dimensional turbulence*, Phys. Fluids **11** (1968), 671–673.

[99] S. Lenhart and J. T. Workman, *Optimal control applied to biological models*, CRC Press, 2007.

[100] D. D. Lilly, *Numerical simulation of two-dimensional turbulence*, Phys. Fluids Suppl. **12**, no. 12.

[101] Edward N Lorenz, *Low order models representing realizations of turbulence*, Journal of Fluid Mechanics **55** (1972), no. 03, 545–563.

[102] J. L. Lumley and G. R. Newman, *The return to isotropy of homogeneous turbulence*, J. Fluid Mech. **82** (1977), no. 01, 161–178.

[103] V. S. L'vov, E. Podivilov, A. Pomyalov, I. Procaccia, and D. Vandembroucq, *Improved shell model of turbulence*, Physical Review E **58** (1998), no. 2, 1811.

[104] ———, *Improved shell model of turbulence*, Physical Review E **58** (1998), no. 2, 1811.

[105] ———, *An optimal shell model of turbulence*, arXiv preprint chao-dyn (1998).

[106] Peter Lynch, *The origins of computer weather prediction and climate modeling*, Journal of Computational Physics **227** (2008), no. 7, 3431–3444.

[107] P. E. Merilees and H. Warn, *On energy and enstrophy exchanges in two-dimensional non-divergent flow*, J. Fluid Mech. **69** (1975), no. 04, 625–630.

[108] F. Molteni, R. Buizza, Tim N. Palmer, and T. Petroliagis, *The ECMWF ensemble prediction system: Methodology and validation*, Quarterly journal of the royal meteorological society **122** (1996), no. 529, 73–119.

[109] B. S. Mordukhovich, *Variational analysis and generalized differentiation i: Basic theory*, Vol. 330, Springer Science & Business Media, 2006.

[110] ———, *Variational analysis and generalized differentiation ii: Applications*, Vol. 330, Springer Science & Business Media, 2006.

[111] B. T. Nadiga and J. M. Aurnou, *A tabletop demonstration of atmospheric dynamics: Baroclinic instability*, Oceanography **21** (2008), no. 4, 196–201.

[112] C. J. Nappo, D. R. Miller, and A. L. Hiscox, *Atmospheric turbulence and diffusion estimates derived from plume image analysis*, 5th joint conf. on the applications of air pollution meteorology with the a&wma, 2008.

[113] L. W. Neustadt, *Optimization: A theory of necessary conditions*, Princeton University Press, 1977.

[114] F. Nicoud and J. Baggett, *On the use of the optimal control theory for deriving wall models for les*, Center for Turbulent Research, Annual Research Briefs (1999), 329–341.

[115] A. M. Obukhov, *The local structure of atmospheric turbulence* **67** (1949), no. 4, 643–646.

[116] ———, *On some general characteristics of the equations of the dynamics of the atmosphere*, Izv. Akad. Nauk SSSR, Fiz. Atmos. Okeana **7** (1971), 695–704.

[117] K. Ohkitani and M. Yamada, *Temporal intermittency in the energy cascade process and local lyapunov analysis in fully-developed model turbulence*, Progress of theoretical physics **81** (1989), no. 2, 329–341.

[118] S. A. Orszag and G. S. Patterson, *Numerical simulation of turbulence: Statistical models and turbulence*, Vol. 12, Springer-Verlag, Berlin, 1972.

[119] C. Pasquero and G. Falkovich, *Stationary spectrum of vorticity cascade in two-dimensional turbulence*, Phys. Rev. E **65**, no. 5.

[120] F. L. Pereira and G. N. Da Silva, *Necessary conditions of optimality for state constrained infinite horizon differential inclusions*, 2011 50th IEEE Conference on Decision and Control and European Control Conference (2011), 6717–6722.

[121] ———, *Necessary conditions of optimality for state constrained infinite horizon differential inclusions, 50th ieee conference on decision and control and european control conference,* (2011), 6717–6722.

[122] G. W. Petty, *A first course in atmospheric thermodynamics*, Sundog Publishing, 2008.

[123] R. F. Phalen and R. N Phalen, *Introduction to air pollution science*, Jones & Bartlett Publishers, 2012.

[124] N. A. Phillips, *On the problem of initial data for the primitive equations*, Tellus **12** (1960), no. 2, 121–126.

[125] ———, *Models for weather prediction*, Ann. Rev. Fluid Mech. **2** (1970), no. 1, 251–292.

[126] L. S. Pontryagin, V. G. Boltyanskiy, R. V. Gamkrelidze, and E. F. Mishchenko, *Mathematical theory of optimal processes*, Wiley Interscience, New York, 1962.

[127] W. H. Press, B. P. Flannery, S. A. Teukolsky, and W. T. Vetterling, *Numerical recipes*, Vol. 3, cambridge University Press, cambridge, 2007.

[128] W. C. Reynolds and A. K. M. F. Hussain, *The mechanics of an organized wave in turbulent shear flow. part 3. theoretical models and comparisons with experiments*, J. Fluid Mech. **54** (1972), no. 02, 263–288.

[129] L. F. Richardson, *Weather prediction by numerical process*, Cambridge University Press, 1922.

[130] D. Ruelle and F. Takens, *On the nature of turbulence*, Comm. math. phys. **20** (1971), no. 3, 167–192.

[131] F. Sanders, A. L. Adams, N. J. .B Gordon, and W. D. Jensen, *Further development of a barotropic operational model for predicting paths of tropical storms*, Monthly Weather Review **108** (1980), no. 5, 642–654.

[132] U. Schimpf, H. Haußecker, and B. Jähne, *Studies of air-sea gas transfer and micro turbulence at the ocean surface using passive thermography*, The Wind-Driven Air-Sea Interface: Electromagnetic and Acoustic Sensing, Wave Dynamics and Turbulent Fluxes (1999), 345–352.

[133] Gavin A Schmidt, *The physics of climate modeling*, Physics Today **60** (2007), no. 1, 72–73.

[134] S. P. Sethi and G. L. Thompson, *Optimal control theory–applications to management science and economics*, Springer, 2000.

[135] F. G. Shuman, *History of numerical weather prediction at the national meteorological center*, Weather and Forecasting **4** (1989), no. 3, 286–296.

[136] J. Smagorinsky, *General circulation experiments with the primitive equations: I. the basic experiment*, Monthly weather rev. **91** (1963), no. 3, 99–164.

[137] S. A. Soldatenko, *Weather and climate manipulation as an optimal control for adaptive dynamical systems*, Complexity **2017** (2017).

[138] S. S. Sritharan, *Optimal control of viscous flow*, SIAM, 1998.

[139] G. W. Swan, *Applications of optimal control theory in biomedicine*, New York (1984).

[140] G. I. Taylor, *Statistical theory of turbulence*, Proc. Roy. Soc. London A **151** (1935), no. 873, 421–478.

[141] C. M. Tchen, *On the spectrum of energy in turbulent shear flow* (1953).

[142] S. A. Thorpe, *An introduction to ocean turbulence*, Cambridge University Press, 2007.

[143] R. S. J. Tol, *Welfare specifications and optimal control of climate change: an application of fund*, Energy Economics **24** (2002), no. 4, 367–376.

[144] A. A. Townsend, *The measurement of double and triple correlation derivatives in isotropic turbulence*, Pro. Camb. Phil Soc. **43** (1947), no. 04, 560–570.

[145] H. J. Tucker and A. J. Reynolds, *The distortion of turbulence by irrotational plane strain*, Journal of fluid mechanics **32** (1968), no. 04, 657–673.

[146] M. S. Uberoi, *Energy transfer in isotropic turbulence*, Phys. of Fluids **6** (1963), no. 8, 1048–1056.

[147] F. Veron, W. K. Melville, and L. Lenain, *The effects of small-scale turbulence on air–sea heat flux*, J. Phys. Oceanography **41** (2011), no. 1, 205–220.

[148] R. B. Vinter, *Optimal control*, Springer, 2000.

[149] R. B. Vinter and F. L. Pereira, *A maximum principle for optimal processes with discontinuous trajectories*, SIAM journal on control and optimization **26** (1988), no. 1, 205–229.

[150] T. Von Kármán, *Some remarks on the statistical theory of turbulence*, Proc. 5th Int. Congr. Appl. Mech., Cambridge, MA **347** (1938).

[151] ———, *Progress in the statistical theory of turbulence*, Pro. Nat. Acad Sci. **34** (1948), no. 11, 530–539.

[152] T. Von Kármán and L. Howarth, *On the statistical theory of isotropic turbulence*, Pro. Roy. Soc. London A **164** (1938), no. 917, 192–215.

[153] Th Von Kármán, *On the statistical theory of turbulence*, Pro. Nat. Acad. Sci. **23** (1937), no. 2, 98–105.

[154] J. Warga, *Optimization-a theory of necessary conditions*, IEEE Transactions on Automatic Control **23** (1978), no. 3, 514–515.

[155] N. Wiener, *The use of statistical theory in the study of turbulence*, Proc. 5th Int. Cong. Appl. Mech (1939), 356.

[156] D. H. Wood and P. Bradshaw, *A turbulent mixing layer constrained by a solid surface. part 1. measurements before reaching the surface*, J. Fluid Mech. **122** (1982), 57–89.

[157] I Wygnanski and H. E. Fiedler, J. Fluid Mech. **38** (1969), 577.

[158] Y. Xue, M. J. Fennessy, and P. J. Sellers, *Impact of vegetation properties on us summer weather prediction*, J. of Geophysical Research: Atmospheres **101** (1996), no. D3, 7419–7430.

[159] M. Yamada and K. Ohkitani, *Lyapunov spectrum of a model of two-dimensional turbulence*, Phys. rev. lett. **60** (1987), no. 11, 983.

[160] M. I. Zelikin and V. F. Borisov, *Theory of chattering control: with applications to astronautics, robotics, economics, and engineering*, Springer Science & Business Media, 2012.


U.PORTO
FACULDADE DE CIÊNCIAS
UNIVERSIDADE DO PORTO